Impact of Cadherin-13 deficiency on the brain serotonin system using mouse models and human iPSC-derived neurons

Einfluss einer Cadherin-13 Defizienz auf das Serotonin- System des Gehirns unter Verwendung von Mausmodellen und humanen iPSC-abgeleiteten Neuronen

Doctoral thesis for a doctoral degree
at the Graduate School of Life Sciences
Julius-Maximilians-Universität Würzburg
Section Neuroscience

submitted by

Andrea Marcela Forero Echeverry

from
Barranquilla, Colombia

Würzburg 2020

Submitted on: ……

Office stamp

Members of the thesis committee:

Chairperson:	Prof. Dr. Charlotte Förster
Primary Supervisor:	Prof. Dr. Klaus-Peter Lesch
Supervisor (Second):	Prof. Dr. Markus Sauer
Supervisor (Third):	PD Dr. Robert Blum

Date of Public Defense: ……

Date of Receipt of Certificates: ……..

Table of contents

List of tables

List of figures

Abbreviations

°C	Degree Celsius
µm	Micrometer
3D	Three dimensional
5-CSRTT	Five-choice serial-reaction time task
5-HT	Serotonin
5-HTT	Serotonin transporter (= SERT)
ACC	Anterior cingulate cortex
ACTB	Actin, Beta
ADHD	Attention-deficit/ hyperactivity disorder
AGP	Autism Genome Project
Akt	Protein kinase B
Amy	Amygdala
ASD	Autism spectrum disorder
ASPD	Antisocial personality disorder
B7d	Dorsal dorsal raphe
B7l	Lateral dorsal raphe
B7v	Ventral dorsal raphe
BDNF	Brain-derived neurotrophic factor
BM	Barnes maze test
bp	Base pair
BPD	Bipolar personality disorder
CA1	*Cornu Ammonis* 1
CCD	Charge-coupled device
CDH2	Cadherin 2
CDH13	Cadherin 13
CG	Cingulate cortex
cKO	Conditional knockout
cm	Centimeter
CNV	Copy number variant
CPu	Caudate putamen
Ctrl	Control
Ctx	Cortex
D	Day
DAPI	4′,6-Diamidin-2-phenylindol
dNTP	Deoxynucleoside triphosphate
Dt	Depression trait
DR	Dorsal raphe
DNA	Deoxyribonucleic acid
E	Embryonic day
EC	Extracellular cadherin repeat

EMCCD	Electron multiplying charge-coupled device
EPM	Elevated plus maze test
ES	Embryonic stem cell
FGF8	Fibroblast growth factor 8
Flp	Flippase
FP	Floor plate
FRT	Flippase recognition target
GABA	γ-aminobutyric acid
GAP43	Growth associated protein 43
GPI	Glycophosphatidylinositol
GWAS	Genome wide association study
h	Hour
HTR1B	5-Hydroxytryptamine Receptor 1B
hCMV	Human cytomegalovirus
IF	Immunofluorescence
IL	Infralimbic
IL-2	Interleukin-2
ir	Immunoreactive
IQ	Intelligence coefficient
IZ	Intermediate zone
iPSC	Induced pluripotent stem cell
IPSC	Inhibitory postsynaptic current
KO	Knockout
L1CAM	L1 cell adhesion molecule
LDT	Laterodorsal thalamus
lx	Lux
LDB	Light dark box test
MHB	Midbrain hindbrain boundary
min	Minute
ml	Milliliter
mM	Millimolar
MR	Median raphe
mRNA	Messenger ribonucleic acid
mTOR	Mammalian target of rapamycin
MZ	Marginal zone
n	Sample size
NA	Numerical aperture
NCAM	Neural cell adhesion molecule
NHS	Normal horse serum
nm	Nanometer
NOR	Novel object recognition
NPC	Neural progenitor cell
OB	Olfactory bulb

OCT	Optimal cutting temperature
OF	Open field test
PBS	Phosphate-buffered saline
PCR	Polymerase chain reaction
PFC	Prefrontal cortex
PVT	Paraventricular thalamus
QTL	Quantitative Trait Locus
RGC	Radial glial cell
RNAi	Ribonucleic acid interference
ROI	Region of interest
rpm	Revolutions per minute
RT	Room temperature
SA	Substance abuse
SCZ	Schizophrenia
sec	Second
sem	Standard error mean
SERT	Serotonin transporter (= 5-HTT)
Shh	Sonic hedgehog
SIM	Structured illumination microscopy
SLC6A4	Solute carrier family 6 member 4 (= 5-HTT gene)
SNP	Single-nucleotide polymorphism
SSC	Simons Simplex Collection
SSC	Somatosensory cortex
STED	Stimulated emission depletion
TDT	Transmission Disequilibrium Test
Th	Thalamus
TPH2	Tryptophan hydroxylase 2
TrkB	Tropomyosin-related kinase B
Trp	Tryptophan
TBS	Tris-buffered saline
V	Voltage
VZ	Ventricular zone
WT	Wildtype

Abstract

Serotonin (5-hydroxytryptamine, 5-HT) is a neurotransmitter involved in early developmental processes such as cell proliferation, migration, and differentiation. Recent research in humans showed that the brain 5-HT system and *CDH13* are interlinked in the genetics of neurodevelopmental disorders including attention-deficit/hyperactivity disorder and autism spectrum disorder (Lesch et al., 2008; Neale et al., 2008; Neale, Medland, Ripke, Anney, et al., 2010; Neale, Medland, Ripke, Asherson, et al., 2010; Sanders et al., 2011; Sanders et al., 2015; Zhou et al., 2008). This study introduces Cadherin-13 (CDH13), a cell adhesion protein, as a contributor to the development and function of the 5-HT system. Our experiments show that the absence of CDH13 increases the density of 5-HT neurons in the developing dorsal raphe (DR) and increases the 5-HT innervation of the prefrontal cortex in mouse embryonic stages. CDH13 is also observed in radial glial cells, an important progenitor cell type linked to neuronal migration. A three-dimensional reconstruction carried out with super-resolution microscopy, identifies 5-HT neurons intertwined with radial glial cells, and CDH13 clusters at contact points between these cells. This indicates a potential contribution of CDH13 to the migration of DR 5-HT neurons. As CDH13 is strongly expressed in 5-HT neurons, we asked whether the selective deletion of CDH13 from these cells is sufficient to generate the alterations observed in the *Cdh13* constitutive knockout mouse line.

In 5-HT conditional *Cdh13* knockout mice (*Cdh13* cKO) an increase in DR 5-HT neurons in the embryonic and adult brains is observed, as well as 5-HT hyperinnervation of cortical regions. Therefore, illustrating that the lack of CDH13 from 5-HT neurons alone impacts DR formation and serotonergic innervation. Behavioral testing conducted on *Cdh13* cKO mice showed delayed learning in visuospatial learning and memory processing, as well as, changes in sociability parameters. To find out how CDH13 localizes in human 5-HT neurons, CDH13 was visualized in neurons that derived from human induced pluripotent stem cells (iPSC). Super-resolution microscopy confirmed CDH13 expression in a subgroup of induced human neurons positive for typical hallmarks of 5-HT neurons, such as expression of Tph2, the neuron-specific tryptophan hydroxylase, and synaptic structures. In summary, the work included in this thesis presents a detailed analysis of CDH13 expression and localization in the 5-HT system and shows that deletion of CDH13 from 5-HT neurons affects specific higher-order functions of the brain.

Zusammenfassung

Serotonin (5-Hydroxytryptamin, 5-HT) ist ein Neurotransmitter, der in frühe Entwicklungsprozesse involviert ist, wie beispielsweise Zellproliferation, Migration und Differenzierung. Aktuelle Forschungsergebnisse im Menschen zeigten eine Verbindung zwischen dem 5-HT System des Gehirns und *CDH13* in der Genetik neurologischer Entwicklungsstörungen, wie die Aufmerksamkeitsdefizit-/Hyperaktivitätsstörung und die Autismus-Spektrum-Störung (Lesch et al., 2008; Neale, Medland, Ripke, Anney, et al., 2010; Neale, Medland, Ripke, Asherson, et al., 2010; Sanders et al., 2011; Sanders et al., 2015; Zhou et al., 2008). Diese Studie präsentiert Cadherin-13 (CDH13), ein Zelladhäsionsprotein, als einen Gegenspieler in der Entwicklung und Funktion des 5-HT Systems. Unsere Experimente zeigen, dass die Abwesenheit von CDH13 die Dichte der 5-HT Neuronen in dem sich entwickelnden dorsalen Raphe (DR) sowie die 5-HT Innervation des Präfrontalen Kortex in den embryonalen Stadien der Maus steigert. CDH13 wird auch in Radialen Gliazellen beobachtet, ein wichtiger Vorläuferzelltyp, der mit neuronaler Migration in Verbindung gebracht wurde. Eine 3-dimensionale Rekonstruktion, durchgeführt mit Superresolutions-Mikroskopie, identifiziert 5-HT Neuronen verflochten mit Radialen Gliazellen und CDH13 in den Kontaktpunkten zwischen diesen Zellen. Dies verdeutlicht eine potenzielle Rolle von CDH13 bei der Migration der DR 5-HT Neuronen. Da CDH13 eine starke Expression in den 5-HT Neuronen aufweist, fragten wir uns, ob die selektive Deletion von CDH13 in den Zellen ausreichend sei, um die in der konstitutiven *Cdh13* Knockout-Mauslinie beobachteten Veränderung zu erzeugen.

In 5-HT konditionalen *Cdh13* Knockout-Mäusen (*Cdh13* cKO) wurde eine Erhöhung der Anzahl der DR 5-HT Neuronen im embryonalen und adulten Gehirn sowie eine 5-HT Überinnervation der kortikalen Regionen beobachtet. Dies veranschaulicht, dass bereits ein Mangel an CDH13 in 5-HT Neuronen die DR-Ausbildung und serotonerge Innervation beeinflusst. Verhaltensversuche, die an *Cdh13* cKO-Mäusen durchgeführt wurden, zeigten verspätetes Lernen im visuell-räumlichen Spektrum und der Gedächtnisverarbeitung sowie Veränderungen der Soziabilitätsparameter. Um herauszufinden, wie CDH13 in humanen 5-HT Neuronen lokalisiert ist, wurde CDH13 in aus humanen pluripotenten Stammzellen (iPSC) erzeugten Neuronen visualisiert. Superresolutions-Mikroskopie bestätigte eine CDH13 Expression in einer Untergruppe induzierter humaner Neuronen, die typische Merkmale von 5-HT Neuronen, wie etwa die Expression der Neuronen-spezifischen Tryptophan-Hydroxylase Tph2 und synaptische Strukturen, aufweisen. Zusammengefasst präsentiert diese Doktorarbeit eine detaillierte Analyse der CDH13 Expression und Lokalisation im 5-HT System und zeigt, dass eine Deletion von CDH13 in 5-HT Neuronen spezifische höhergradige Funktionen des Gehirns beeinflusst.

1 | General Introduction

1.1. *CDH13*: one gene, multiple disorders

The genetic and molecular underpinning of psychiatric disorders is a complex network composed of both shared, common factors, as well as specific markers for each individual disorder. Recent studies show that neurodevelopmental/ psychiatric disorders, such as autism spectrum disorder (ASD), attention-deficit/hyperactivity disorder (ADHD) and schizophrenia, are not only influenced by multiple genetic alterations, but that the altered genes are in many cases shared among the disorders (Brainstorm et al., 2018). Numerous genetic studies identified *CDH13* as one of these genetic factors which is associated to different psychiatric conditions (for review: Hawi et al., 2018; Rivero et al., 2013) (Figure 1.1-1).

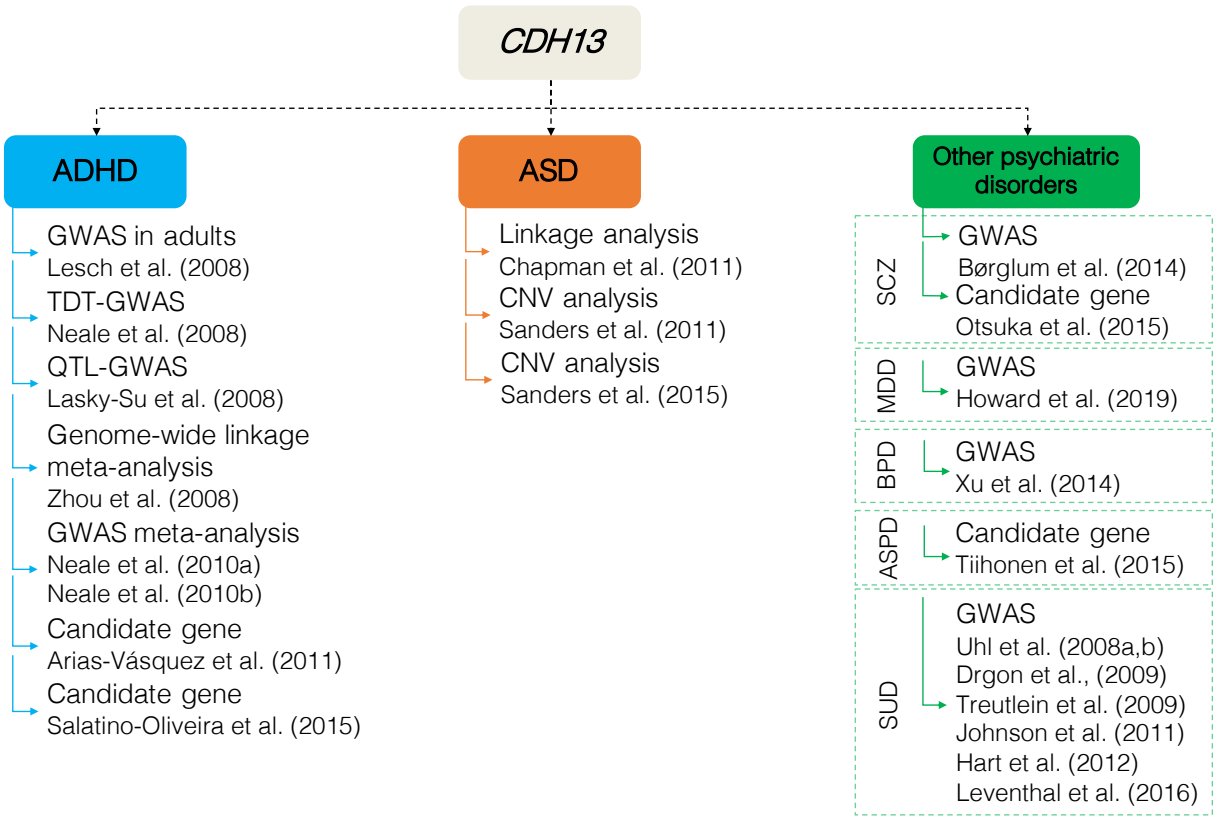

Figure 1.1-1. *CDH13* and neuropsychiatric / neurodevelopmental disorders. Numerous genetic studies have associated *CDH13* to neurodevelopmental/ psychiatric conditions such as attention-deficit/hyperactivity disorder (ADHD), autism spectrum disorder (ASD), schizophrenia (SCZ), major depressive disorder (MDD), Bipolar disorder (BPD), antisocial personality disorder (ASPD) and substance use disorders (SUD). Abbreviations: genome-wide association study (GWAS); copy number variant (CNV).

CDH13 and Attention-deficit/hyperactivity disorder

A pooling-based genome-wide association study (GWAS) of adult ADHD patients and matched controls placed *CDH13* variants among the top-ranked 30 SNPs studied (Lesch et al., 2008). In another study, a family-based analysis also found significant associations mapped to *CDH13* after a phenotype/genetic model combination based on six quantitative traits derived from ADHD clinical measures (Lasky-Su et al., 2008). The relevance of the *CDH13* gene in ADHD was further consolidated by a meta-analysis looking at seven genome-wide linkage scans of ADHD, with a total of 2,084 cases, which reported *CDH13* as the only chromosomal region that yielded genome-wide significant linkage to ADHD (Zhou et al., 2008). Another case-control GWAS investigating ADHD genetics advanced the support for the association *CDH13*-ADHD (Neale et al., 2010a), while a meta-analysis of ADHD GWAS carried out to boost statistical power identified CDH13 as a potential candidate gene (Neale et al., 2010b).

However, it is noteworthy to clarify that none of the GWAS here previously mentioned have identified any genes associated with ADHD at a genome-wide level of significance, probably due to insufficient sample size. Given the genetic heterogeneity of ADHD, only very recent GWAS with very large sample sizes (such as Demontis et al., 2019) have been able to detect variants reaching genome-wide significance, although unfortunately *CDH13* variants were not included among them. However, *CDH13* still continues to be one of the most relevant genes on ADHD and related comorbid conditions. Recently, the association between *CDH13* and executive function tasks as endophenotypes of ADHD was tested and a significant link between SNP rs11150556 and verbal working memory performance was found (Arias-Vasquez et al., 2011). Similarly, the *CDH13* SNP rs11150556 CC genotype was identified as being significantly associated with hyperactive/impulsive symptoms in adolescents with ADHD (Salatino-Oliveira et al., 2015).

CDH13 and Autism Spectrum Disorder

Three main genetic studies have associated *CDH13* with ASD. An initial linkage analysis suggested *CDH13* as a candidate gene underlying the discrepancy in the verbal IQ of autistic children (Chapman et al., 2011). Later, a rare recurrent *de novo* Copy Number Variant (CNV) at *CDH13* was identified in a genome-wide analysis conducted with 1124 ASD families from the Simons Simplex Collection (SSC) (Sanders et al., 2011). By extending the original study to a larger cohort with 2591 families; *CDH13 de novo* deletions correlated with ASD and reached genome-wide significance (Sanders et al., 2015). However, this significance was lost when these data were pooled with previously published data from the Autism Genome Project (AGP) dataset (Pinto et al., 2014).

CDH13 and other psychiatric conditions

The genetic studies presented in this section have correlated *CDH13* with psychiatric conditions identified as comorbidities to ADHD. A study conducted with prisoners in Finland revealed an association between *CDH13* and extremely violent behavior (Tiihonen et al., 2015). Here, violent behavior was defined as having at least 10 committed homicides, attempted homicides or batteries (Tiihonen et al., 2015). *CDH13* has also been strongly associated with substance use disorders (Liu et al., 2006), more specifically with methamphetamine (Uhl, Drgon, et al., 2008), *d*-amphetamine (Hart et al., 2012; Leventhal et al., 2017) and alcohol dependence (Johnson, Drgon, Walther, & Uhl, 2011; Treutlein et al., 2009) as well as cigarette smoking (Drgon et al., 2009; Uhl, Liu, et al., 2008). The comorbidity of conduct disorders and/or substance use with ADHD emphasizes the relevance of these studies.

Regarding affective disorders, *CDH13* has been recognized as a potential risk gene in depression (Howard et al., 2019) and in bipolar disorder (Cho et al., 2015; Prata, Costa-Neves, Cosme, & Vassos, 2019; W. Xu et al., 2014). Additionally, a case-control GWAS carried out with 888 patients diagnosed with schizophrenia and 882 controls identified *CDH13* SNP rs8057927 as one of the most significantly associated factors with the disorder (Borglum et al., 2014). A following candidate gene analysis in a Japanese population identified five additional SNPs in the promoter region of *CDH13* to be significantly associated with schizophrenia (Otsuka et al., 2015).

1.2. Cadherin-13 and neurodevelopment

Just as *CDH13* has been associated to a wide range of psychiatric disorders and symptoms of neurodevelopmental origin, Cadherin-13 (CDH13), the protein coded by this gene, has also been linked to numerous neurobiological developmental functions. The most prominent functions related to its expression can be grouped in three main categories: (1) migration, (2) axonal outgrowth/pathfinding, and (3) synapse formation. These effects on cellular processes influence the brain function and behavior, as shown with the help of various *Cdh13* knockout mouse lines (Figure 1.2-1).

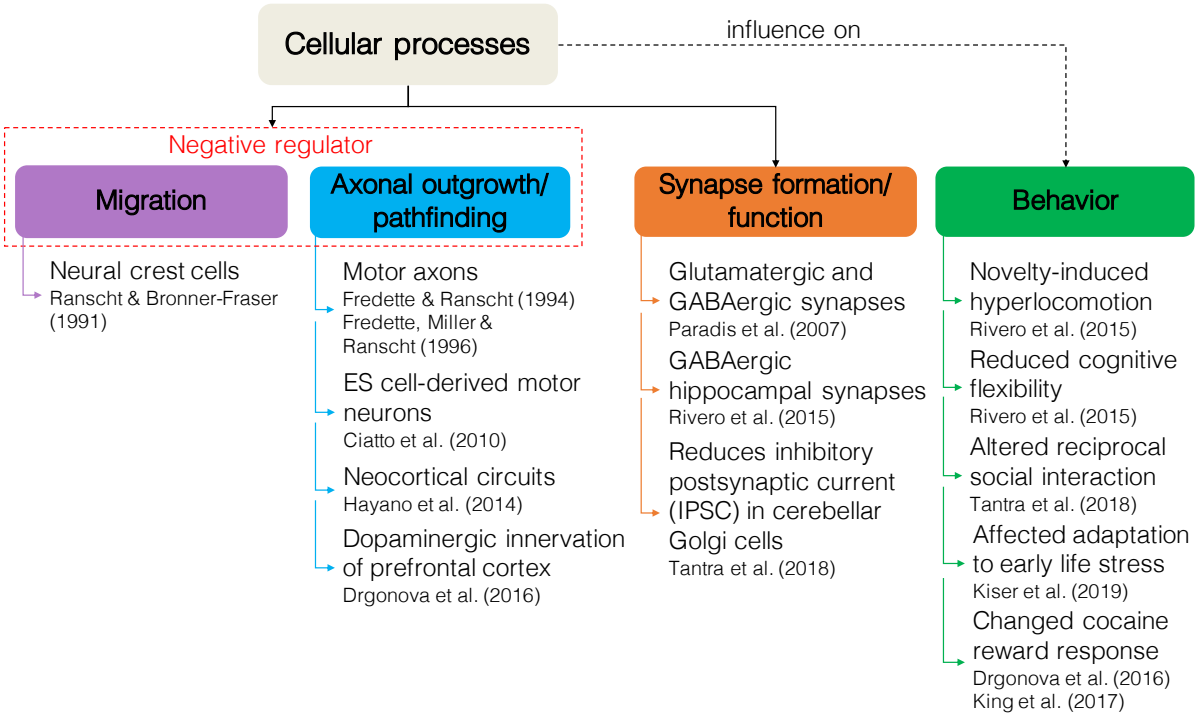

Figure 1.2-1. Cadherin-13 and neurodevelopmental functions. Many functions have been attributed to CDH13 in neurodevelopment and neuron function, with the most prominent ones being related to (1) axonal outgrowth/pathfinding, (2) migration, and (3) synapse formation/ function. These cellular functions have also been directly or indirectly linked to (4) behavioral alterations in various *Cdh13* knockout mouse models. Abbreviations: embryonic stem cell (ES); Inhibitory postsynaptic current (IPSC).

The implication of CDH13 in this wide range of neuronal functions could be due to the fact that CDH13 expression has been reported in a variety of cell types and systems. For instance, initial work showed CDH13 expression in motor neurons and inhibition of their peripheral projections (Ciatto et al., 2010; Fredette, Miller, & Ranscht, 1996; Fredette & Ranscht, 1994). Later studies identified CDH13 expression in diverse neuronal cell types including cortical neurons, GABAergic interneurons, and dopaminergic neurons (Drgonova et al., 2016; Hayano et al., 2014; Paradis et al., 2007; Rivero et al., 2015). However, it is still unclear whether the protein functions are the same among all cell types and systems, or if it executes different, but cell-type specific molecular functions.

Cadherin-13, an atypical cadherin

Cadherin-13 (CDH13), also known as T-Cadherin or H-Cadherin, is a calcium-dependent cell adhesion molecule belonging to the cadherin superfamily (Philippova et al., 2009). Cadherins were originally identified as cell surface glycoproteins that require calcium to form homophilic interactions between cells (Takeichi, 1988). The main function attributed to cadherins is to generate and maintain stable cell-cell contacts due to their link to the cell's cytoskeleton through the interaction with ß- and α-catenin (Takeichi, 1988). However, more than 100 members of the Cadherin family have been identified (Seong, Yuan, & Arikkath, 2015). Although they all share the characteristic extracellular cadherin repeats (ECs), they have diverse protein structures and have been linked to diverse cell-cell adhesion and cell signaling functionalities (Maitre & Heisenberg, 2013; Saito, Tucker, Kohlhorst, Niessen, & Kowalczyk, 2012).

Cadherins are categorized into three main groups: classical cadherins, protocadherins, and atypical cadherins. Like classic cadherins, such as CDH2 (also known as N-cadherin), CDH13 possess the distinct five ECs in the extracellular domain (Patel et al., 2006). However, CDH13 is atypical; (1) it lacks the cytoplasmic and transmembrane domains, and instead is attached to the cell membrane through a glycophosphatidylinositol (GPI)-anchor (Ranscht and Dours-Zimmermann, 1991), and (2) it lacks the conserved tryptophan residues also typical of classical cadherins (Figure 1.2-2) (Ciatto et al., 2010).

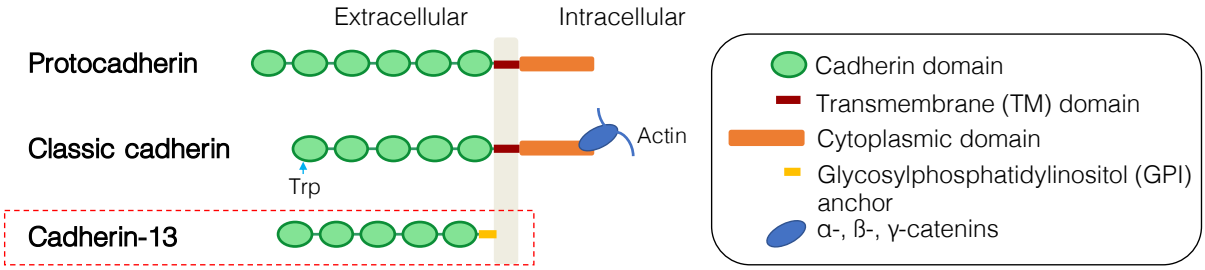

Figure 1.2-2. Structural comparison of protocadherin, classical cadherin and Cadherin-13. CDH13, similarly to protocadherins and classical cadherins, possesses the typical extracellular cadherin domains. However, it is lacking the transmembrane and cytoplasmic domains and instead is attached to the cell membrane through a GPI-anchor and is also lacking the conserved tryptophan (Trp) residues in EC1.

The absence of the conserved tryptophan residues present in classical cadherins, limits the capacity of CDH13 to form dimers in which the N-terminal ß-strands of the EC1 domains 'swap' between partner molecules. Instead, the protein is able to form X dimers through an alternative non-swapped interface near the EC1-EC2 calcium-binding sites (Ciatto et al., 2010; Harrison et al., 2010) (Figure 1.2-3). Nevertheless, this lack of tryptophan side chains, and of the cytoplasmic and transmembrane domains, does not interfere with its ability to promote cell-cell

adhesion, but instead only hinders the strength of the adhesion (Harrison et al., 2010; Vestal & Ranscht, 1992).

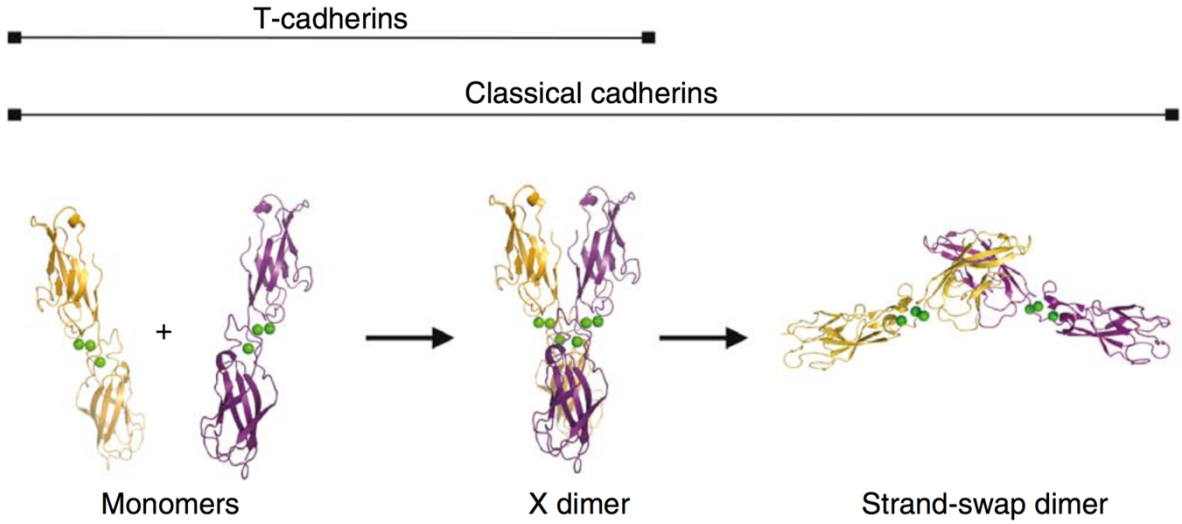

Figure 1.2-3. Two-step model of classical cadherin binding. Classical cadherins are capable of generating a strand-swap dimer, while CDH13 can only form the initial X dimer due to its lack of tryptophan residues in the EC1. Reprinted with permission from "Two-step adhesive binding by classical cadherins" by Harrison et al. (2010), *Nat Struct Mol Biol, 17*(3), 348-357. Copyright Springer Nature (License number 4766391365180).

Similarly, the truncated nature of CDH13 due to the absence of transmembrane and cytoplasmic domains does not limit its ability to function as a signaling molecule. Extensive studies conducted in vascular endothelial and smooth muscle cells as well as in cancer cells have identified possible signaling pathways through which CDH13 might act to generate effects in proliferation, migration and survival (Figure 1.2-4) (for review: Rivero et al., 2013).

CDH13 induces changes in cell morphology through homophilic interactions mediated by small Rho GTPases by acting through two complementary components: (1) the RhoA/ROCK pathway, which generates actin stress fibers leading to cell contraction, and (2) Rac-dependent pathway, which modulates the formation of lamellipodia in migrating cells (Philippova et al., 2005). More recent work showed that CDH13 affects smooth muscle cell survival and dedifferentiation through MEK1/2/Erk1/2 axis activation and GSK3ß inactivation, respectively (Frismantiene et al., 2016; Kyriakakis et al., 2017). CDH13 has also been shown to play a role in the activation of the Akt and mTOR pathways, both of which are of importance in processes including cell survival, neurite outgrowth and synapse formation (Joshi, Ivanov, Philippova, Erne, & Resink, 2007; Joshi et al., 2005; Read & Gorman, 2009). Studies conducted in endothelial cells identified integrin-linked kinase as an interacting partner of CDH13 (Joshi et al., 2007) as well as integrin $ß_3$ and GABA-A receptor α1 subunit (Philippova et al., 2008). Work carried out in our laboratory has led us to suspect that CDH13 may interact with the brain-

derived neurotrophic factor (BDNF) receptor, tropomyosin-receptor kinase B (TrkB), and possibly with lipid raft proteins that have been associated with CDH13 (for review: Rivero et al., 2013).

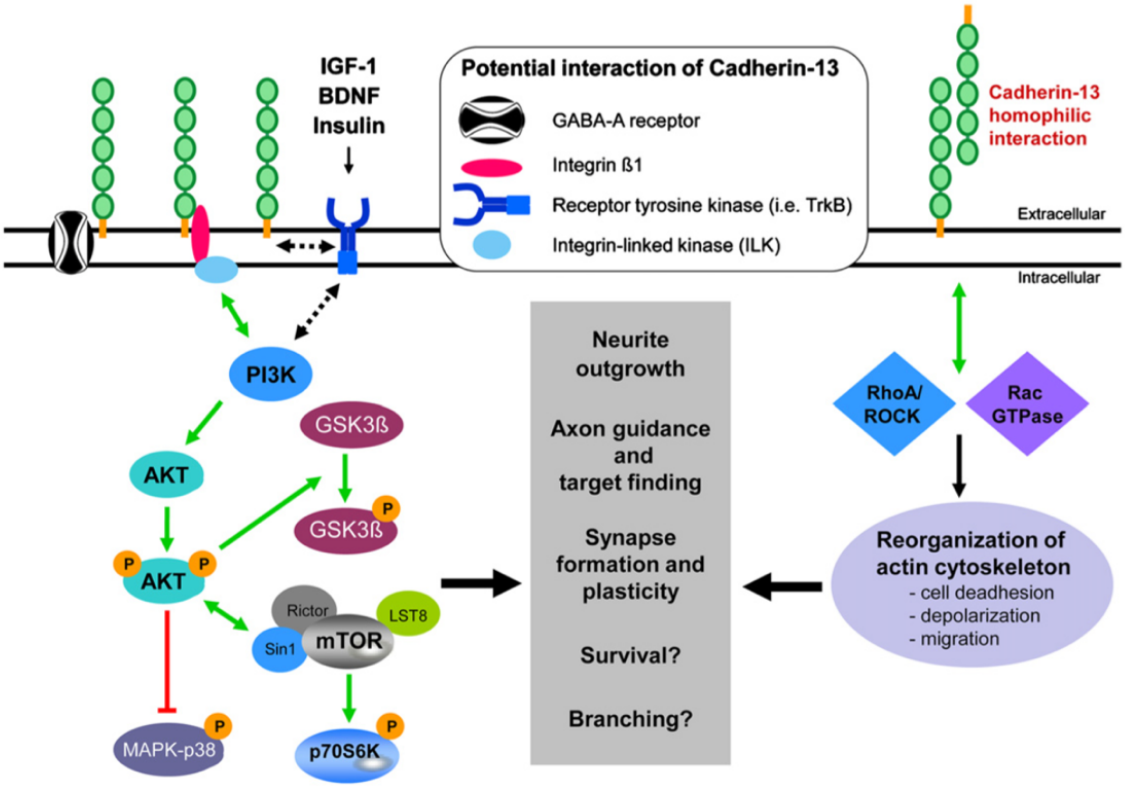

Figure 1.2-4. Intracellular signaling pathways of Cadherin-13 and its putative involvement in neuronal function. *In vitro* studies in vascular cells have revealed the role of CDH13 as a signaling molecule via the regulation of the AKT pathway and small GTPases. Reprinted with permission from "Impact of the ADHD-susceptibility gene CDH13 on development and function of brain networks" by Rivero et al. (2013), *Eur Neuropsychopharmacol,* 23(6), 492-507. Copyright Elsevier (License number 4774170222878).

Cadherins are known to form homophilic and heterophilic interactions with other members of the cadherin superfamily (Brasch et al., 2018; Prakasam, Maruthamuthu, & Leckband, 2006). Even though the interaction between CDH13 and other cadherins has not been reported yet, it is very likely that it occurs, since it shares a common structure with classical cadherins. For instance, the sequence identity of the five cadherin extracellular domains EC1-EC5 of mouse CDH13 is 47% identical to that of N-cadherin (Ranscht & Dours-Zimmermann, 1991). CDH13 and N-cadherin proteins are co-expressed on the surface of individual neurons *in vitro* (Sacristan, Vestal, Dours-Zimmermann, & Ranscht, 1993), and while N-cadherin promotes neurite outgrowth, CDH13 inhibits this process (Fredette & Ranscht, 1994). Therefore, we predict that CDH13 serves as an antagonist for other cadherins, such as N-cadherin, and blocks their downstream activation of cytoskeleton dynamics which promote neuronal processes including migration and axonal pathfinding.

Cadherin-13 as a negative regulator in neurodevelopment

One of the main functions of CDH13 is that it serves as a negative regulator of migration and axonal outgrowth/pathfinding (Ciatto et al., 2010; Fredette et al., 1996; Fredette & Ranscht, 1994; Hayano et al., 2014; Ranscht & Dours-Zimmermann, 1991). In the avian embryo, it was shown that CDH13 expression alternated in neural crest cells during their migration, which suggests that it works as a signaling molecule to delimit their migration path or to maintain the polarity of the migrating somite (Ranscht & Bronner-Fraser, 1991). A posterior study also conducted in chick embryos observed that CDH13 was expressed uniformly in motor neurons as they projected between the spinal cord and the base of the hindlimb. However, CDH13 expression decreased as the axons formed the muscle nerve trunks. Additionally, ectopic expression of CDH13 modified the trajectory in which the motor axons extended, showing that these avoid regions positive for CDH13 (Fredette & Ranscht, 1994).

Two *in vitro* studies have further contributed to understanding the negative regulation of CDH13 on neurite outgrowth in motor axon projections. The first showed how CDH13 inhibits neurite extension of cultured sympathetic, ciliary or dorsal root ganglia via homophilic interaction when used as a substratum and as a soluble recombinant protein (Fredette et al., 1996). The second study confirmed CDH13-mediated inhibition of neurite outgrowth, and additionally unveiled the mechanism that allows this inhibition (Ciatto et al., 2010). By generating a set of mutants, it was shown that the cell-adhesion mechanism used by CDH13 involves an X dimer configuration (Figure 1.2-3) and is necessary for inhibition of motor neuron extensions (Ciatto et al., 2010).

CDH13 regulation of axonal outgrowth also contributes to circuit formation of neocortical neurons (Hayano et al., 2014). CDH13 expression is present in deep-layer cell axons in the developing mouse cortex that project to subcortical structures, but not in upper layer callosal axons projecting to the contralateral cortex. Alteration of this developmental expression pattern, either through ectopic expression of CDH13 or suppression of CDH13 expression through RNAi, causes an aberrant projection of these axons (Hayano et al., 2014). More recently, it was shown that *Cdh13* KO mice have elevated levels of dopamine in cortical regions as well as a higher dopaminergic innervation of the prefrontal cortex, therefore providing evidence for an inhibitory role of CDH13 in monoaminergic neuron fiber projection (Drgonova et al., 2016).

Cadherin-13 as a mediator in synapse formation and function

The contribution of CDH13 to synapse formation and function has been explored in hippocampal and cerebellar Golgi cells (Paradis et al., 2007; Rivero et al., 2015; Tantra et al., 2018). An initial study which screened 22 cadherin family members using RNAi in mouse hippocampus neurons, demonstrated that CDH13 is required for adequate formation of glutamatergic and GABAergic synapses on pyramidal neurons (Paradis et al., 2007). More recent results confirmed an increase in miniature inhibitory postsynaptic currents (IPSC), in CA1 pyramidal neurons of the hippocampus of *Cdh13*$^{-/-}$ mice, while no alterations in excitatory transmission were observed (Rivero et al., 2015). This is in accordance with an observation in cerebellar Golgi cells of the cerebellum. Here, conditional deletion of *Cdh13* reduces spontaneous inhibitory postsynaptic current (IPSC) without altering the excitatory postsynaptic response (Tantra et al., 2018).

Cadherin-13 deficiency and its effect on murine behavior

The effects of CDH13 deficiency on murine behavior have been studied through the use of constitutive and conditional knockout mouse lines. Animals with a constitutive deletion of *Cdh13* show novelty-induced hyperlocomotion and reduced cognitive flexibility in learning and memory tasks (Rivero et al., 2015). Furthermore, when subjected to early-life stress due to prolonged maternal separation, *Cdh13*$^{-/-}$ mice show less exploration as well as an increase in anxiety-like behavior in the light-dark and open field tests (Kiser et al., 2019). In the same study, *Cdh13*$^{-/-}$ mice present altered cognitive flexibility and a mild decrease in freezing behavior during a fear extinction paradigm (Kiser et al., 2019). The conditional deletion of *Cdh13* in cerebellar Golgi cells was shown to impair reciprocal social interaction (Tantra et al., 2018). All these behavioral alterations are in line with genetic studies showing an association of *CDH13* dysregulation with neurodevelopmental conditions such as ADHD or autism, in which impairment in learning and memory and sociability are described. Furthermore, the association of *CDH13* with substance use disorders has prompted various studies focused on the effects of CDH13 deficiency on addiction-related behavioral phenotypes, specifically, intravenous cocaine self-administration, cocaine conditioned cue/ place preference, cocaine- conditioned taste aversion (Drgonova et al., 2016; King et al., 2017). *Cdh13*$^{-/-}$ mice display evidence for changed cocaine rewards, specifically a shifted dose response in a cocaine-conditioned place preference test (Drgonova et al., 2016). A preference for a place paired with a dose of 5 mg/kg of cocaine is observed in *Cdh13*$^{-/-}$ mice, while *Cdh13*$^{+/+}$ control mice required a dose of 10 mg/kg to generate this preference (Drgonova et al., 2016). *Cdh13*$^{-/-}$ rats were also found to have an increased cue-induced reinstatement of intravenous cocaine self-administration compared to *Cdh13*$^{+/+}$ animals (King et al., 2017).

1.3. Cadherin-13 and the serotonin system

Even though CDH13 is known to regulate processes including cell migration, neurite outgrowth, axon guidance and target finding in many cell types, the relationship between this protein and the development of the serotonin (5-HT) system has not been thoroughly studied. A transcriptome analysis of specific neuronal subpopulations from mouse hindbrain, performed by combining intersectional fate mapping, cell sorting, and genome-wide RNA-sequencing, identified several cell adhesion molecules in rostral raphe nuclei, with the expression of CDH13 being specifically restricted to 5-HT neurons of the dorsal raphe (DR) (Okaty et al., 2015). Additionally, *Cdh13* mRNA is present in DR 5-HT neurons of the adult mouse brain (Rivero et al., 2013) (Figure 1.3-1).

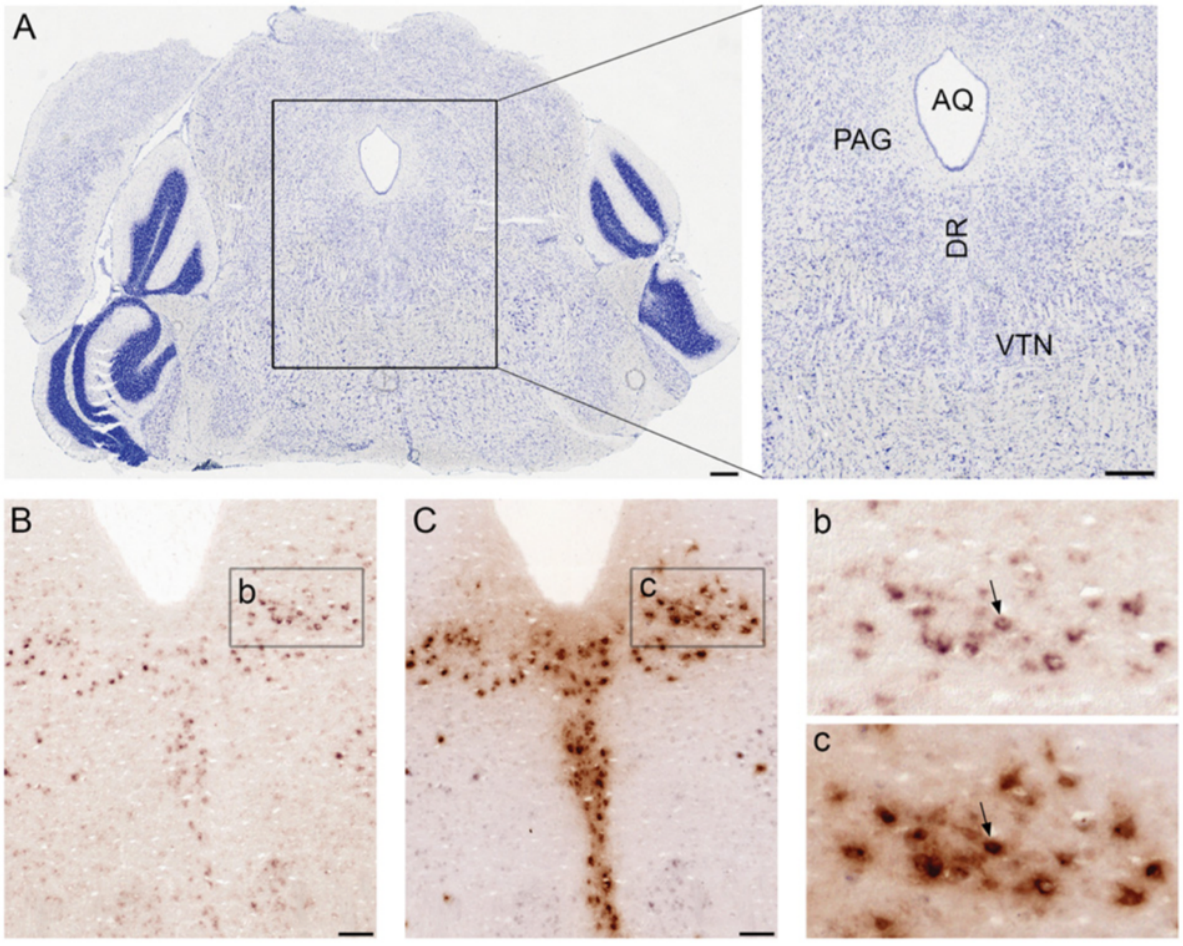

Figure 1.3-1. Colocalization of Cdh13 expression and tryptophan hydroxylase-2 (Tph2) in 5-HT neurons. (B) Expression of *Cdh13* mRNA in the brain stem of adult mice was investigated using in situ hybridization (ISH). (C) Subsequently the same sections were stained using anti-Tph2 antibody to confirm the presence of Cdh13 in 5-HT neurons. Colocalization of Cdh13 mRNA and Tph2 in raphe nuclei is demonstrated especially in the DR. (A) Nissl-stained section of the brain stem. Representative images (b, c) of a cluster of 5-HT neurons and colocalization is indicated by an arrow. AQ, cerebral aqueduct; VTN, ventral tegmental nucleus. Scale bars: A=300 mm; B, C=100 mm. Reprinted with permission from "Impact of the ADHD-susceptibility gene CDH13 on development and function of brain networks" by Rivero et al. (2013), *Eur Neuropsychopharmacol,* 23(6), 492-507. Copyright Elsevier (License number 4774170222878).

Neurodevelopmental function of serotonin

5-HT is an important regulator in early developmental processes such as cell proliferation, migration, and differentiation. Due to its vast innervation of brain regions including the prefrontal cortex, the hippocampus, the amygdala, among many others, it has been linked to brain functions ranging from first order activities such as motricity and sensory processing to more complex operations including emotional regulation and cognitive control (for review: Lesch & Waider, 2012). For instance, the 5-HT receptors 5-HT1A, 5-HT1B and 5-HT2 were shown to contribute to cell proliferation in the various subgroups of the hippocampus (Banasr, Hery, Printemps, & Daszuta, 2004), while in the prefrontal cortex, the 5-HT2A receptor was shown to modulate 5-HT-induced neuronal activity during early postnatal stages of neurodevelopment (Zhang, 2003). Both increased and decreased 5-HT neurotransmission compromises cortical development at different periods of embryonic and postnatal development (Garcia-Gonzalez et al., 2017; Gaspar, Cases, & Maroteaux, 2003; Riccio et al., 2009; Teissier, Soiza-Reilly, & Gaspar, 2017; Vitalis, Cases, Passemard, Callebert, & Parnavelas, 2007).

5-HT is also critical for the development and functioning of other neurotransmission systems in the brain (Garcia-Gonzalez et al., 2017; Whitaker-Azmitia, 2001). Initial studies showed that 5-HT projections densely innervate the dopaminergic nuclei in the substantia nigra and ventral tegmental area in rodent animal models (Dray, Davies, Oakley, Tongroach, & Vellucci, 1978; Herve, Pickel, Joh, & Beaudet, 1987), and was later proven to be consistent in human brains (Wallman, Gagnon, & Parent, 2011). 5-HT modulation of glutamatergic and GABAergic synaptic release has also been extensively studied, indicating its role in regulating synaptic transmission (Ciranna, 2006; Lesch & Waider, 2012).

The development of socio-emotional brain circuits is also modulated by 5-HT. Dysfunction of 5-HT transmission has been implicated in neurodevelopmental disorders and subsequent psychiatric conditions in which social cognitive functions are compromised (Lesch & Waider, 2012). This is particularly interesting when studying neurodevelopmental disorders such as ASD and ADHD.

Development of the serotonin system

The development of the 5-HT system commences early in prenatal stages, with 5-HT initially being supplemented from a placental source (Bonnin et al., 2011; Wallace & Lauder, 1983). It begins with the migration of 5-HT specific neurons for the arrangement of nine anatomically distinct groups of cells known as the raphe nuclei. These nuclei are subdivided into two main clusters: a caudal cluster in the medulla (B1–B5), and a rostral cluster in the pons (B6–B9).

The identity of the 5-HT neuron population comprising the rostral cluster is determined by a transcription code that shows some variation along dorsoventral and anteroposterior axes (Gaspar et al., 2003; Kiyasova & Gaspar, 2011; Ye, Shimamura, Rubenstein, Hynes, & Rosenthal, 1998). The dorsoventral orientation is dependent on a molecule produced by the notochord and floorplate known as Sonic hedgehog (Shh). Alterations in Shh signaling pathway dorsalize 5-HT precursors and cause 5-HT neurons to be misplaced to the cerebellum (Hynes et al., 2000). Meanwhile, the midbrain-hindbrain boundary (MHB), an organizing center between the midbrain and hindbrain that expresses fibroblast growth factor 8 (Fgf8), serves as a rostral limit (Wurst & Bally-Cuif, 2001). A shift in the MHB leads to a corresponding rostral or caudal displacement of 5-HT neurons (Brodski et al., 2003), while the lack of functional Fgf8 in zebrafish embryos reduces the number of 5-HT neurons in the hindbrain (Teraoka et al., 2004). Following these genetic landmarks, 5-HT neurons migrate radially through somal translocation, that is, without the aid of radial glial cells, at very early stages of neurodevelopment (Hawthorne, Wylie, Landmesser, Deneris, & Silver, 2010). Additional tangential migrations also occur during this developmental process (Alonso et al., 2013; Hawthorne et al., 2010).

The innervation from these nuclei to their corresponding target regions is a process that also begins early in prenatal stages of development. Only one day after 5-HT neurons of the rostral cluster are born at embryonic day (E)10- E11, they start projecting towards forebrain regions (Lidov & Molliver, 1982; Wallace & Lauder, 1983). These axons project through the marginal zone (MZ) and below the cortical plate to the intermediate zone (IZ) and reach the developing cortex at around E16 (Wallace & Lauder, 1983). Then, perpendicular axons begin to extend to innervate brain regions along the cortical plate (Vitalis, Ansorge, & Dayer, 2013). Alterations in molecules implicated in anterior-posterior orientation, midline guidance, as well as axon elongation and maintenance have been shown to affect the guidance of serotonergic axons (Kiyasova & Gaspar, 2011).

The use of conditional anterograde and retrograde tracing has allowed a detailed analysis showing that the rostral 5-HT cell groups (B5-B9) distinctly project to a broad number of regions in the forebrain and brainstem (Muzerelle, Scotto-Lomassese, Bernard, Soiza-Reilly, & Gaspar, 2016; Ren et al., 2018; Sargin, Jeoung, Goodfellow, & Lambe, 2019; Waselus, Valentino, & Van Bockstaele, 2011). For instance, while the dorsal (B7l) subcomponent of the DR targets primarily areas such as the lateral thalamus and prepositus nucleus, the ventral (B7v) portion of this nucleus innervates the amygdala and cortical regions such as the prefrontal cortex (Muzerelle et al., 2016). Functional differences are also observed in these DR sub-systems; frontal cortex- projecting 5-HT neurons are shown to promote active coping behavior, while amygdala-projecting 5-HT neurons promote anxiety behaviors in mice (Ren et al., 2018).

1.4. Aim of the thesis

The overall aim of this thesis was to study the relationship between CDH13 and the development of the brain 5-HT system. Two initial projects were carried out using a constitutive *Cdh13* knockout mouse line (Project 1) and a 5-HT neuron-specific *Cdh13* knockout mouse line (*Cdh13* cKO; Project 2). With the use of mouse models, we aimed to identify alterations in 5-HT nuclei formation and innervation associated to CDH13 deficiency. Behavior was also analyzed in the newly developed *Cdh13* cKO mouse line. Additional to the experiments conducted with mice, a third project was conducted that aimed to study CDH13 expression in TPH2-positive neurons derived from human induced pluripotent stem cells (iPSCs). A more detailed description of the specific objectives of each of the projects is given in the results section.

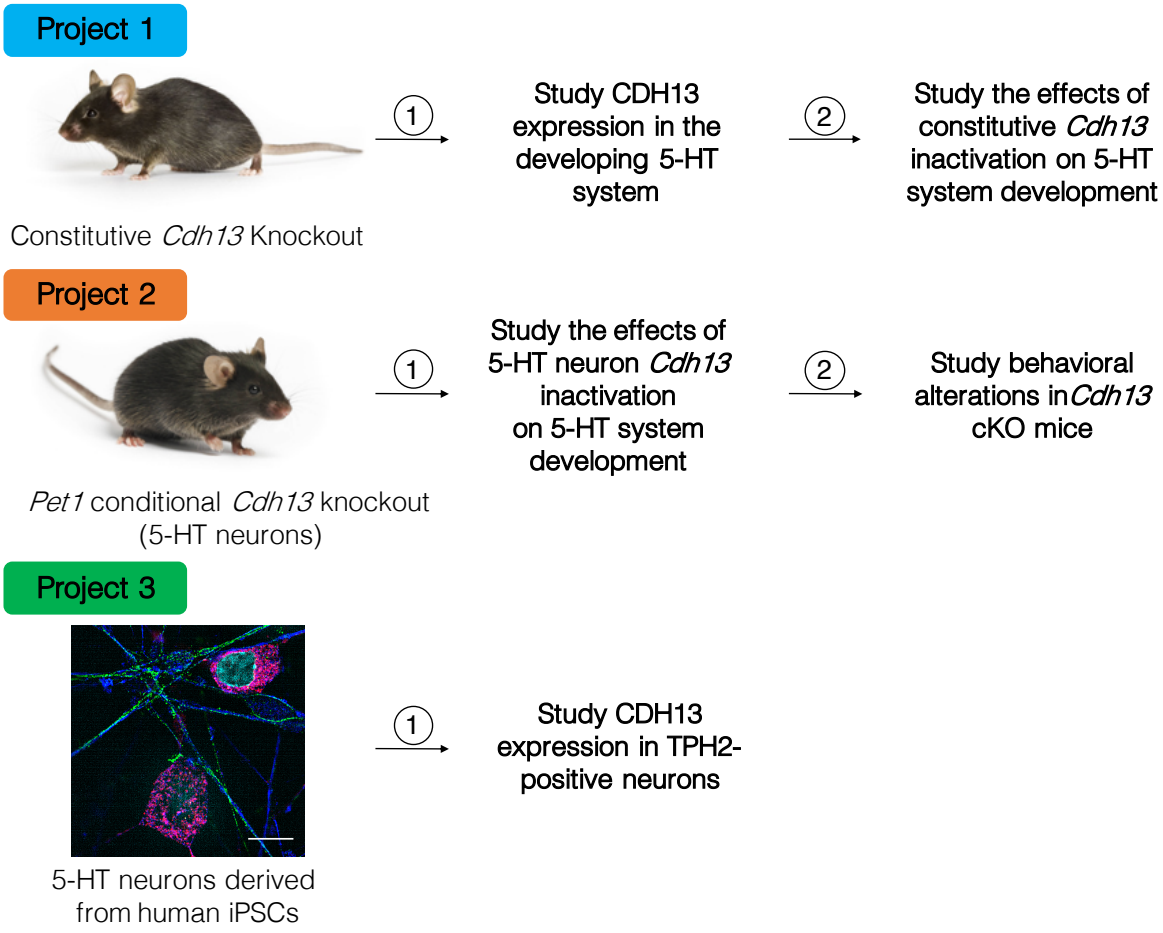

Figure 1.4-1. Aim of the thesis. The thesis was composed of three projects, all of which aimed to study the relationship between CDH13 and the development of the brain 5-HT system. The first two projects were conducted with a constitutive *Cdh13* knockout mouse line (Project 1) and a *Pet1* conditional *Cdh13* knockout mouse line (Project 2), while Project 3 was conducted with neurons derived from human iPSCs.

2 | Materials and methods

2.1. Animals and ethics

All the experimental procedures carried out with live mice were previously approved by the boards of the University of Würzburg and the Government of Lower Franconia (55.2-2531.01-92/13) and performed in accordance with the guidelines for animal care and use provided by the European Community. Mice were housed in groups of 3–5 per cage at the facilities of the Center of Experimental Molecular Medicine, under a 12 h light/dark cycle with food and water *ad libitum*. Mice were kept on a C57Bl/6N background. For the generation of mouse embryos, timed breedings were conducted overnight; midday controls of plug positive animals and weight controls 12 days after breeding were considered to determine pregnancy.

Constitutive Cdh13 knockout mouse line. The constitutive *Cdh13* knockout mouse line (*Cdh13*$^{-/-}$) was previously generated at the Division of Molecular Psychiatry, Center of Mental Health, University of Würzburg (Rivero et al., 2015). A scheme of its generation is presented in Figure 2.1-1. The validation of this mouse line was confirmed by *in situ* hybridization and Western blot (Rivero et al., 2015). For this project, littermates were used for both the embryonic and adult mouse experiments. *Cdh13*$^{-/-}$ and *Cdh13*$^{+/+}$ embryos were obtained by crossing heterozygous animals (*Cdh13*$^{+/-}$).

Conditional Cdh13 knockout mouse line. The 5-HT neuron-specific *Cdh13* knockout (*Cdh13*$^{loxP/loxP}$::*Pet1-Cre*$^{+/-}$; in the following referred to as *Cdh13* cKO) was generated by subsequently crossing *Cdh13*$^{loxP/loxP}$ mice (Rivero et al., 2015) with *Pet1-Cre* mice generated by Song et al. (2011). *Pet1-Cre* deleter mice express Cre recombinase under the control of the *Pet1* promoter (Dai et al., 2008). A scheme of its generation is presented in Figure 2.1-2. Once established, the mouse line was maintained by breeding *Cdh13*$^{loxP/loxP}$ animals that were negative for Cre (in the following referred to as Ctrl) with *Cdh13* cKO mice. The validation of this mouse line was confirmed by microdissection of the DR followed by quantitative real-time PCR (qRT-PCR) and immunohistochemistry (Forero et al., 2020). Littermates were used for both the embryonic and adult mouse experiments.

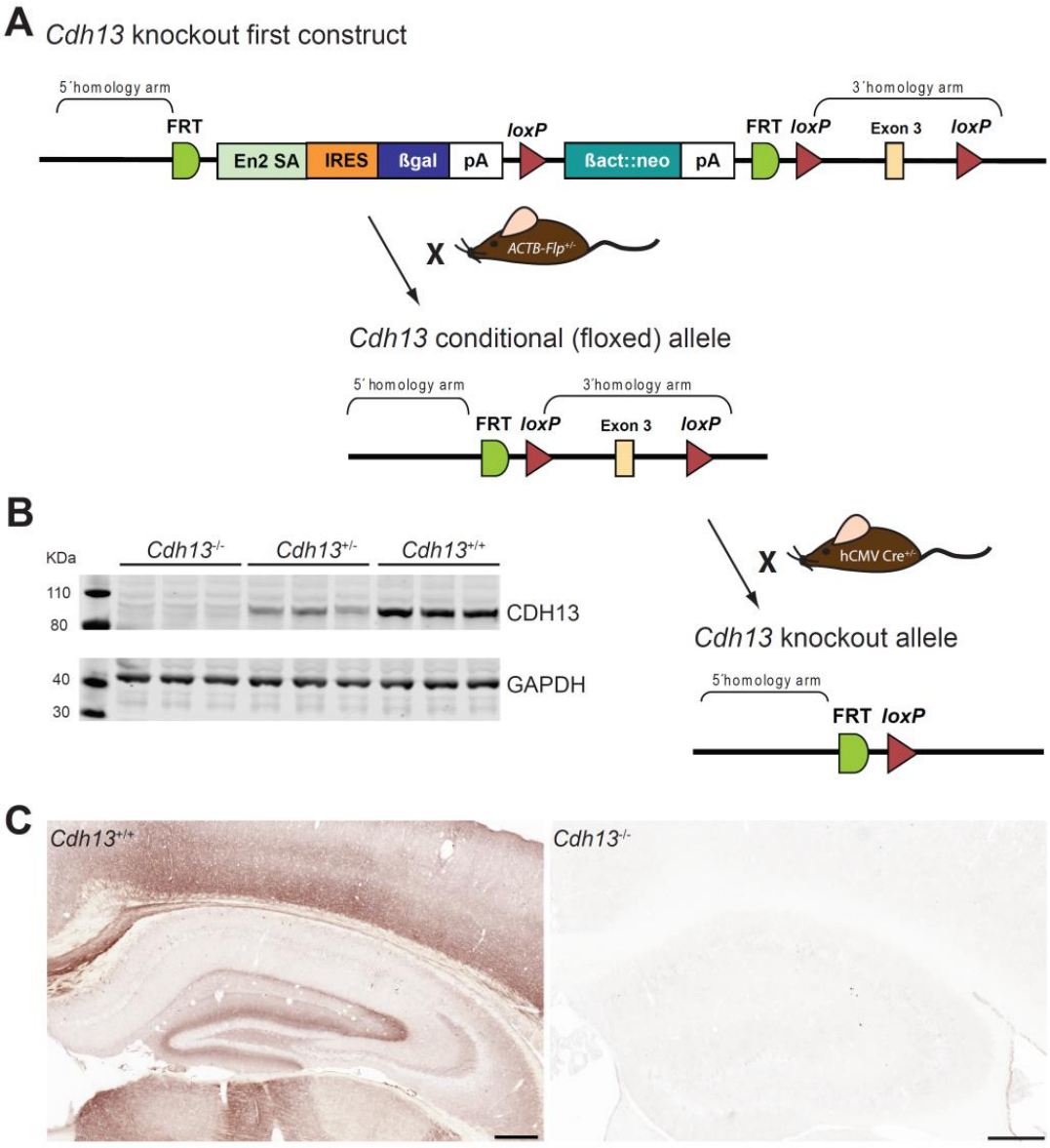

Figure 2.1-1. Generation of constitutive *Cdh13* knockout mouse line. (A) Schematic representation of the *Cdh13* knockout first targeting construct expressed in ES cells that were injected into C57Bl6/N blastocysts. Afterwards, *Cdh13* knockout first mice were bred with Flp-deleter mice in order to remove the FRT-flanked cassette (containing both the LacZ reporter gene and the neomycin resistance gene). The resulting *Cdh13* conditional (floxed) mice were intercrossed with constitutive Cre-deleter mice, which induced the recombination of exon 3 and the generation of a truncated protein in the *Cdh13*$^{-/-}$ mice. (B) Western blot analysis of mouse brain lysates shows, in Cdh13$^{+/+}$ mice, a prominent band of approximately 90 kDa corresponding to the mature CDH13 protein. This band could not be detected in Cdh13$^{-/-}$ mice, whereas reduced levels were observed in heterozygote (Cdh13$^{+/-}$) mice, suggesting a gene dose effect. GAPDH antibody was used to confirm the equal loading in all lanes. (C) Absence of CDH13 protein in the brains of Cdh13$^{-/-}$ mice was also confirmed by immunohistochemistry. No stained cells or fibers were found in any region of the brain (i.e. cortex or hippocampus). Scale bars 300µm. Abbreviations: FRT, Flippase Recognition Target; En2 SA, splice acceptor of mouse En2 exon; IRES, Internal Ribosome Entry Site; ßgal, ß- galactosidase; pA, polyadenylation sequence; loxP, locus of X-over P1; ßact: ß-actin; Neo, Neomicin resistance gene; ACTB, ß-actin gene; Flp, Flippase; hCMV, human cytomegalovirus; +, wildtype; -, knockout; GAPDH, Glyceraldehyde 3-phosphate dehydrogenase. Taken from Rivero et al. (2015).

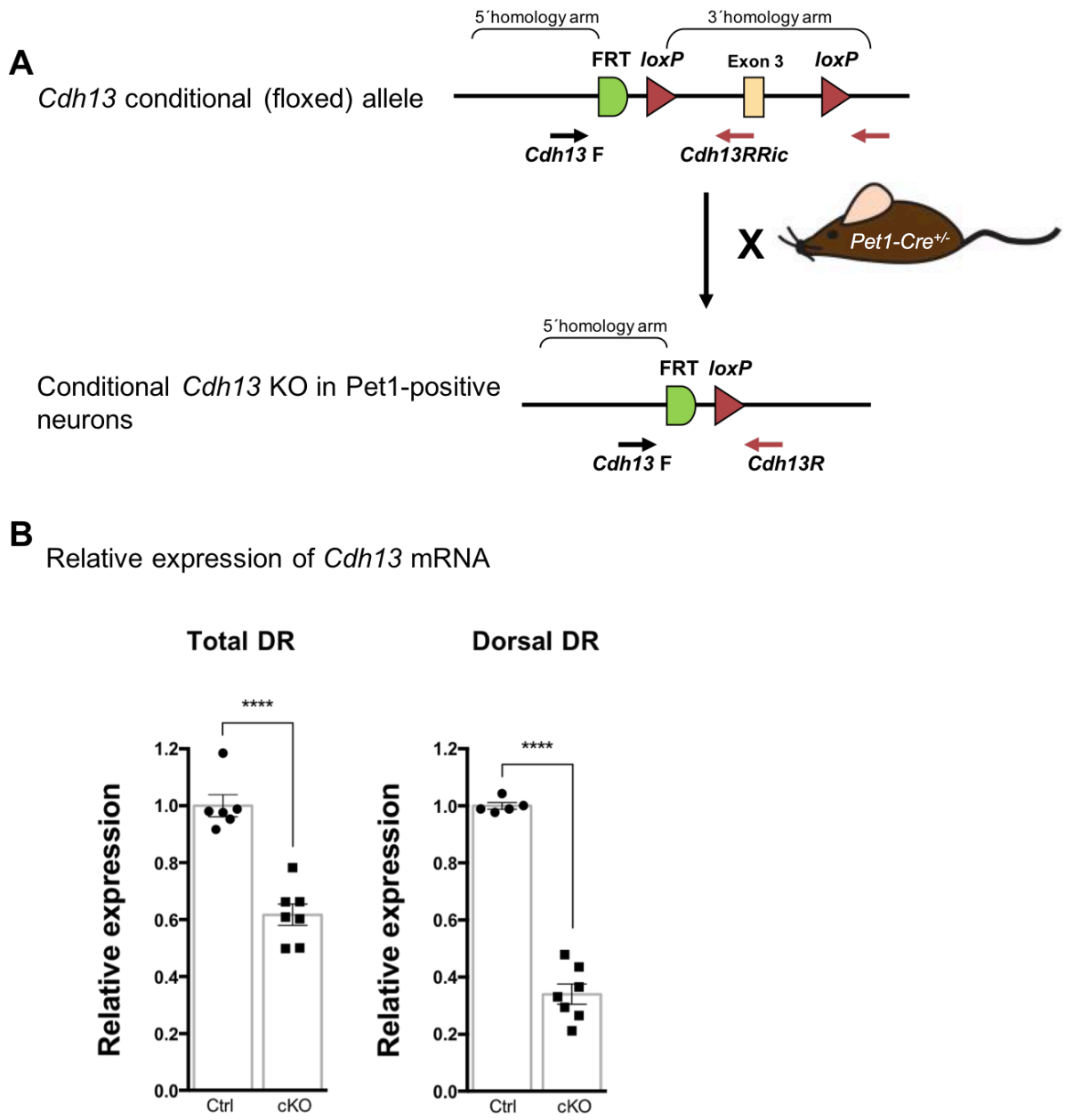

Figure 2.1-2. Generation of 5-HT neuron-specific *Cdh13* knockout mouse line. (A) Schematic representation of the crossbreeding of *Cdh13* floxed mice previously described (Rivero et al., 2015) with *Pet1-Cre* mice generated by Song et al. 2011. The breeding induces the recombination of *Cdh13* exon 3 in *Pet1*- positive neurons, which leads to the generation of a truncated CDH13 protein. (B) qRT-PCR analysis revealed a significant reduction of *Cdh13* mRNA in the DR of *Cdh13* cKO when compared to Ctrl mice ($p<0.0001$). Specifically, in the dorsal DR subgroup, where the anatomical locality allowed microdissection with the highest precision, the *Cdh13* mRNA level decreased approximately 66%. We assumed that the reduction was likely close to the latter estimation when we overcome the influence of the limited visualization methodology. ****P*<0.001. (A) Adapted from Rivero et al. (2015) (B) Taken from Forero et al. (2020).

2.2. Cell lines

One human induced pluripotent stem cell (iPSC) line was used in this project, referred to as CJ1. It was provided by doctoral student C. Jansch (Division of Molecular Psychiatry, Center of Mental Health, University of Würzburg), and the method by which it was generated is described in the lab resource publication Jansch et al. (2018). The process by which this cell line was differentiated into TPH2-positive neurons was also conducted by C. Jansch and is described in Jansch et al. (submitted).

In general terms, fibroblasts isolated from a skin biopsy of a control individual were reprogrammed into iPSCs with Sendai virus, a single stranded non-integrating RNA virus. The iPSCs were then differentiated into TPH2-expressing neurons by first generating free-floating embryoid bodies, which were converted to rostral hindbrain progenitors by exposure to neural progenitor cell medium containing Sonic hedgehog (Shh), followed by platting and addition of Fgf4 to specify the serotonergic fate (Jansch et al., submitted).

2.3. Embryo extraction and preparation

Table 1. Materials, solutions and equipment used for embryo extraction and tissue preparation.

Material	**Company**
Isoflurane	Cp-pharma, Burgdorf
Phosphate buffered saline (PBS) 1x	Lonza, Basel, Switzerland
Phosphate buffered saline (PBS) 10x	Lonza, Basel, Switzerland
Paraformaldehyde (PFA)	Carl Roth, Karlsruhe
D(+)-Sucrose	AppliChem, Darmstadt
Isopentane (2-methylbutane)	AppliChem, Darmstadt
Tissue-Tek O.C.T.	Sakura, Nagano, Japan
Solution	**Composition**
4% paraformaldehyde	Paraformaldehyde in 1x PBS, dissolved at 60°C; pH 7.4
10% Sucrose	D(+)-Sucrose dissolved in 1x PBS at RT

20% Sucrose	D(+)-Sucrose dissolved in 1x PBS at RT
Equipment	**Company**
Dissection tools	Fine Science Tools, Vancouver, Canada
Leica CM 1950 cryostat	Leica, Wetzlar
Histobond®+ adhesive microscope slides	Paul Marienfeld, Lauda-Königshofen

Timed-pregnant dams were sacrificed by administration of an overdose of isoflurane. Through a Y-shaped incision in the abdomen, embryos were extracted at three different developmental stages: embryonic day (E)13.5, E15.5, and E17.5. The brains from E15.5 and E17.5 embryos were dissected from the skull, while the complete head was processed for E13.5, both carried out in 1x PBS. A small sample of the most caudal part of each embryo was taken for genotyping of the *Cdh13* locus. Fixation was done by immersion in 4% paraformaldehyde (1x PBS; pH 7.4) at 4°C overnight, followed by cryoprotection in 10% and 20% sucrose solutions for 1 day each consecutively. The brains were frozen in isopentane cooled with dry ice and cryosectioned in Tissue-Tek O.C.T. (Sakura, Japan). Coronal/sagittal 20 or 60 µm sections were mounted on Histobond®+ adhesive microscope slides (Paul Marienfeld. Lauda-Königshofen, Germany). The slides with the sections were then stored at -80°C until needed.

2.4. Adult mouse brain perfusion

Table 2. Materials, solutions and equipment used for adult mice perfusion.

Material	**Company**
Isoflurane	Cp-pharma, Burgdorf
Phosphate buffered saline (PBS) 10x	Lonza, Basel, Switzerland
Heparin sodium salt (5 units/µL)	Ratiopharm, Ulm
Paraformaldehyde (PFA)	Carl Roth, Karlsruhe
D(+)-Sucrose	AppliChem, Darmstadt
Isopentane (2-methylbutane)	AppliChem, Darmstadt
Tissue-Tek O.C.T.	Sakura, Nagano, Japan

Solution	Composition
heparinized PBS (20 units/mL)	20 units/mL heparin in 1x PBS at RT
4% paraformaldehyde	Paraformaldehyde in 1xPBS, dissolved at 60°C; pH 7.4
10% Sucrose	D(+)-Sucrose dissolved in 1xPBS at RT
20% Sucrose	D(+)-Sucrose dissolved in 1xPBS at RT
Equipment	**Company**
Dissection tools	Fine Science Tools, Vancouver, Canada
Perfusion micropump	Ismatec ISM827B, Wertheim
Venofix "Luer Lock" 21G 0,8 x 20 mm, long 30 cm	B Braun Medical Inc., Schwalm-Eder-Kreis
Leica CM 1950 cryostat	Leica, Wetzlar
Histobond®+ adhesive microscope slides	Paul Marienfeld, Lauda-Königshofen

Mice aged 3–4 months were sacrificed with isoflurane and subjected to transcardial perfusion. The perfusion consisted of an initial prewash using heparinized PBS (20 units/mL) for 11 min followed by 11 min of ice-cold 4% paraformaldehyde (1x PBS; pH 7.5) at a flow rate of 2.75 mL/min. A small sample of the tip of the tail of each mouse was taken for genotyping of the *Cdh13* locus. Brains were dissected and kept in 4% paraformaldehyde (1xPBS; pH 7.4) for 48 h, and consecutively placed in 10% and 20% sucrose solutions for 1 day each for cryoprotection. The brains were then frozen in isopentane cooled with dry ice and cryosectioned in coronal or sagittal 20 µm sections onto Histobond®+ adhesive microscope slides (Paul Marienfeld. Lauda-Königshofen, Germany). Sections were finally stored at -80°C until used.

2.5. DNA extraction and genotyping

Table 3. Materials, solutions and equipment used for DNA extraction and genotyping.

Material	Company
Tris	Carl Roth, Karlsruhe
EDTA	Carl Roth, Karlsruhe

Isopropanol	AppliChem, Darmstadt
70% Ethanol	AppliChem, Darmstadt
Proteinase K	Sigma-Aldrich, St. Louis, MO, USA
dNTPs	Promega, Fitchburg, WI, USA
Taq Polymerase	Uniklinikum, Würzburg
Ethidium bromide	Sigma-Aldrich, St. Louis, MO, USA
100-bp DNA ladder	Thermo Fisher Scientific, Waltham, MA, USA
Agarose type A	AppliChem, Darmstadt
Solution/ Buffer	**Composition**
Lysis buffer	1,5 M Tris-HCl pH8.5 5 M NaCl 0,5 M EDTA pH 8.0 20% SDS ddH_2O
TE buffer	10 mM Tris-HCl 1 mM EDTA-Na_2 pH 8.0
TAE buffer	40 mM Tris-acetate 1 mM EDTA
Agarose gel	3 % Agarose in 1xTAE
Loading buffer	10 mM Tris-HCl 0.03% Bromophenol Blue 0.03% Xylene Cyanol FF 60% Glycerol 60 mM EDTA
Equipment	**Company**
Centrifuge	Hettich MIKRO 220R, Tuttlingen
Water bath	JB Aqua 12, Grant Instruments, Cambridge, UK
Nanodrop spectrophotometer	Nanodrop ND-1000, Peqlab Biotechnologie GmbH, Erlangen
Thermocycler	Tpersonal Thermocycler Scientific, BioRad, Hercules, CA, USA
Electrophoresis power supply	Consort E844, Turnhout, Belgium
Ultraviolet transilluminator	Universal hood II, BioRad, Hercules, CA, USA

For DNA extraction, the piece of peripheral tissue previously clipped from each embryo/mouse was used. This sample was placed in 500 µl of lysis buffer and 5 µl of proteinase K and kept overnight in a water bath at 55°C to break down the cells in the tissue. The next day, the samples were centrifuged at 14000 rpm at 4°C for 10 min, then the suspension was transferred into a new 1.5 ml microcentrifuge tube with isopropanol for DNA precipitation. The samples were then centrifuged again at 14000 rpm at 4°C for 10 min to pellet the precipitated DNA, and now the isopropanol was replaced with 70% ethanol to wash away residual salt, and centrifuged once more at 14000 rpm at 4°C for 10 min. Finally, the 70% ethanol was discarded, and the samples were dried in a 37°C oven. When the ethanol had completely evaporated, 50 µl of TE buffer were added to reconstitute the DNA and placed on a shaker at 4°C overnight. The following day, the DNA concentration of each sample was measured using a nanodrop spectrophotometer.

Genotyping was carried out through polymerase chain reaction (PCR). 1 µl of DNA from each sample was combined with the appropriate primers (Tables 5 and 6), dNTPs, DNA polymerase, and nuclease-free water, and the solution was run in a thermocycler, under the conditions presented on Table 4.

Table 4. PCR program used for genotyping.

Temperature	Time	Repetitions
95°C	1 min	1 time
95°C	15 sec	
64°C	15 sec	
72°C	1 min	2 times
95°C	15 sec	
61°C	15 sec	
72°C	1 min	2 times
95°C	15 sec	
58°C	15 sec	
72°C	1 min	20 times
95°C	15 sec	
55°C	15 sec	
72°C	1 min	10 times
72°C	10 min	1 time
10°C	Pause	

The PCR products were combined with a loading buffer and then separated by gel electrophoresis at 120 V for approximately 40 min in a 3% agarose gel containing the fluorescent dye ethidium bromide (final concentration 0.5 µg/ml). DNA fragments were visualized using an ultraviolet transilluminator. The band sizes depending on the primers used were as shown in Table 5 for constitutive *Cdh13* KO mice and Table 6 for *Cdh13* cKO mice.

Table 5. List of primers and amplicon sizes used for the genotyping of constitutive *Cdh13* KO mice.

PCR 1 (to detect the *Cdh13* wildtype allele)	
Cdh13-F	5' – TGGTTCTGCTCCAAGACTCAG – 3'
Cdh13-RRic	5' – ATTAGGGACTATCCTGGGCTA – 3'
Internal control (IL-2)-F	5' – CTA GGC CAC AGA ATT GAA AGA TCT – 3'
Internal control (IL-2)-R	5' – GTA GGT GGA AAT TCT AGC ATC ATC C – 3'
Wildtype *Cdh13* allele	233 bp
Internal control (IL-2)	324 bp
PCR 2 (to detect the *Cdh13* KO allele, and in some cases the wildtype allele[1])	
Cdh13-F	5' – TGGTTCTGCTCCAAGACTCAG – 3'
Cdh13-R	5' – CCAGGAAGAGATAAAGCCAGG – 3'
Internal control (IL-2)-F	5' – CTA GGC CAC AGA ATT GAA AGA TCT – 3'
Internal control (IL-2)-R	5' – GTA GGT GGA AAT TCT AGC ATC ATC C – 3'
Cdh13 ko allele	478 bp
Wildtype Cdh13 allele	1190 bp
Internal control (IL-2)	324 bp

Table 6. List of primers and amplicon sizes used for the genotyping of *Cdh13* cKO mice.

PCR 1 (to detect the *Cdh13* floxed allele)	
Cdh13 fl-F	5' – TGGTTCTGCTCCAAGACTCAG – 3'
Cdh13 fl-R	5' – ATTAGGGACTATCCTGGGCTA – 3'
Cdh13 floxed	437 bp
Cdh13 wildtype	233 bp

[1] Given its large size, the wildtype allele is sometimes not properly amplified and therefore PCR1 is needed to confirm its presence or absence.

PCR 2 (to detect the presence of *Cre* transgene)	
Cre-F	5’ – GCGGTCTGGCAGTAAAAACTATC – 3’
Cre-R	5’ – GTGAAACAGCATTGCTGTCACTT – 3’
Internal control (IL-2)-F	5’ – CTA GGC CAC AGA ATT GAA AGA TCT – 3’
Internal control (IL-2)-R	5’ – GTA GGT GGA AAT TCT AGC ATC ATC C – 3’
Pet-1 Cre	100 bp
Internal control	324 bp

2.6. Indirect immunofluorescence

2.6.1. Mouse tissue

Table 7. Materials and solutions used for indirect immunofluorescence in mouse tissue.

Material	**Company**
Tris	Carl Roth, Karlsruhe
Sodium Chloride	Sigma-Aldrich, St. Louis, MO, USA
Citric acid monohydrate	AppliChem, Darmstadt
Normal horse serum (NHS)	Vector Laboratories, Burlingame, CA, USA
Triton-X 100	Sigma-Aldrich, St. Louis, MO, USA
4′,6-Diamidin-2-phenylindol (DAPI)	Sigma-Aldrich, St. Louis, MO, USA
Fluorogel	Electron Microscopy Sciences, Hatfield, PA, USA
Solution/ Buffer	**Composition**
Tris-buffered solution (TBS)	50 mM Tris 150 mM NaCl in ddH2O; pH 7.5
Citrate buffer	10 mM citric acid monohydrate in ddH_2O; pH 6

Blocking solution	10% Normal Horse Serum (NHS) 0,2% Triton X-100 in 1x TBS

Indirect immunofluorescence was used to study the expression pattern of CDH13 in the developing 5-HT system. Brain sections were allowed to air dry for 45-60 min at room temperature (RT) and then washed in TBS and treated with citrate buffer (10 mM, pH 6) at 80°C in a water bath for antigen retrieval. Sections were blocked with 10% NHS and 0.2% Triton X-100 in TBS for 1 h, and incubated overnight at 4°C in a wet chamber with primary antibodies: polyclonal goat anti-CDH13 (1:200, R&D Systems, Minneapolis, USA, cat# AF3264), polyclonal rabbit anti-5-HT (1:500, Acris, Herford, Germany, cat# 20080), monoclonal mouse anti-RC2 IgM (1:80, Developmental Studies Hybridoma Bank, Iowa, USA, cat# AB531887), monoclonal mouse anti-nestin (1:200, Santa Cruz Biotechnology, Dallas, TX, USA, cat# SC-33677), rabbit anti-serotonin (5-HT) transporter (1:500, Merck Millipore, cat# PC177L), polyclonal rabbit anti-tryptophan hydroxylase 2 (TPH2) (1:1,000, generated and validated as reported in Gutknecht et al., 2018; Gutknecht et al., 2019) and/or polyclonal rabbit anti-OTX2 (1:500, Merck Millipore, cat# AB9566). The next day, sections were washed with TBS and incubated at room temperature with the corresponding secondary antibody: donkey anti-Goat IgG (H+L) Alexa Fluor 555, donkey anti-Mouse IgG (H+L) Alexa Fluor 488, donkey anti-Mouse IgM (H+L) Alexa Fluor 488, donkey anti-Rabbit IgG (H+L) Alexa Fluor 488, and/or donkey anti-Rabbit IgG (H+L) Alexa Fluor 647. Finally, 4′,6-Diamidin-2-phenylindol (DAPI, Sigma-Aldrich; 300nM) was applied as a nuclear counterstain to the sections, which were then embedded with Fluorogel as mounting medium.

2.6.2. Human iPSC-derived neurons

Table 8. Materials and solutions used for indirect immunofluorescence in human iPSC-derived neurons.

Chemical	**Company**
Phosphate buffered saline (PBS)	Lonza, Basel, Switzerland
Roti®-Histofix (PFA 4 %)	Carl Roth, Karlsruhe
Fetal Bovine Serum, qualified, heat inactivated	Thermo Fisher Scientific, Waltham, MA, USA
Triton-X 100	Sigma-Aldrich, St. Louis, MO, USA
4′,6-Diamidin-2-phenylindol (DAPI)	Sigma-Aldrich, St. Louis, MO, USA
D-(+)-Glucose solution	Sigma-Aldrich, St. Louis, MO, USA
ß-mercaptoethylamine	Sigma-Aldrich, St. Louis, MO, USA

Solution/ Buffer	Composition
Blocking solution	5%FBS 0.2% Triton X-100 in 1x PBS; pH of 8.0
Photoswitching buffer	1% glucose 100 mM ß-mercaptoethylamine in 1x PBS; pH of 8.0

Structured Illumination Microscopy (SIM). A live cell imaging protocol was followed for the staining of CDH13. The cells were washed with PBS to remove culture medium residues and then blocking solution (5%FBS, 0.2% Triton X-100 in PBS) was applied for 45 min while the cells were kept on ice. The cells were then incubated with the primary antibody polyclonal goat anti-CDH13 (1:200, R&D Systems, Minneapolis, USA, cat# AF3264) diluted in blocking solution for 60 min on ice. Following 3 washes of 5 min each with PBS, the cells were fixed using 4% PFA for 15 min at RT and washed again 3 times 5 min each to remove any excess PFA. Then blocking solution was applied for 45 min, and incubation overnight at 4°C was conducted with the additional primary antibodies: polyclonal rabbit anti TPH2 (1:1000, Novus Biologicals, cat# NB100-74555, Weisbaden Nordenstadt, Germany), monoclonal mouse anti-ßIII Tubulin (1:1000, Promega, cat# G7121, Mannheim, Germany). The next day, cells were washed and incubated with the corresponding secondary antibodies for 1 h at RT together with DAPI (4',6-diamidino-2-phenylindole, Sigma-Aldrich; 300nM): donkey anti-Goat IgG (H+L) Alexa Fluor 647, donkey anti-Rabbit IgG (H+L) Alexa Fluor 555, donkey anti-Mouse IgG (H+L) Alexa Fluor 488.

Direct Stochastic Optical Reconstruction Microscopy (dSTORM). Cells were washed with PBS to remove culture medium residues, followed by fixation using 4% PFA for 15 min at RT. Blocking solution was applied (5%FBS, 0.2% Triton X-100 in PBS) for 45 min at RT. Primary antibodies were applied and incubated overnight at 4°C: polyclonal rabbit anti TPH2 (1:1000, Novus Biologicals, cat# NB100-74555, Weisbaden Nordenstadt, Germany), polyclonal Guinea pig anti-Bassoon (1:200, Synaptic Systems, cat# 141-004, Göttingen, Germany), monoclonal mouse anti-Homer (1:200, Synaptic Systems, cat# 160-011, Göttingen, Germany). The next day, cells were washed and incubated with the corresponding secondary antibodies (1 h, RT) together with DAPI (4',6-diamidino-2-phenylindole, Sigma-Aldrich; 300nM): donkey anti-Rabbit IgM (H+L) Alexa Fluor 488, donkey anti-Guinea pig IgG (H+L) Alexa Fluor 647, and/or goat anti-Mouse IgG (H+L) Alexa Fluor 532.

2.7. Imaging

The following microscopy techniques were used: (1) epifluorescence microscopy, (2) confocal microscopy, (3) structured illumination microscopy (SIM), (4) *direct* stochastic optical reconstruction microscopy (*d*STORM).

Epifluorescence microscopy. Images were generated using an Olympus motorized inverted system microscope IX81, equipped with a X-Cite fluorescence illuminator, and an XM10 camera. Pictures were taken at 10× and/or 20× (air), through the exposure channels for Alexa Fluor 488, Cy3/Alexa Fluor 555, and DAPI. Images were then processed using software CellSense (Olympus, Leinfelden-Echterdingen, Germany), and corrected for contrast using ImageJ v2.0.0 (Schneider, Rasband, & Eliceiri, 2012).

Confocal microscopy. Images were obtained using a FluoView FV1000 confocal microscope (Olympus) with 20× UPlanSAPO, NA 0.75 (air) and 40X UPlanFLN, NA 1.30 (oil) objectives. Stack images were taken by laser illumination at 561 nm (Alexa Fluor 555), 488 nm (Alexa Fluor 488), and 405 nm (DAPI). 12-bit raw images were processed with the imaging software Fluoview, version 4.1.a (Olympus).

Structured illumination microscopy (SIM). The SIM setup was operated by doctoral student Dr. S. Wäldchen (at the time doctoral student at the Department of Biotechnology and Biophysics, Biocenter, University of Würzburg). Images were captured with a commercial inverted SIM microscope (Zeiss ELYRA, Oberkochen, Germany) using a Plan-Apochromat 63×/1.4 Oil Dic M27 objective (Gustafsson, 2000; Wegel et al., 2016). Excitation of the fluorophores was performed by laser illumination at 642 nm (Alexa Fluor 647), 561 nm (Alexa Fluor 555), 488 nm (Alexa Fluor 488), and 405 nm (DAPI) and fluorescence light was filtered by appropriate detection filters: LP 655 (Alexa Fluor 647), BP 570–620 + LP 750 (Alexa Fluor 555), BP 495–550 + LP 750 (Alexa Fluor 488), and BP 420–480 + LP 750 (DAPI). Images were recorded with five rotations and five phase steps of the illumination pattern. Recorded data were processed with the ZEN imaging software (Zeiss). They were processed under standard ELYRA settings of the manual mode, selecting the Raw Scale option to keep the original dynamic range and therefore ensure a reliable comparison of the actual sample and the control samples. Following the structured illumination processing, the four channels were aligned (ZEN imaging software).

Direct Stochastic Optical Reconstruction Microscopy (dSTORM). To reveal synaptic structures in TPH2-positive neurons *d*STORM was performed on a wide-field setup for localization microscopy (van de Linde et al., 2011). The *d*STORM setup was operated by Dr. S. Wäldchen (Department of Biotechnology and Biophysics, Biocenter, University of Würzburg), as well as the selection of the

following parameters. A diode laser with a wavelength of 640 nm (iBeam smart, TOPTICA Photonics, maximum power of 200 mW) and a diode-pumped solid-state laser with a wavelength of 532 nm (gem, Laser Quantum, maximum power of 500 mW) were used for excitation of Alexa Fluor 647 and Alexa Fluor 532 respectively. Laser beams were cleaned-up by bandpass filters (Semrock) and combined by appropriate dichroic mirrors (LaserMUX filters, Semrock). Afterwards they were focused onto the back focal plane of the high numerical oil-immersion objective (alpha Plan-Apochromat 100×/1,46 Oil DIC, Carl Zeiss Microscopy), which is part of an inverted fluorescence microscope (Zeiss Axio Observer.Z1, Carl Zeiss Microscopy) equipped with an autofocus system (Definite Focus, Carl Zeiss Microscopy). To separate the excitation light from the fluorescence light, a suitable dichroic beam splitter (Semrock) was placed into the light path before the laser beams enter the objective. Fluorescence light of Alexa Fluor 647 and Alexa Fluor 532 was collected by the objective and split by a dichroic mirror (Chroma) to two separate EMCCD cameras (iXon Ultra 897, Andor Technology). Before entering the cameras, it was filtered by appropriate detection filters (Semrock/Chroma). For every image, 15000 frames were taken with an integration time of 10 ms per frame. Data analysis was performed using ThunderSTORM (Ovesný et al., 2014). Gold beads were used for drift correction (Jansch et al., submitted).

Three-dimensional reconstruction. For three-dimensional (3D) visualization of SIM images, z-stacks with intervals of 125 nm were recorded (usually ~50 slices). 3D reconstruction and animation of the processed SIM images were performed in Imaris (Bitplane, Zurich, Switzerland). The fluorescence signal was represented by surface visualization. Resulting 3D renderings were animated by rotation and zooming and exported as avi files.

2.8. Data quantification

2.8.1. Constitutive *Cdh13* knockout mouse line

Cell density in dorsal and median raphe. Cell density measurements of the DR were quantified at E13.5, E17.5, and in the adult brain using ImageJ v2.0.0 by an observer unaware of genotype. At E13.5 the complete DR was imaged and selected as the region of interest (ROI). Within this ROI, five areas of 50 × 50 pixels were randomly selected. The number of 5-HT immunoreactive (ir) cells in these areas (including the cells on the left and bottom borders) was counted using the 'Cell Counter' plug-in. This was done through the entire stack of images, using DAPI as a counterstaining to count only cells with a focused nucleus and therefore avoid double counts. Then the average number of cells for each brain was calculated. At E17.5 and in the adult brain, sections at a distance of 120 µm were imaged, ~4–5

images per brain. In these images, the DR was selected as the ROI and then all the 5-HT-ir cells for E17.5 and Tph2-ir cells for adult brains were counted using the Cell Counter plugin, avoiding double counts through the use of DAPI. Finally, the average number of cells per brain was calculated.

Area measurement of dorsal raphe. The area of the DR was measured at E13.5 using ImageJ v2.0.0. Six sections stained for 5-HT, where the DR was clearly visible, were selected per brain and the area of the group of 5-HT-ir cells was measured. Images where the DR extended out of the image were excluded.

Radial glial cells endfeet analysis. This analysis consisted in the quantification of the number of radial glial cells with club-like or branched endfeet in the rostral hindbrain region as conducted by Yokota et al. (2010). A total of three images per brain were taken with confocal microscopy at 60x magnification and were then processed using ImageJ v2.0.0. Radial glial cell endfeet that could not be clearly categorized as club-like or branched were excluded.

Serotonergic fiber density in prefrontal cortex

Embryos. The area of the 5-HT-ir fibers was measured at E17.5 using ImageJ v2.0.0 as described previously (Gomez et al., 2007). Earlier developmental stages were not analyzed because 5-HT afferents have not reached the cortex by then. Six images of the prefrontal cortex were taken per brain. A threshold was set for each image to balance the signal-to-noise ratio by an observer unaware of genotype, so that the serotonergic fibers were clearly distinguishable from the background. Then, the images were transformed into binary images in which only immunostained elements were visible. A ROI of 100 × 100 pixels in the center of the intermediate zone (IZ) was set and the area of the fibers was calculated using the "Analyze Particles" option.

Adults. Images of infralimbic (IL) and cingulate (CG) cortices from three to four sections at intervals of 120 µm were taken at 20× magnification. After backgrounds were subtracted and fibers were skeletonized, an evenly spaced square grid (70 × 70 μm^2) was laid over the composite images. Finally, the area of the fibers within this ROI was calculated using the "Analyze Particles" option.

2.8.2. Conditional *Cdh13* knockout mouse line

Cell density quantification in dorsal raphe

Embryos. The 5-HT cell density of the DR at E13.5 was analyzed using ImageJ v2.0.0 by an observer unaware of genotype. The complete DR was imaged using a FluoView FV1000 confocal microscope (Olympus) with 20×/0.75 UPlanSAPO

objective. In each image, the DR was selected as the ROI and then the 'Cell Counter' plug-in (ImageJ) was used to count 5-HT-ir cells. The DAPI counterstain was used to ensure that only those cells with a visible and focused nucleus were counted, in order to avoid double counts. Then the average number of cells for each brain was determined. In addition, the area of the ROI was also determined using the 'Measure' plug-in on ImageJ.

Adults. The density of 5-HT neurons in the DR was calculated for each of its three main subgroups: (1) dorsal (B7d), (2) ventral (B7v) and (3) lateral (B7l). Images from three to four sections at intervals of 120 µm were taken with a FluoView FV1000 confocal microscope (Olympus) with 20×/0.75 UPlanSAPO objective. The images were then processed using ImageJ. The background was subtracted with a rolling ball value of 20, and the image palette was changed to "Fire" to better identify Tph2-ir cells. The number of cells for each subcomponent was counted, and the mean number of Tph2-positive cells was calculated for each brain.

Serotonergic innervation of target regions

Embryos. The serotonergic innervation of two cortical regions, the prefrontal cortex and the somatosensory cortex, was quantified at E17.5 using ImageJ v2.0.0. In the images taken, the intermediate zone (IZ), where the serotonergic fibers are located at this developmental stage, was selected as the ROI and rotated when necessary to make the ROI lie horizontally. In order to make the serotonergic fibers clearly distinguishable from the background, image background was removed using the 'Subtract background' function on ImageJ with 'Rolling' values of 5, 10 and 15 consecutively. Images were made binary and a rectangle of 100 × 800 pixels was drawn surrounding the IZ. Having selected the ROI, 5-HT-ir fibers were counted using the 'Analyze particles' ImageJ function. The total number of pixels occupied by the 5-HT-ir fibers was calculated.

Adults. The serotonergic innervation of several target regions was analyzed in adult brains. The regions were the following: (1) prefrontal cortex (including cingulate and infralimbic cortices), (2) thalamus (including median and lateral thalamus), (3) caudate putamen, and (4) amygdala. These regions were previously identified as the main target regions of the lateral (B7l) and ventral (B7v) DR (Muzerelle et al., 2016). Each region was imaged by confocal microscopy on 3-4 brain slides per hemisphere. Section interval was 120 µm. The images were processed using ImageJ. Initially the background was subtracted with a "Rolling ball" value of 1.45 or 1.5 depending on the region (Table 9). Then the contrast was enhanced, and the image was made binary allowing only immunostained elements to be visible. A section was selected in the center of the image (Supplementary Table 9), and the total number of pixels occupied by the 5-Htt-positive fibers was measured using the "Analyze Particles" option in each individual image.

Table 9. 5-HTT innervation in adult brains: Rolling ball values and selected area.

Region	Rolling ball value	Selected area (µm²)
PFC (CG and IL)	5	120062.250
PVT	1.5	86819.040
LDT	1.45	168087.150
Amygdala	1.45	104590.440
Caudate putamen	1.5	120062.250

Abbreviations: prefrontal cortex (PFC); cingulate cortex (CG); Infralimbic cortex (IL); paraventricular thalamus (PVT); laterodorsal thalamus (LDT)

2.9. Behavioral assessment

An extensive behavioral repertoire was conducted in the *Cdh13* cKO mice to better understand whether CDH13 deficiency in the serotonergic network affects mouse behavior. Due to the relationship between *CDH13* and neurodevelopmental disorders ADHD and ASD (for review: Hawi et al., 2018; Rivero et al., 2013) we aimed to apply behavioral tests commonly used to investigate impulsivity, attention, cognitive abilities and sociability. Anxiety-like behavior was also tested, because anxiety has been identified as a comorbidity of ADHD (Schatz & Rostain, 2006). To this end, a cohort of adult male *Cdh13* cKO (n=8-14) and $Cdh13^{LoxP/LoxP}$ control littermates (n=8-10) were subjected to a series of behavioral tests from 3-4 months of age to assess anxiety-like behavior (elevated plus maze, light-dark box, open field), sociability and preference for social memory (social interaction test), locomotor activity (open field test) as well as visuospatial learning and memory (Barnes maze test).

Behavioral testing was performed during the light cycle between 9 am and 5 pm. The behavior was recorded and analyzed using VideoMot2 software (TSE Systems) unless otherwise specified. The examiner was blinded to the genotypes. The test arenas were thoroughly disinfected with 70% ethanol between trials to prevent olfactory cues. The order in which the tests were carried out was from least to most stressful and was as presented below. All the tests were conducted as previously described by Rivero et al. (2015) with minor modifications.

Elevated Plus Maze. The elevated plus maze (EPM) is used to evaluate anxiety-like behavior (Pellow, Chopin, File, & Briley, 1985; Walf & Frye, 2007). The mice were placed in the center of the maze which consists of an elevated platform approximately 60 cm from the floor, with two open arms (illumination of 50 lx) and two closed, dark arms (15 cm high walls, illumination of 5 lx), each arm with a dimension of 30 × 5 cm and semi-permeable to infrared light (TSE Systems, Bad Homburg, Germany). The test was conducted for 10 min, during which the

animals' trajectory was tracked using a CCD camera. The videos were then analyzed to calculate the total distance traveled, the number of entries and time spent in each of the arms.

Light-Dark Box. The light-dark box (LDB) test also allows the evaluation of anxiety-like behavior. The test apparatus consists of a square box (50 × 50 × 40 cm) semi-permeable to infrared light that contains a black insert measuring one third of the total area of the box with a small opening that allows access to the rest of the box. The illumination of the light compartment is approximately 100 lx, while the illumination of the dark compartment is between 0 and 5 lx. Each mouse was individually placed in the dark compartment and its movement was tracked for 10 min using the VideoMot2 software (TSE Systems). The measurements analyzed were the number of entries and latency to enter the light compartment, the time spent in each compartment, and the total distance travelled.

Open Field. The open field (OF) test was performed to measure locomotor activity as well as anxiety-like behavior. The OF is composed of a square box semi-permeable to infrared light (50 × 50 × 40 cm) with an illumination gradient between 50 and 100 lx from the walls to the center of the arena. The mice were placed individually in one of the corners of the arena and their movement was monitored for a duration of 30 min using a CCD camera positioned above the center of the setup. The total distance traveled as a measure of locomotor activity, as well as the amount of time spent in the central and border areas and the latency to enter the center of the arena as measures for anxiety-like behavior were then calculated.

Two-trial social interaction test. The social interaction test was performed in the OF arena to which the animals had already been habituated. This test measures both sociability and preference for social novelty in two consecutive trials. In the first trial (sociability test), the mice were placed in the arena for 10 min and were given the opportunity to explore either an unfamiliar mouse that was enclosed in a small plastic grid cage or an identical empty plastic grid cage. The small cages were located in the upper left and right corners of the arena and the positions of the cage with the unfamiliar animal and the empty cage were randomly alternated between trials to prevent possible effects of side preference. During the second trial that was performed 5 min later (test of preference for social novelty), the mice were placed in the arena and were given the choice to explore the first, now familiar mouse, or a novel, unfamiliar mouse, both enclosed in small plastic cages. The behavior was recorded, and measurements of the total distance traveled, the number of visits and time spent within each interaction zone (animal vs cage; familiar animal vs novel animal), as well as the latency to explore each, were taken. Sociability was defined as interaction time with an unfamiliar mouse over

an empty cage. Preference for social novelty was defined as time spent interacting with the novel mouse over the familiar mouse.

Novel object recognition test. The novel object recognition (NOR) test, used to measure learning, memory and object discrimination, consisted of two 10-min trials and was also conducted in the OF arena. In the first trial, the mice were placed in the arena for 10 min with two identical objects, 50 ml glass bottles filled with a white cloth. During the second trial, which was performed 30 min later, one of the glass bottles (now familiar object) was replaced by a rectangular Lego® brick construction about the same height as the glass bottle (novel object). The mice were again allowed to freely explore both the familiar and novel objects. The objects were located in the upper left and right corners of the OF arena and the positions of the familiar and novel objects were randomly alternated between animals to prevent possible effects of side preference. The behavior was recorded, and total distance traveled, latency to explore each object, as well as the number of visits and time spent in the area surrounding each object were measured in each trial. In addition, in trial 2, the discrimination index was defined as the time spent interacting with the novel object minus the time spent interacting with the familiar object, over the total exploration time of both objects.

Barnes Maze Test. The Barnes maze (BM) test was performed to evaluate visuospatial learning and memory. The testing apparatus (TSE Systems) consists of a circular grey platform (120 cm in diameter) with 40 holes around its circumference (each 5 cm in diameter); one of the holes was randomly chosen to hold an escape box. Visual cues to allow visuospatial orientation were located around the maze at a distance of approximately 10 cm. At each trial, a mouse was individually placed in the center of the maze and covered with a start cylinder. After removing the cylinder, the mouse was allowed to explore the maze and behavior was recorded until the mouse found the escape hole. If the mouse was unable to find the escape hole within 3 min, the mouse was carefully guided to the escape hole. Mice were trained to find the hidden escape box for 9 days (2 trials per day), with a resting period of 24 h between days 4 and 5. The latency to start exploring, latency to escape as well as the total distance travelled were automatically measured by the Videomot2 software. The number of primary errors, defined as the number of times the mouse poked its head into a wrong hole before the first encounter with the escape hole, were manually scored.

2.10. Statistical analysis

Histological analysis. Statistical analysis was performed using Prism, version 7.0a (GraphPad Software, La Jolla, CA, USA). The normality of the data sets was verified using the Kolmogorow-Smirnow test and the Shapiro-Wilk test. Genotype effects were analyzed by a two-tailed unpaired *t*-test, otherwise the nonparametric Mann-Whitney test was conducted.

Behavioral testing. Statistical analyses were performed using Prism, version 7.0a (GraphPad Software) and/or SPSS Statistics, version 25.0 (IBM Corp., Armonk, NY). The normality of the data sets was verified using the Kolmogorow-Smirnow test and the Shapiro-Wilk test. Once a normal distribution was confirmed, genotype effects were analyzed by a two-tailed unpaired *t*-test, otherwise the nonparametric Mann-Whitney test was conducted. For the Barnes Maze, a repeated-measures mixed analysis of variance was also used, with genotype as between-subject factor and test session as the repeated measure. Animals that were statistically identified as outliers were excluded from the analysis.

3 | Cadherin-13 deficiency impacts dorsal raphe formation and 5-HT prefrontal cortex innervation in the mouse embryo

3.1. Objectives

CDH13 has a role in a wide range of neurodevelopment processes including cell migration, axon pathfinding, and synaptogenesis. However, there is a lack of knowledge regarding its relationship to the brain 5-HT system. The study of this relationship is important because of the involvement of CDH13 in psychiatric disease with serotonergic impact. Given the expression of CDH13 in 5-HT neurons and its role as a negative regulator of axon outgrowth and migration, we hypothesize that the deletion of CDH13 will alter 5-HT neuron migration and innervation of frontal target regions. The aim of the first project of this doctoral thesis consisted in characterizing the expression pattern of CDH13 during mouse brain development at different embryonic stages with special emphasis on the 5-HT system. Additionally, the consequence of CDH13 deficiency on brain 5-HT system development was investigated in a constitutive *Cdh13* knockout mouse, a model for loss-of function mutations at the *CDH13* locus presumed to associate with neurodevelopmental disorders (Figure 3.1-1). The presented work and figures have been published in Forero et al. (2017).

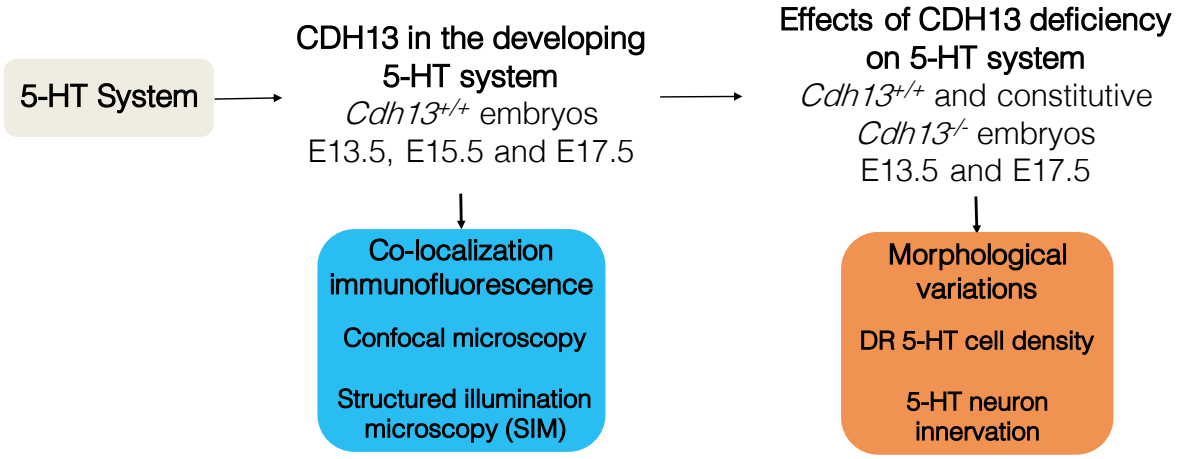

Figure 3.1-1. Outline of principal objectives of Project 1. The project focuses on the expression of CDH13 in 5-HT neurons in *Cdh13*$^{+/+}$ mice at different embryonic stages, followed by the study of the effects of CDH13 deficiency using a *Cdh13* constitutive knockout mouse line on DR morphology and 5-HT neuron innervation.

3.2. Results

3.2.1. CDH13 follows a caudal to rostral progression in the developing mouse brain

Considering the limited knowledge available regarding the expression of CDH13 in the developing mouse brain, we conducted an analysis that allowed us to determine the regional and cellular specificity of CDH13 at three developmental stages (E13.5, E15.5 and E17.5) using the Allen Developing Mouse Brain Atlas (2008) as a reference.

Our findings show that the expression pattern of CDH13 follows a caudal to rostral progression through prenatal development. We began our analysis at developmental stage E13.5 since there is very low detection of CDH13 expression in the mouse brain prior to this stage (Rivero et al., 2015). In this initial embryonic stage (E13.5), we observed that CDH13 is present in fiber-like structures that extend along the hindbrain and into the midbrain. However, at this stage CDH13 is almost completely lacking from the neocortex, with only a very faint staining in the outer most cortical layer (Figure 3.2.1-1a, top).

At E15.5, CDH13 protein is distributed throughout the different brain regions and spreads from the hindbrain to the telencephalon. Only the thalamus and part of the developing pallium show lower immunoreactivity for CDH13 (Figure 3.2.1-1a, middle).

At the latest stage analyzed (E17.5), a shift in the expression pattern of CDH13 compared to its expression in earlier developmental stages was observed. At this timepoint, the strongest CDH13 abundance was found in the developing cortex. Low immunoreactivity was also observed in other brain regions (Figure 3.2.1-1a, bottom).

Along with its caudal-to-rostral progression, CDH13 expression was restricted to regions of neuronal maturation and fiber extension as it advances. Little to no CDH13 expression was detected in areas of neurogenesis. Specifically, CDH13 was not detected in ventricular zones positive for nestin, a marker of neural stem cells or progenitor cells (Lendahl, Zimmerman, & McKay, 1990). Instead, CDH13-immunoreactive (ir) fibers delimit these regions of neurogenesis both in cortical areas as well as in the developing hindbrain (Figure 3.2.1-1b).

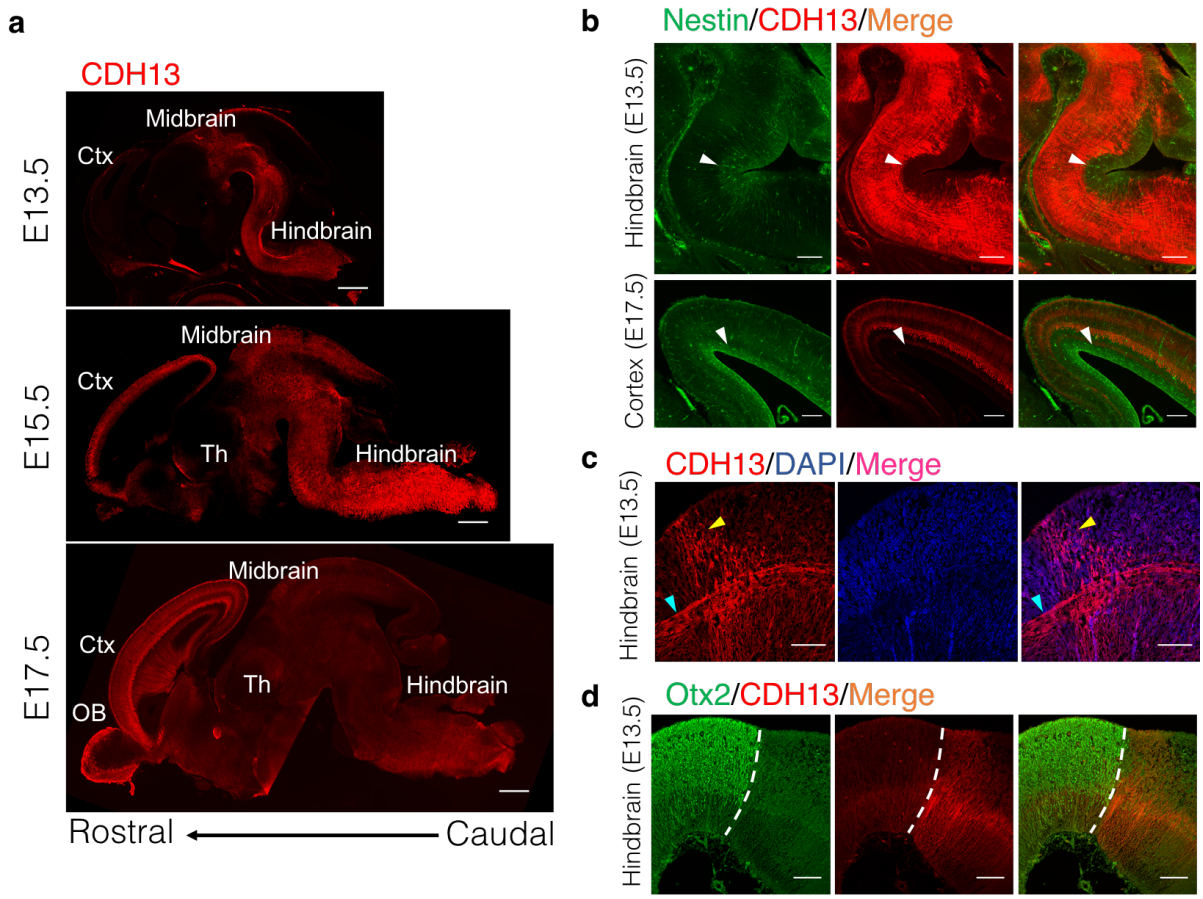

Figure 3.2.1-1. CDH13 expression at prenatal embryonic stages. (a) CDH13 immunoreactivity varies in the brain at E13.5, E15.5 and E17.5. (b) Regions of neurogenesis positive for nestin (white arrows) are negative for CDH13 expression. (c) At E13.5, CDH13 is found in two groups of fibers in the hindbrain, one extending longitudinally (cyan arrow) and another transversally (yellow arrow). (d) CDH13 hindbrain immunoreactivity is juxtaposed to Otx2 midbrain expression, delimiting the MHB (white dotted lines) at E13.5. Orientation: sagittal. Microscopy technique: (a, b) epifluorescence, (c, d) confocal. Scale bars: (a) 500 µm, (b) 200 µm, (c, d) 100 µm. Ctx, cortex; OB, olfactory bulb; Th, thalamus. Adapted from Forero et al. (2017).

A more detailed analysis of developmental stage E13.5 showed that CDH13-positive fibers adjacent to the midbrain-hindbrain boundary (MHB) in rhombomere 1 of the hindbrain follow two distinct perpendicular directions (Figure 3.2.1-1c). While one group of fibers was found to extend longitudinally from the caudal end of the hindbrain to the midbrain, another group projected transversally and extended from the ventricular zone of the hindbrain to the corresponding floorplate (Figure 3.2.1-1c). Double-staining with Otx2, a protein that delimits the caudal boundary of the MHB (Li & Joyner, 2001), confirmed that CDH13-positive fibers extend transversally in the hindbrain until this midbrain boundary at E13.5 (Figure 3.2.1-1d).

3.2.2. CDH13 expression in 5-HT neurons of the dorsal raphe

We hypothesized CDH13 expression in 5-HT neurons and a potential role in their innervation of anterior target regions, such as the developing prefrontal cortex due to two main reasons; (1) the high detection of CDH13 at the region adjacent to the MHB which corresponds with the location of the DR (Figure 3.2.2-1a) (2) the orientation and extension of serotonergic fibers colocalized with the CDH13-expressing trajectory.

To confirm this, we conducted immunofluorescence using 5-HT as a marker for serotonin-positive neurons. Examination of the hindbrain region using confocal microscopy revealed that the DR expresses high amounts of CDH13. Additionally, bundles of 5-HT neurons with an elongated migratory morphology located in the DR were accompanied by CDH13-positive fibers (Figure 3.2.2-1b). However, this was not observed in the developing median raphe (MR), where CDH13 expression is almost completely absent (Figure 3.2.2-1c).

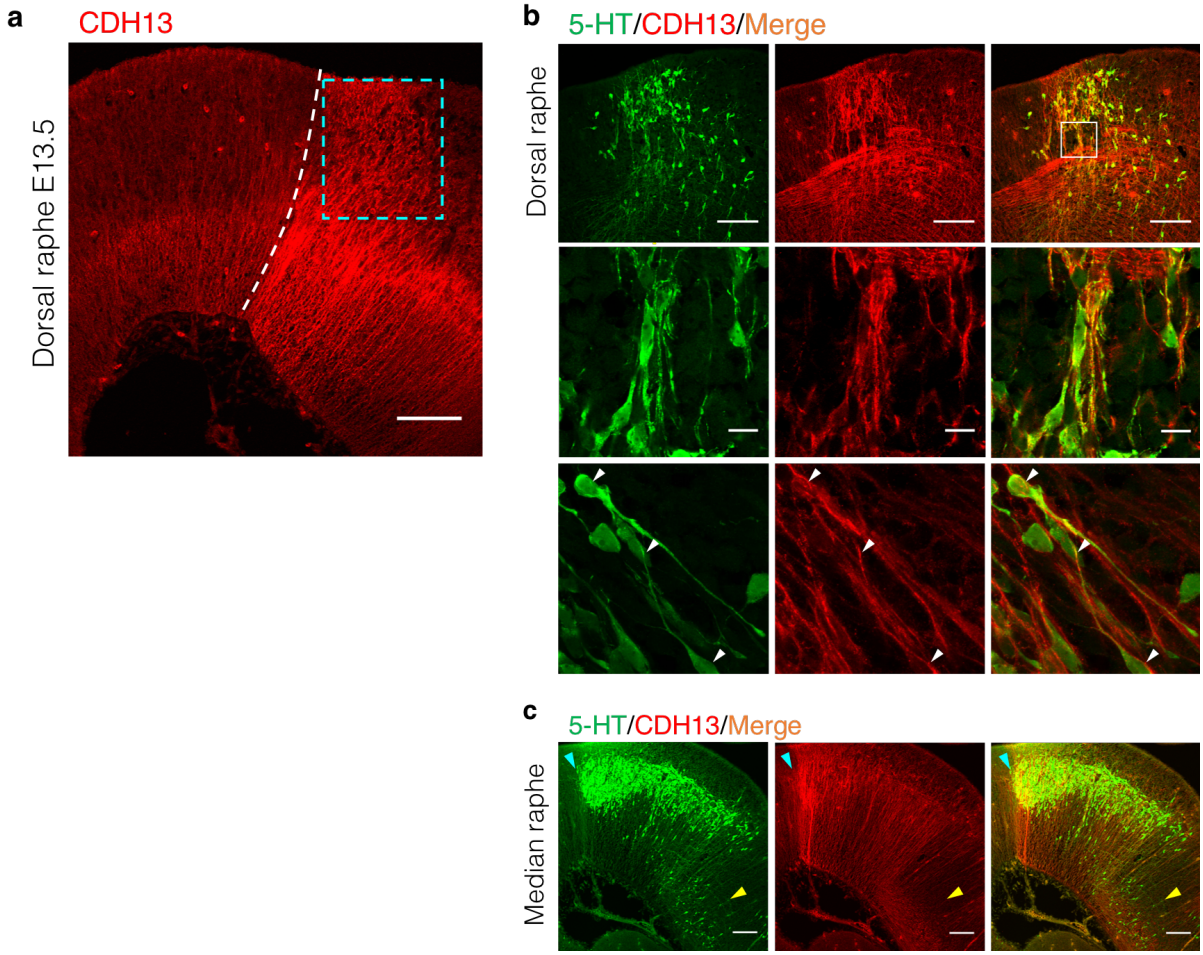

Figure 3.2.2-1. CDH13 expression in the developing dorsal and median raphe nuclei. (a) Strong detection of CDH13 is observed in the region juxtaposed (dotted cyan square) to the MHB (dotted white line) at E13.5. (b) Using confocal microscopy, CDH13 is detectable in 5-HT-positive neurons in the DR. (c) CDH13 expression is considerably lower in the MR (yellow arrow) compared to the DR (cyan arrow). Orientation: sagittal. Microscopy technique: confocal. Scale bars: 100 µm. Adapted from Forero et al. (2017).

In order to more precisely determine the patterning of CDH13 protein on these 5-HT neurons, we applied the super-resolution technique SIM, which provides a two-fold increase in resolution compared to confocal microscopy (Gustafsson, 2000; Wegel et al., 2016). This work was done together with Dr. S. Wäldchen (Department of Biotechnology and Biophysics, Biocenter, University of Würzburg).

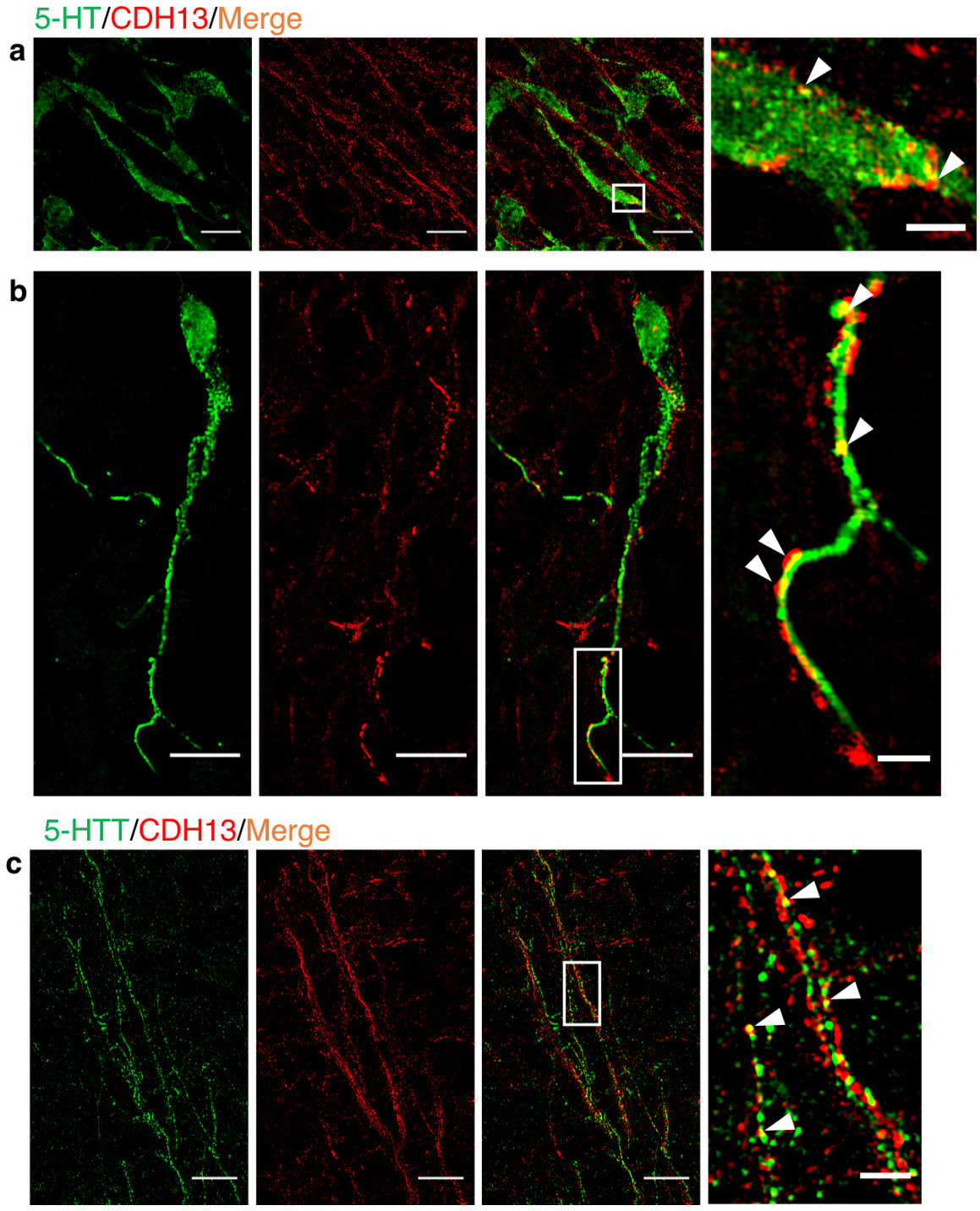

Figure 3.2.2-2. Cellular localization of CDH13 in 5-HT neurons of the dorsal raphe. (a) CDH13 is detected on the soma of 5-HT-positive neurons showing a punctate pattern along the cell membrane. (b) Expression of CDH13 is also found on the extending neurites of 5-HT neurons. (c) Some colocalizations (white arrows) with 5-Htt are observed. Orientation: sagittal. Microscopy technique: SIM. Scale bars: full images (a) 100 µm, (b, c) 10 µm; magnified boxed regions (a, b, c) 2 µm. Adapted from Forero et al. (2017).

The use of SIM allowed us to identify CDH13 on the soma of 5-HT-positive neurons with its characteristic punctate pattern around the cell membrane and clustering at some discrete locations (Figure 3.2.2-2a). Moreover, CDH13 is not only limited to the cell body, but is also present on the 5-HT neuron extension, with punctate immunoreactivity along parts of the neurite (Figure 3.2.2-2b). Immunofluorescence staining for the 5-HT transporter (5-Htt/Sert) showed that there are some colocalization sites with CDH13, confirming its expression on the axons of these neurons (Figure 3.2.2-2c).

3.2.3. CDH13 is present at intersecting points between 5-HT neurons and radial glial cells in the dorsal raphe

The foregoing analysis of the expression pattern in the region adjacent to the MHB revealed that CDH13 is present not only on 5-HT-positive neurons of the DR but may be found also on neighboring cells. Additional CDH13-ir cell extensions were observed in this region, extending in parallel across the neuroepithelium. The structures appeared to create a scaffold for 5-HT neurons. The pattern observed suggested that CDH13 is present on radial glial cells (RGCs). By using an isoform of the intermediate filament protein nestin (RC2), a marker for RGCs (Park et al., 2009), we detected consistent co-localization between CDH13 and RC2 immunoreactivity in the developing hindbrain (Figure 3.2.3-1). This overlap of expression confirmed the identity of CDH13-positive cell extensions as being distinct from serotonergic neurites.

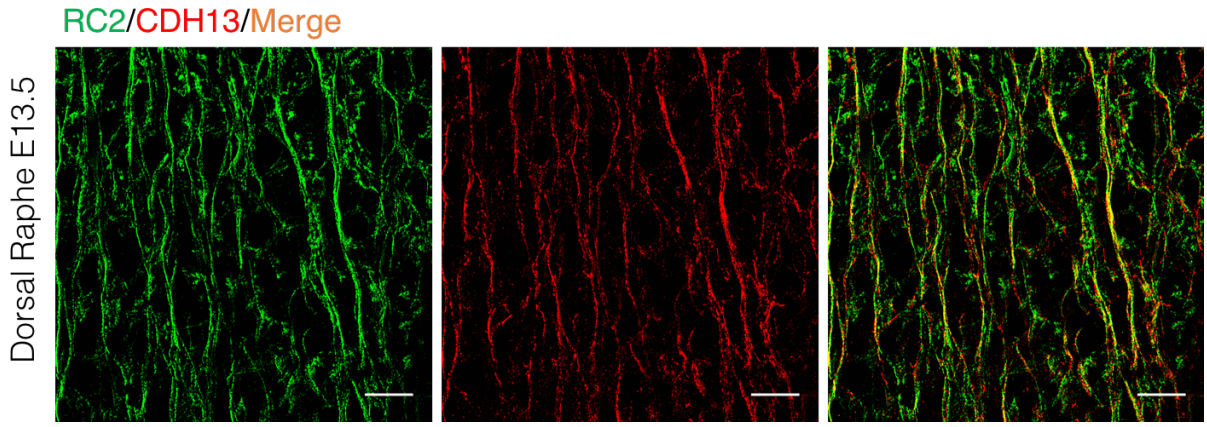

Figure 3.2.3-1. CDH13 expression in radial glial cells in the developing hindbrain. RC2-ir fibers are shown to also be positive for CDH13. Orientation: sagittal. Microscopy technique: SIM. Scale bar: 100 µm. Adapted from Forero et al. (2017).

The presence of CDH13 on both 5-HT neurons and adjacent RGCs suggests a role for CDH13 in RGC-mediated locomotion of 5-HT neurons. Triple immunofluorescence staining for 5-HT, RC2 and CDH13 (Figure 3.2.3-2a) and reconstruction of spatial alignment of the three molecules (Figure 3.2.3-2b) yielded two findings in support of this mechanistic association: first, 5-HT neurons in the DR are intertwined with RGCs in early developmental stages, an organization

suggesting that these neurons are using RGC structure as a physical guide to migrate. Second, CDH13 is present at points of intersection between the 5-HT specific and RGC types, both at the soma and the extending neurites, which indicates that cooperativity, possibly by homophilic interaction, may contribute to the migration process.

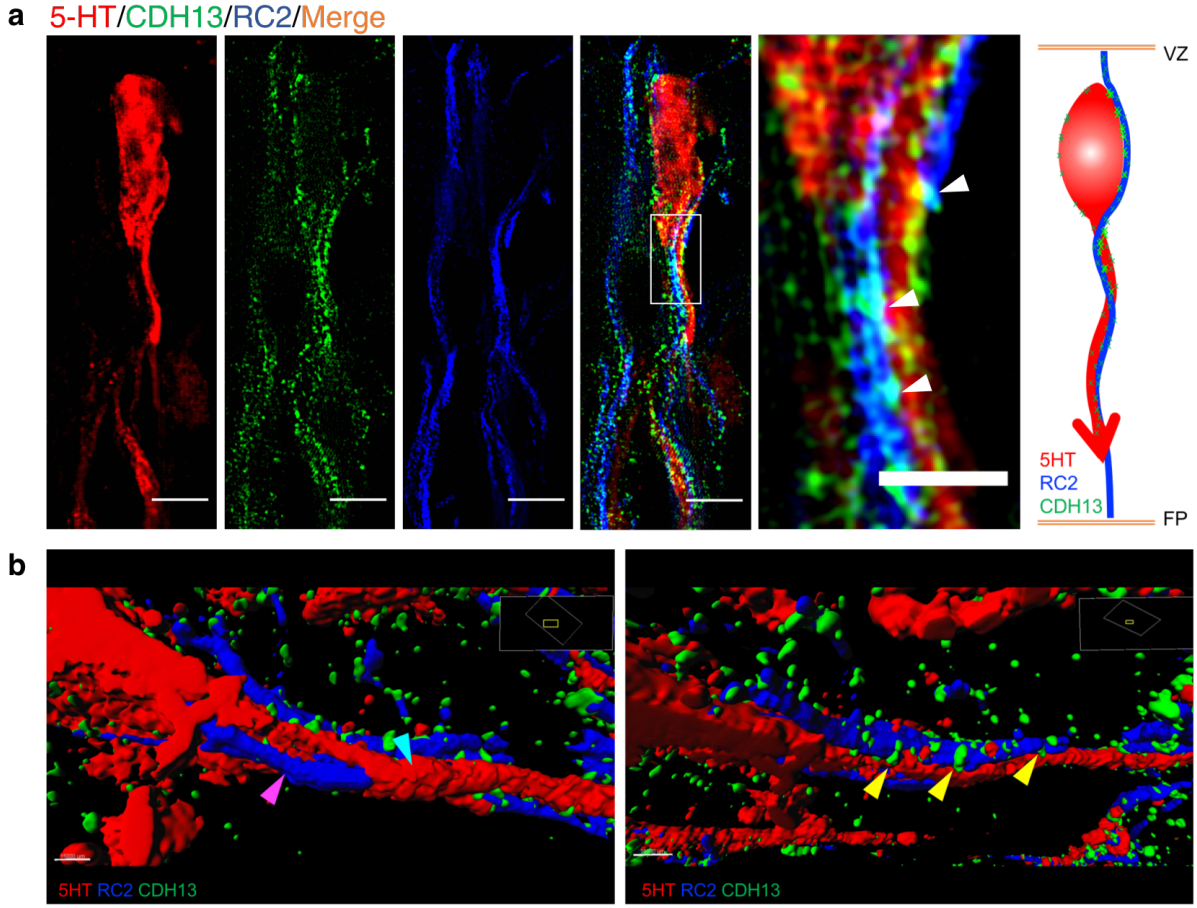

Figure 3.2.3-2. CDH13 expression in interacting 5-HT neurons and radial glial cells. (a) CDH13 is present in both 5-HT neurons and RGCs, and CDH13 clusters are observed at points of intersection between these two cell types (yellow arrows). (b) Reconstruction of triple IF of 5-HT, RC2 and CDH13 using Imaris. The 5-HT neuron (cyan arrow) is intertwined with the RGC fiber (magenta arrow). CDH13 immunoreactivity is found at the interface between both cells (yellow arrows). Orientation: sagittal. Microscopy technique: SIM. Scale bar: (a) 5 µm in full images, 2 µm in magnified boxed region. FP, floor plate; VZ, ventricular zone. Adapted from Forero et al. (2017).

3.2.4. CDH13 deficiency increases 5-HT cell density in the dorsal raphe in early prenatal stages

The evidence for the high expression of CDH13 in DR and a possible role in 5-HT neuron migration and fiber extension prompted us to study the effects of CDH13 deficiency on the development of the DR-cortex 5-HT subsystem. We first investigated the effect of CDH13 deficiency on the formation of the DR by measuring the density of 5-HT-positive neurons in *Cdh13*$^{-/-}$ animals at E13.5 and E17.5. At E13.5, we found a significant increase of DR 5-HT neuron density

in *Cdh13*$^{-/-}$ mice (P = 0.0014 vs. wildtype controls; Figure 3.2.4-1a). The same measurement was conducted in the MR, where CDH13 is not highly detected, yielding no significant difference (Figure 3.2.4-1b).

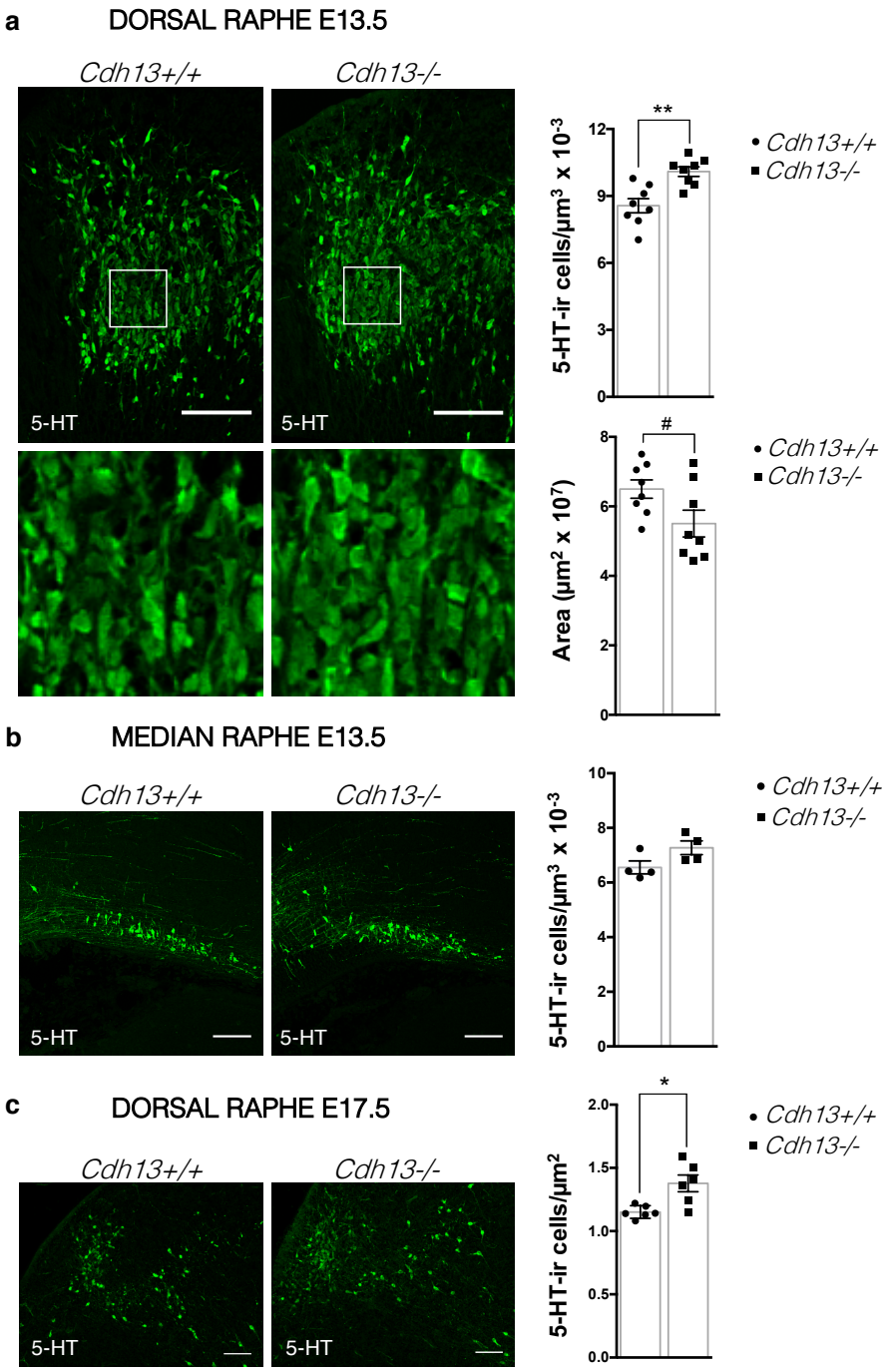

Figure 3.2.4-1. CDH13 deficiency affects the dorsal raphe 5-HT neuron density at E13.5 and E17.5. (a) Representative images of the DR at E13.5. A significantly higher cell density of 5-HT neurons (n=8 per genotype; P=0.0014) and a trend toward reduced DR area (n=8 per genotype; P=0.051) are observed in *Cdh13*$^{-/-}$ mice compared to *Cdh13*$^{+/+}$ controls. (b) Representative images of the MR at E13.5. No significant difference is observed in 5-HT neuron density in the MR between *Cdh13*$^{-/-}$ and *Cdh13*$^{+/+}$ embryos. (c) Representative images of the DR at E17.5. A significantly higher 5-HT neuron density is observed in *Cdh13*$^{-/-}$ mice compared to *Cdh13*$^{+/+}$ controls (n=6 per genotype; P=0.0227). Orientation: sagittal. Microscopy technique: confocal. Scale bars: 100 µm. Data presented as mean ± s.e.m. *P<0.05, **P<0.01. Adapted from Forero et al. (2017).

We observed a similar increase in the cell density of DR 5-HT-positive neurons at E17.5 (P = 0.0227; Figure 3.2.4-1c) with a significant increase in *Cdh13*$^{-/-}$ mice compared to *Cdh13*$^{+/+}$ animals. Moreover, there was a tendency at E13.5 for the area occupied by DR 5-HT neurons in *Cdh13*$^{-/-}$ mice to be smaller than in *Cdh13*$^{+/+}$ controls (P = 0.051; Figure 3.2.4-1a).

Given the importance of the proper formation of the MHB in the development of the DR nucleus (Brodski et al., 2003; Teraoka et al., 2004), in collaboration with doctoral student H.P. Ku (Ku, 2017), we compared the MHB location and integrity between *Cdh13* $^{-/-}$ and *Cdh13*$^{+/+}$ mice at E13.5. As shown in Figure 3.2.4-2, no alterations in the MHB could be observed in *Cdh13*$^{-/-}$ mice. The midbrain marker OTX2, which delimits the boundary of the midbrain with the hindbrain, does not appear to be displaced to more rostral or caudal brain regions when compared to the corresponding location in *Cdh13*$^{+/+}$ animals.

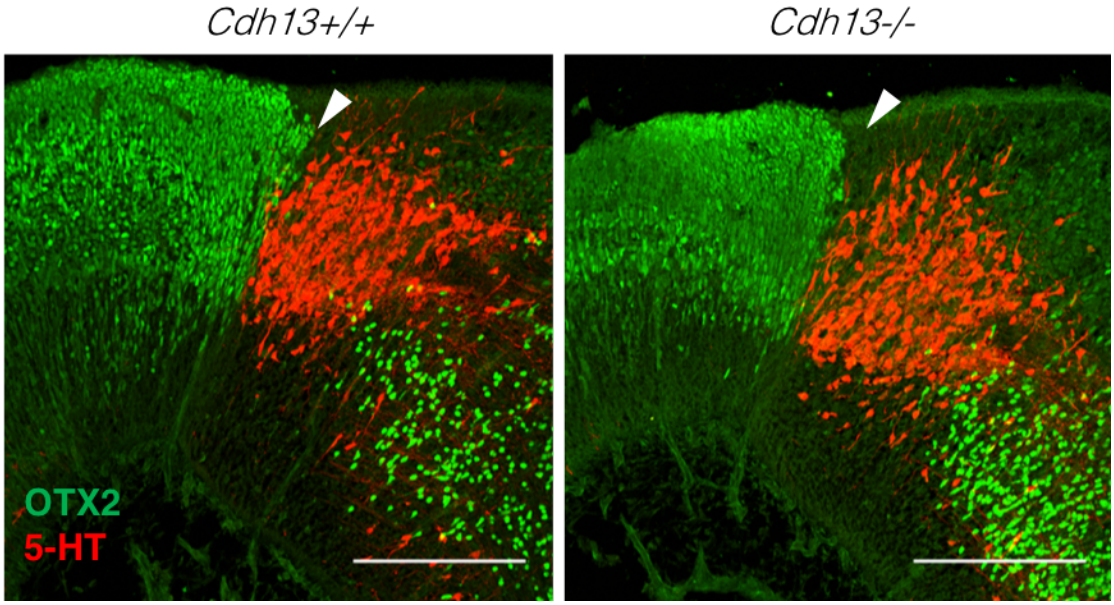

Figure 3.2.4-2. CDH13 deficiency does not affect midbrain-hindbrain boundary formation at E13.5. Representative images of the DR stained with 5-HT and midbrain boundary marker OTX2 at E13.5. Qualitative observation did not show a difference in the location and integrity of the MHB between *Cdh13*$^{-/-}$ and *Cdh13*$^{+/+}$ embryos. Orientation: sagittal. Microscopy technique: confocal. Scale bars: 200 µm. These data were processed and analyzed together with doctoral student H.P. Ku and were part of the work she presented in her Master thesis (Ku, 2017).

Additionally, we asked whether the absence of CDH13 in RGCs might cause alterations that may influence their interaction with 5-HT neurons. To this end, we investigated the morphology of the endfeet of RGCs in *Cdh13*$^{-/-}$ and *Cdh13*$^{+/+}$ animals. RGC endfeet can be characterized as either club-like or branched based on their shape (Yokota et al., 2010). Club-like endfeet structures allow a rapid rate of extension towards a target, and therefore are more abundant in later embryonic stages (E16.5) when the cortex is expanding.

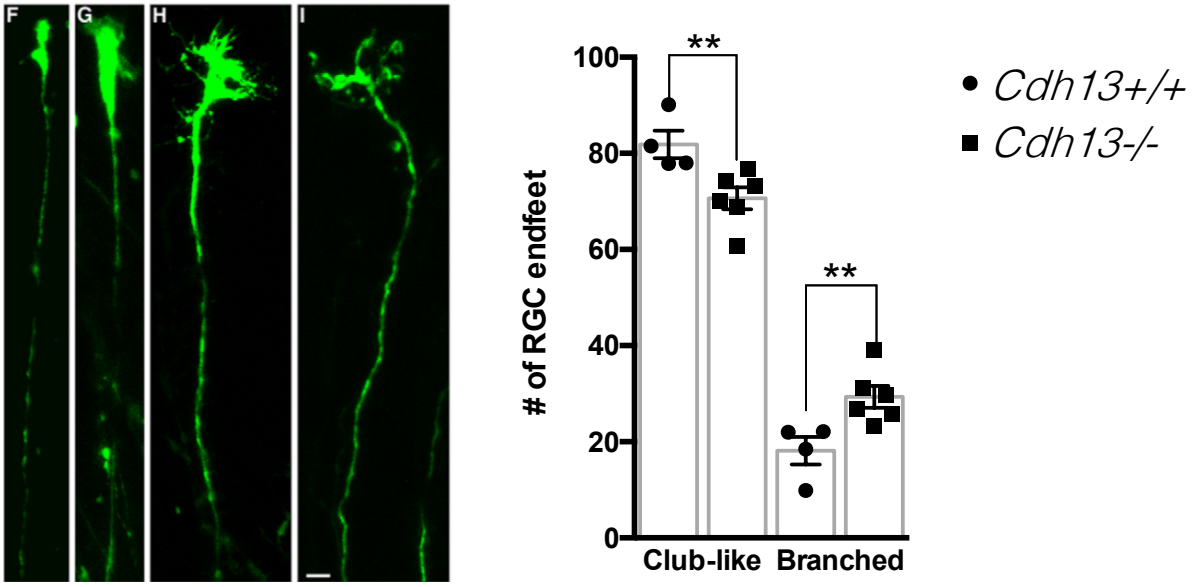

Figure 3.2.4-3. Radial glial cell endfeet analysis of *Cdh13*$^{-/-}$ and *Cdh13*$^{+/+}$ mice. Representative images of club-like (F, G) and branched (H, I) RGC endfeet are shown (taken from Yokota et al., 2010). A significant difference is observed in the percentage of club-like and branched RGC endfeet (P=0.0095) present in *Cdh13*$^{-/-}$ and *Cdh13*$^{+/+}$ embryos (*Cdh13*$^{+/+}$ n=4; *Cdh13*$^{-/-}$ n=6). Scale bar: 66 µm. Data presented as mean ± s.e.m. **P<0.01.

The analysis of RGC endfeet was conducted in collaboration with intern student M. C. Rincón. Our results show a significant difference in the structure of the RGC endfeet structures between *Cdh13*$^{-/-}$ *and Cdh13*$^{+/+}$ mice. *Cdh13*$^{-/-}$ embryos have less club-like and more branched RGCs (P = 0.0095; Figure 3.2.4-3). It will be important to find out how this structural difference in endfeet structures affects RGCs function, and whether and how they interact with 5-HT neurons.

3.2.5. CDH13 expression in the developing prefrontal cortex

Given the role of CDH13 in neurite outgrowth and axon guidance, we also examined its expression in one of the DR target regions, the prefrontal cortex (PFC). This was conducted at E17.5 when 5-HT afferents from the DR have started to innervate the cortex (Wallace & Lauder, 1983). As shown in Figure 3.2.5-1a, at this developmental stage CDH13 is strongly detected in all the cortical layers except for the zone adjacent to the lateral ventricle (LV). 5-HT projections are observed mostly in the intermediate zone (IZ) and, in a lower quantity, in the marginal zone (MZ). Our results show that both layers present strong immunoreactivity for CDH13 (Figure 3.2.5-1b).

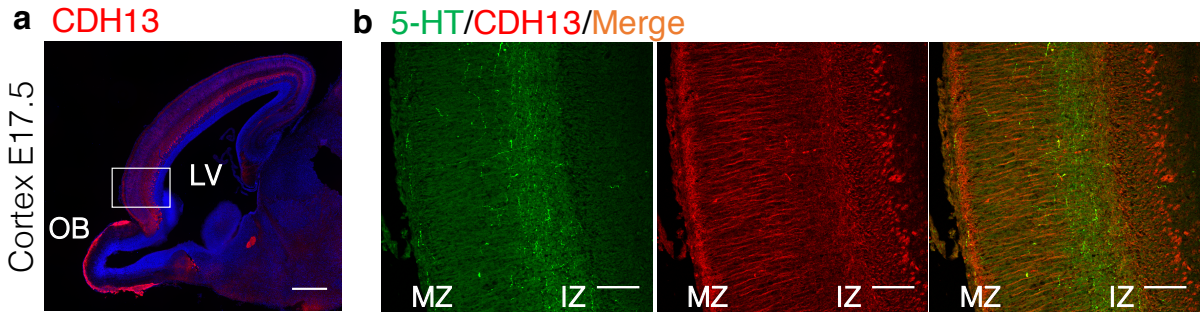

Figure 3.2.5-1. CDH13 and 5-HT expression in the developing prefrontal cortex. (a) Immunoreactivity of CDH13 in the developing cortex at E17.5 (PFC is labeled with a white square). (b) 5-HT innervation is seen at the MZ and IZ of the cortex, while CDH13 is present in almost all the cortical layers. Orientation: sagittal. Microscopy technique: (a) epifluorescence, (b) confocal. Scale bar: 100 µm. OB, olfactory bulb; LV, lateral ventricle; MZ, marginal zone; IZ, intermediate zone. Adapted from Forero et al. (2017).

3.2.6. CDH13 deficiency increases serotonergic innervation of the prefrontal cortex in early prenatal stages

Following, the presence of CDH13 in the developing PFC led us to investigate whether CDH13 deficiency alters serotonergic innervation of this region. The area occupied by 5-HT-positive fibers in the IZ of the PFC at E17.5 was calculated for *Cdh13*$^{-/-}$ and *Cdh13*$^{+/+}$ mice. This work was carried out with bachelor student Y. Gärtner. We found an increase in the area covered by serotonergic fibers in *Cdh13*$^{-/-}$ embryos ($P = 0.042$ vs. wildtype controls; Figure 3.2.6-1).

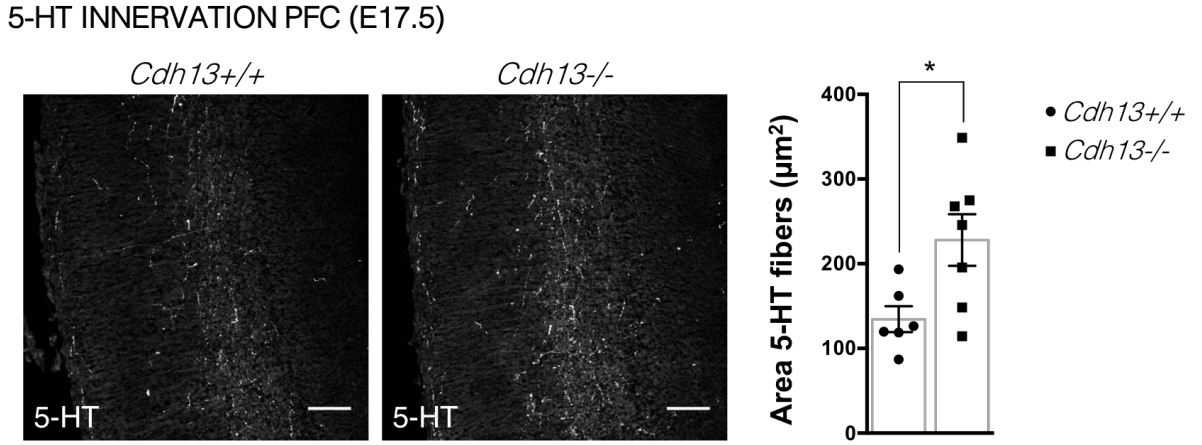

Figure 3.2.6-1. 5-HT innervation of the prefrontal cortex in *Cdh13*$^{-/-}$ and *Cdh13*$^{+/+}$ E17.5 embryonic brains. Representative images of 5-HT fibers in the IZ of the PFC in *Cdh13*$^{-/-}$ and *Cdh13*$^{+/+}$ E17.5 embryos. A larger area occupied by 5-HT-positive fibers is observed in *Cdh13*$^{-/-}$ mice compared to *Cdh13*$^{+/+}$ controls (n=7 per genotype; P=0.042). Scale bars: 100 µm. Microscopy technique: confocal. Data presented as mean ± s.e.m. *P<0.05. Adapted from Forero et al. (2017).

3.2.7. CDH13 deficiency increases Tph2 neuron density in the adult mouse brain but does not alter 5-Htt innervation in the prefrontal cortex

In order to observe if the DR alteration present in *Cdh13*$^{-/-}$ mice in prenatal stages of development persists into adulthood, we compared 5-HT neuron density in the adult brain of *Cdh13*$^{-/-}$ and *Cdh13*$^{+/+}$ mice. As mentioned previously, Tph2 is the neuron-specific tryptophan hydroxylase required for 5-HT synthesis. The number of Tph2-specific neurons in the complete DR as well as the area occupied by this nucleus were calculated to asses Tph2 neuron density. As shown in Figure 3.2.7-1a, *Cdh13*$^{-/-}$ mice have an elevated number of Tph2-positive neurons in the DR compared to *Cdh13*$^{+/+}$ mice (P=0.0191).

The analysis of prefrontal cortex 5-HT innervation in the adult mouse brain shows that the hyperinnervation present in embryonic stages is no longer observed in the adult mouse brain. No difference was detected in the area occupied by 5-Htt-fibers in two main regions of the PFC, the infralimbic (IL) and cingulate (CG) cortices, between *Cdh13*$^{-/-}$ and *Cdh13*$^{+/+}$ adult mice (Figure 3.2.7-1b).

These data were processed and analyzed together with doctoral student H.P. Ku and were part of the work she presented in her Master thesis (Ku, 2017).

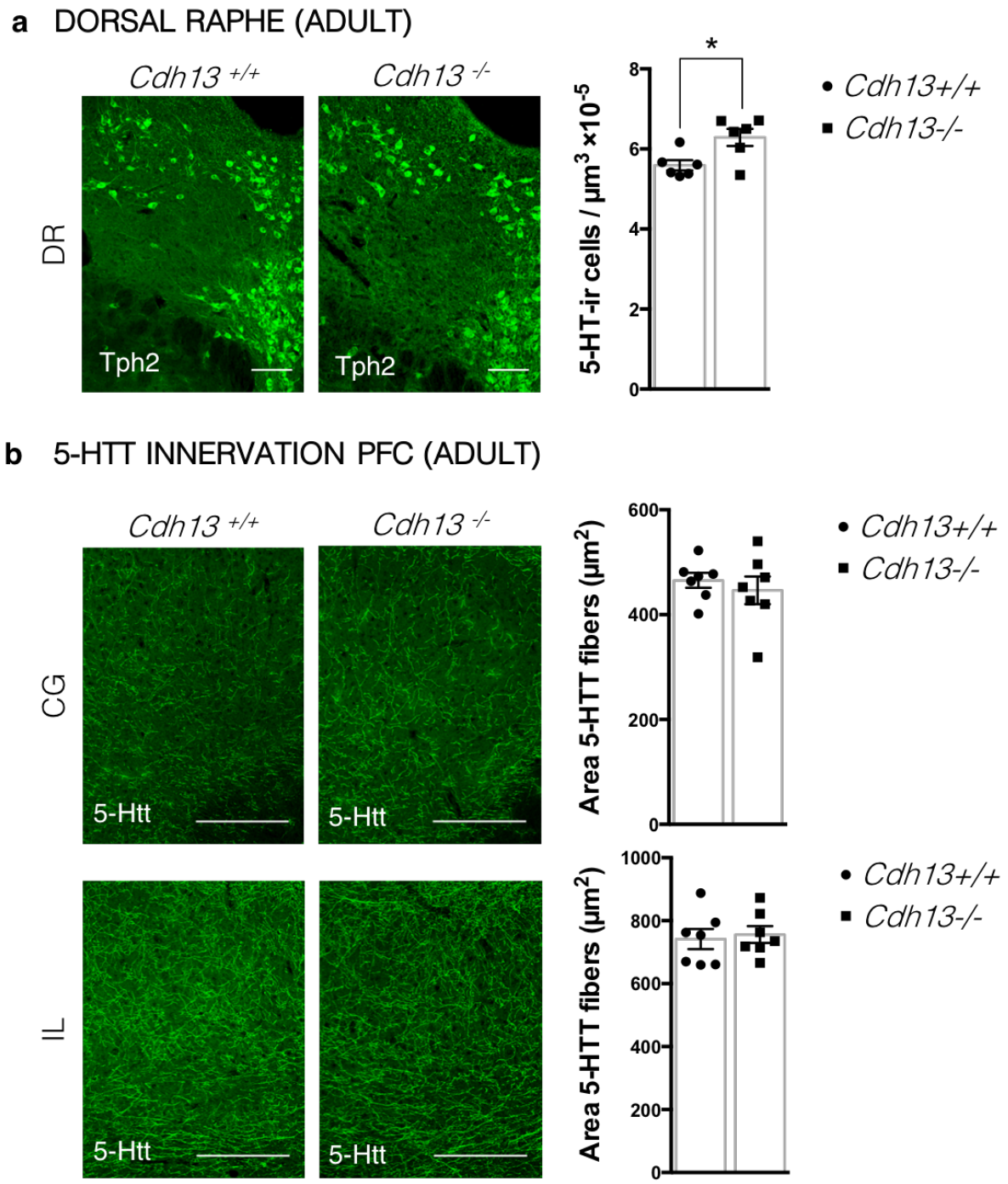

Figure 3.2.7-1. Tph2 neuron density and 5-Htt prefrontal cortex innervation in *Cdh13*$^{-/-}$ and *Cdh13*$^{+/+}$ adult mouse brains. (a) Representative images of Tph2-ir neurons in the DR of *Cdh13*$^{-/-}$ and *Cdh13*$^{+/+}$ adult brains. The density of Tph2 neurons in *Cdh13*$^{-/-}$ mice is increased compared to *Cdh13*$^{+/+}$ controls (n=6 per genotype; P=0.0191) (b) Representative images of 5-Htt innervation in the CG and IL cortices of *Cdh13*$^{-/-}$ and *Cdh13*$^{+/+}$ adult brains. No difference is observed in the area occupied by 5-Htt fibers in these two prefrontal cortical regions. Scale bars: (a) 100 µm, (b) 200 µm. Microscopy technique: confocal. Data presented as mean ± s.e.m. *P<0.05. These data were processed and analyzed together with doctoral student H.P. Ku and were part of the work she presented in her Master thesis (Ku, 2017). Adapted from Forero et al. (2017).

3.3. Discussion

The development of the raphe nuclei and their subsequent projections to target brain regions is determined by intrinsic and extrinsic molecular factors (for review: Deneris & Gaspar, 2018). In the present project, we identify CDH13 as a new molecular player in 5-HT neuron migration and development of serotonergic forebrain projections. Our results demonstrate that in the mouse embryonic brain, CDH13 is strongly expressed on 5-HT specific neurons of the DR and hindbrain RGCs. 3D reconstruction of 5-HT and RC2 immunofluorescence showed the intertwining of 5-HT neurons with RGCs in the embryonic DR, a morphology suggesting that 5-HT neurons undergo RGC-guided migration. Additionally, super-resolution microscopy confirmed the presence of CDH13 at points of intersection between 5-HT neurons and RGCs. Overall, we describe a profile of alterations in 5-HT system development in *Cdh13* constitutive knockout mice (Forero et al., 2017).

While *Cdh13* mRNA has been identified in 5-HT neurons of the adult murine brain (Okaty et al., 2015; Rivero et al., 2013; Wylie et al., 2010), our findings confirm the presence of CDH13 protein in this cell type already at early embryonic stages. Our data indicate that during prenatal development CDH13 expression is preferentially detected in the DR, one of the major sources of 5-HT innervation to the forebrain (Lesch & Waider, 2012). The migratory pattern of CDH13-positive cellular structures closely follows the temporal progression of serotonergic fibers originating from the rostral raphe nuclei (Forero et al., 2017). A structurally detailed expression pattern of CDH13 achieved by super-resolution microscopy shows its presence on both the soma and extending neurites of 5-HT neurons (Forero et al., 2017). CDH13 also co-localizes with the 5-Htt suggesting that it might contribute to target recognition and synaptogenesis (Forero et al., 2017).

Further analysis of the unique expression pattern of CDH13 in the hindbrain revealed a strong localization in RGCs (Forero et al., 2017). Studies have reported that CDH2 (N-cadherin), a classical cadherin, is present on RGC extensions and is required for migration as well as axon formation of cortical neurons (Shikanai, Nakajima, & Kawauchi, 2011; C. Xu et al., 2015). Although both CDH13 and CDH2 were identified in RGCs, the distribution of their expression in the raphe nuclei appears to be different, with CDH2 being more restricted to the MR region (Okaty et al., 2015). Further studies determining the function of CDH2 in the hindbrain are lacking, however our results indicate that CDH13 is present at the interface between 5-HT neurons and RGCs, indicating a potential role in 5-HT neuron migration and thereof in the developmental formation of the DR (Forero et al., 2017).

The observation that 5-HT neurons are intertwined with RGCs in the hindbrain led us to consider that RGCs might be implicated in their migratory and axon guidance processes. RGCs assist migration of specific neuronal cell types and the projection of their neurites at late prenatal stages of neurodevelopment (Campbell & Gotz, 2002; Gupta, Tsai, & Wynshaw-Boris, 2002; Nadarajah & Parnavelas, 2002). The RGCs-assisted migratory mechanism has almost exclusively been established for the telencephalon, with the exception of studies focused on radial migration of granule neurons in the cerebellum (Adams, Tomoda, Cooper, Dietz, & Hatten, 2002; Edmondson & Hatten, 1987).

In our 3D reconstruction (Figure 3.2.3-2), we observe the grasping and intertwining of 5-HT neurons to RGCs. These morphological hallmarks are similar to those observed in migrating neurons during RGC-mediated locomotion (Forero et al., 2017; Rakic, 1978, 2003). Additionally, we observed that the absence of CDH13 affects the morphology of RGC endfeet structures in the hindbrain. Defects in these typical structures can lead to placement deficits of corresponding neurons (Haubst, Georges-Labouesse, De Arcangelis, Mayer, & Gotz, 2006; Yokota et al., 2010). A thorough analysis conducted with three mouse lines carrying mutations that hinder the attachment of RGC endfeet to the basement membrane of the cortex presented alterations in the positioning of neuronal subtypes, including cortical interneurons (Haubst et al., 2006). However, further confirmation of migratory defects in 5-HT neurons in *Cdh13*$^{-/-}$ mice through live cell imaging is still pending.

At developmental day E12, 5-HT neurons migrate across the neuroepithelium through dynamin-mediated somal translocation, a form of neuronal migration that does not require the aid of RGCs (Hawthorne et al., 2010). However, it is likely that numerous additional regulators contribute to the fine-tuning of this complex process at later prenatal stages. Our results complement this finding by showing that at subsequent developmental stages, 5-HT neurons are intertwined with RGCs, an organization that suggests that they undergo RGC-mediated locomotion. Therefore, the principle of migration observed for cortical neurons which states that somal translocation occurs at early phases of development and that in later phases the migration is guided by RGCs (Campbell & Gotz, 2002; Gupta et al., 2002; Nadarajah & Parnavelas, 2002), might also hold true for 5-HT neurons in the hindbrain (Forero et al., 2017).

Regarding the contribution of CDH13 to the formation of the DR, we observe that the absence of CDH13 modifies the 5-HT neuron density of the DR. A higher number of 5-HT-producing cells per μm^3 is reported in *Cdh13*$^{-/-}$ mice (Forero et al., 2017). Previous studies have provided evidence that alterations in the MHB lead to a misplacement and/or reduction of 5-HT neurons (Brodski et al., 2003; Teraoka et al., 2004). Even though, our results show that CDH13 rich fibers delimit the

caudal boundary of the OTX2-positive MHB, no alterations in the orientation nor location of this isthmic organizer is observed in CDH13 deficient mice.

Previous studies implicating CDH13 in neurite outgrowth and axonal pathfinding (Bai, Ghoshal, & Jacob, 2006; Fredette et al., 1996; Fredette & Ranscht, 1994; Ranscht & Bronner-Fraser, 1991) prompted us to analyze the effect of CDH13 deficiency on the serotonergic innervation of the developing PFC. The PFC is a relevant region of study due to its associations with higher-order brain functions, such as attentional processes, working memory, and social cognition (Blakemore, 2008; Miller & Cohen, 2001). Our results revealed that at E17.5, CDH13 is strongly expressed throughout the developing cortex, including the PFC, a time point at which innervation of 5-HT afferents is also starting to develop (Vitalis et al., 2013). Alterations in molecules implicated in anterior-posterior orientation, midline guidance as well as axon elongation and maintenance, have been shown to affect projection of 5-HT axons (Kiyasova & Gaspar, 2011).

Our data indicate that in *Cdh13*$^{-/-}$ embryos, the innervation of serotonergic fibers in the PFC is increased (Forero et al., 2017). This is consistent with initial findings that CDH13 functions as a negative regulator in neurite outgrowth (Bai et al., 2006; Fredette et al., 1996; Fredette & Ranscht, 1994; Ranscht & Bronner-Fraser, 1991). The mechanism underlying CDH13-mediated inhibition of axon growth is not well-understood. The interaction of CDH13 with molecules such as lipid raft proteins (for review: Rivero et al., 2013), as well as the possible interaction with other members of the cadherin superfamily, such as CDH2 (N-Cadherin), might contribute to its inhibitory function in axonal pathfinding. For instance, it is known that the growth associated protein-43 (GAP43), a phosphoprotein that is essential in the wiring of serotonergic circuits, interacts with neural cell adhesion molecules associated with neurite outgrowth and axon guidance, such as NCAM, L1CAM and CDH2 (Donovan, Mamounas, Andrews, Blue, & McCasland, 2002). Likewise, CDH13 may also be among the cell adhesion molecules that GAP43 interacts with, thus impacting projection of 5-HT neurons (Forero et al., 2017).

Interestingly, the increase in 5-HT innervation present in embryonic *Cdh13*$^{-/-}$ mice does not persist into adulthood. In adult mice, 5-HT fiber density in the PFC is no longer significantly different compared to *Cdh13*$^{+/+}$ animals (Forero et al., 2017). This calls for the need of a longitudinal study of 5-HT innervation in relation to CDH13, in order to determine at which developmental timepoint this hyperinnervation is compensated and which are the mechanisms mediating this action.

The impact of CDH13 dysfunction on the development of the 5-HT system specifically and brain function in general may be relevant for the etiopathogenesis of neurodevelopmental disorders. For instance, disruption of *CDH13* by rare *de*

novo and inherited deletions that has been linked to autism spectrum disorders can generate changes in 5-HT system function (Sanders et al., 2011; Sanders et al., 2015). The relationship between altered 5-HT system function and these conditions has been amply discussed and reviewed (Gaspar et al., 2003; Kiser, Rivero, & Lesch, 2015; Lesch, 2016; Lesch & Waider, 2012). Our findings of altered 5-HT system development in *Cdh13*-deficient mice resulting in serotonergic hyperinnervation of the cortex is in line with the notion of a CDH13-driven pathogenetic mechanism affecting brain 5-HT system function in neurodevelopmental disorders.

Common *CDH13* variation is amply associated with neurodevelopmental and psychiatric disorders, particularly ADHD and comorbid conditions (Lasky-Su et al., 2008; Lesch et al., 2008; Lionel et al., 2011; Neale et al., 2008; Neale, Medland, Ripke, Anney, et al., 2010; Treutlein et al., 2009; Uhl, Drgon, et al., 2008; Uhl, Liu, et al., 2008; Zhou et al., 2008). Common variation in genes coding for various components of 5-HT transmission (e.g., *HTR1B, SLC6A4/5-HTT, TPH2*) has previously been associated with a susceptibility to ADHD, which may epistatically interact with *CDH13* variants. Alterations in the 5-HT system, such as reduced brain 5-HT function and 5-HT hyperinnervation, have been identified in animal model for ADHD (Banerjee & Nandagopal, 2015). 5-HT is believed to contribute to ADHD and its treatment indirectly through its interaction with the dopamine system (Gainetdinov et al., 1999). A connection between CDH13 and the brain dopamine system has been recently described (Drgonova et al., 2016). *Cdh13*$^{-/-}$ mice displayed alterations in the cortex including increased dopaminergic innervation, reduced levels of dopamine and an altered dopamine/metabolites ratio. In addition to alterations in 5-HT system function, dysregulation of dopaminergic signaling has consistently been implicated in ADHD. This combined involvement of at least two monoaminergic systems may thus represent a basis for the pervasive pathogenetic mechanisms of ADHD (Forero et al., 2017).

In conclusion, the results presented here provide evidence linking CDH13 with the formation of the 5-HT system in early embryonic stages. We show how dysregulation of CDH13 expression during development may contribute to alterations in 5-HT neuron migration and density in the DR. Additionally, constitutive CDH13 deficiency leads to impaired organization of serotonergic innervation and circuit formation in frontal cortex, thus impacting cognitive function, which may underlie the emergence of neurodevelopmental disorders (Forero et al., 2017). Nevertheless, further research is required to directly attribute 5-HT system alterations specifically to CDH13 function in 5-HT neurons.

4 | Altered serotonin system development in 5-HT neuron-specific Cadherin-13 knockout: impact on cognitive function

4.1. Objectives

In order to further clarify the relevance of CDH13 expression in the 5-HT system, a conditional knockout mouse line was developed where *Cdh13* is selectively eliminated from Pet1 expressing neurons. Pet1 is a transcription factor that is required for the acquisition of serotonergic specification and is active during the development of 5-HT neurons in the raphe nuclei (Hendricks et al., 2003; Kiyasova et al., 2011; Wyler, Donovan, Yeager, & Deneris, 2015; Wyler et al., 2016). Similar to the studies performed in the constitutive *Cdh13* knockout mouse model, a detailed morphological analysis was performed, which included the evaluation of 5-HT neuron density in the DR, as well as alterations in the innervation of its target regions in both adult and embryonic murine brains. In addition, due to the lack of behavioral data on this mouse line, a series of behavioral tests was also performed (Figure 4.1-1). The presented work and figures have been accepted for publication (Forero et al., 2020).

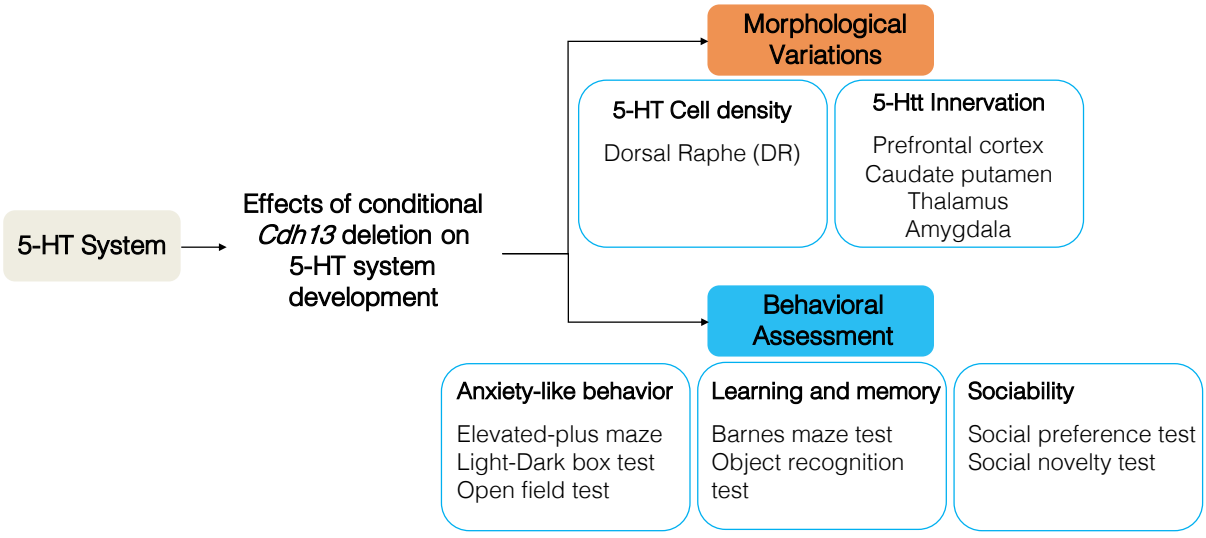

Figure 4.1-1. Outline of principal objectives of Project 2. This project focused on the effects of the conditional deletion of *Cdh13* in 5-HT neurons on morphological features such as 5-HT neuron density and 5-Htt target region innervation. Furthermore, a behavioral assessment of the *Cdh13* cKO mouse line was conducted.

4.2. Results

4.2.1. Conditional *Cdh13* inactivation in Pet1-positive neurons increases 5-HT neuron density in the developing dorsal raphe

Given the contribution of CDH13 to the proper formation of the DR and 5-HT innervation of the PFC in early embryonic stages of development (Forero et al., 2017), we aimed to study if the specific deletion of *Cdh13* from 5-HT neurons is sufficient to generate the altered phenotypes observed in constitutive *Cdh13* knockout embryos. We generated a conditional knockout mouse line where CDH13 is selectively eliminated from *Pet1* expressing neurons (Dai et al., 2008). Pet1 is a transcription factor that is required for the acquisition of serotonergic identity and expression of 5-HT system-related genes in all 5-HT neurons of the raphe nuclei (Hendricks et al., 2003; Kiyasova et al., 2011; Wyler et al., 2015; Wyler et al., 2016).

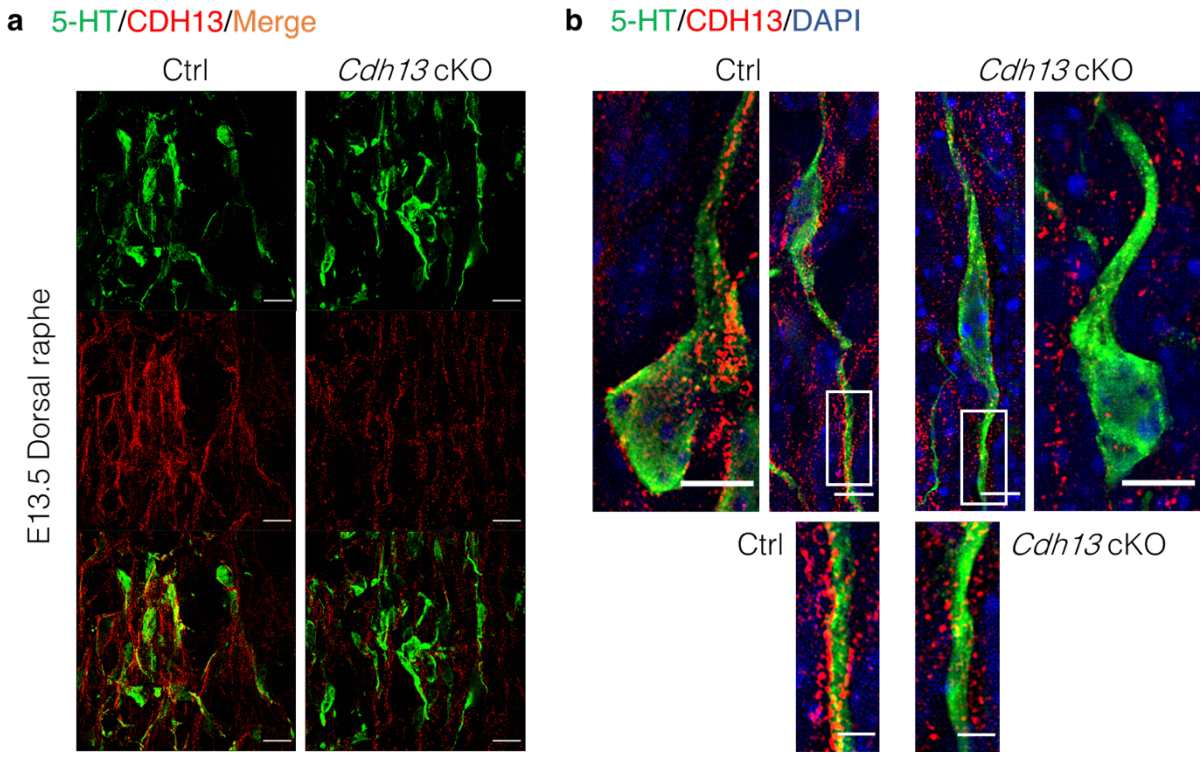

Figure 4.2.1-1. Comparative immunofluorescence of CDH13 in *Cdh13* conditional knockout vs. control embryonic brains using SIM. (a) CDH13 immunoreactivity in the DR is considerably lower in *Cdh13* cKO mice compared to Ctrl mice. (b) Close up image showing expression of CDH13 in a 5-HT-positive neuron; at a cellular level, CDH13 does not cluster along 5-HT neuron extensions in *Cdh13* cKO brains as it does in Ctrl animals. Orientation: sagittal. Scale bars: (a) 10 µm, (b) 5 µm; close-up 2 µm. Adapted from Forero et al., 2020.

As shown in Figure 4.2.1-1a, immunofluorescence staining of both CDH13 and 5-HT in combination with super-resolution imaging by SIM (Gustafsson, 2000; Wegel et al., 2016) confirmed a considerable decrease of CDH13 in the DR of *Cdh13* cKO mice compared to Ctrl mice. Additionally, super-resolution microscopy at single 5-HT-positive neurons in *Cdh13* cKO embryos revealed that CDH13 does not appear to cluster in the extending neurites or soma of these cells, as it is observed in Ctrl mice (Figure 4.2.1-1b). Traces of CDH13-ir were still observed and outline 5-HT-positive neurons. This indicates that this immunoreactivity is most likely coming from adjacent cells, such as RGCs (Forero et al., 2017).

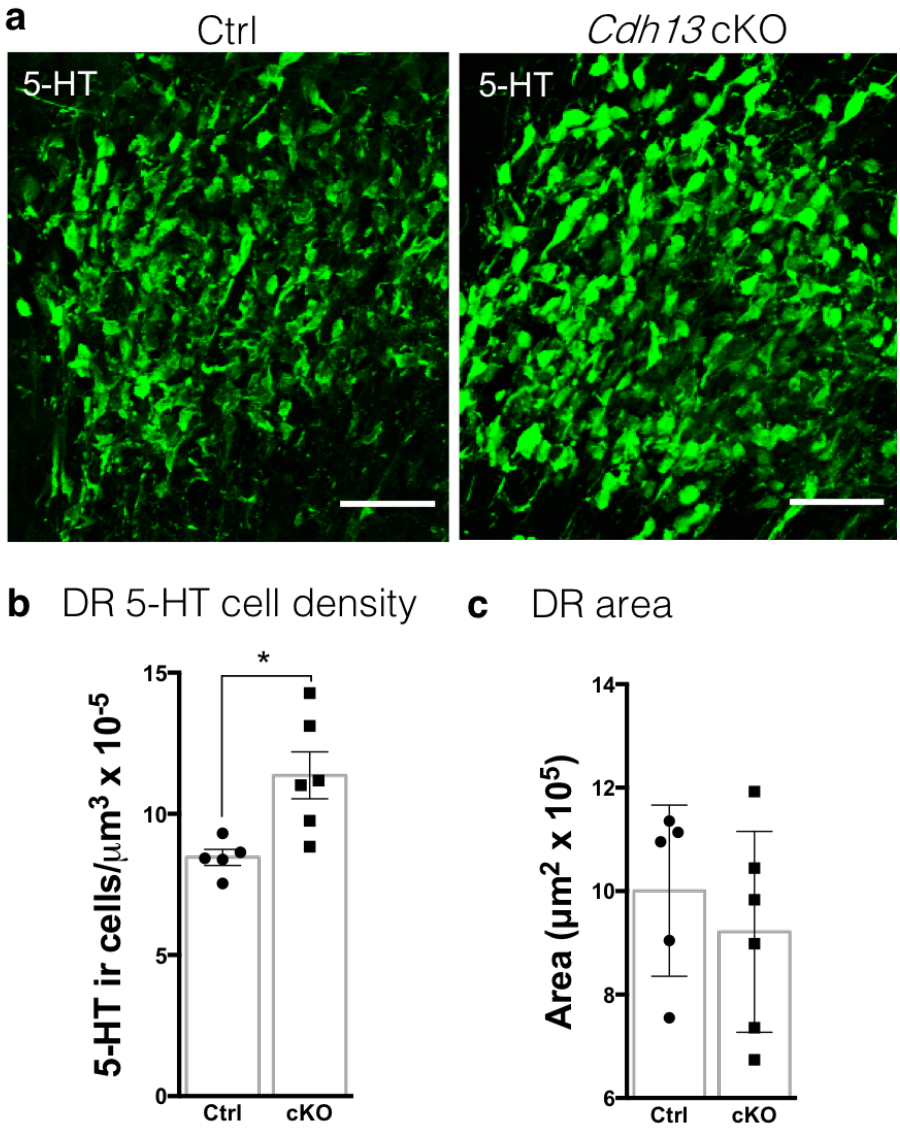

Figure 4.2.1-2. Dorsal raphe 5-HT neuron density and area at E13.5. (a) Representative images of the DR show an increase in 5-HT neuron density in *Cdh13* cKO embryonic brains compared to Ctrls. (b) Quantification of these cells results in a significant increase of 5-HT-positive neurons (Ctrl, n=5; *Cdh13* cKO, n=6; P=0.0138). (c) No difference is observed in the area occupied by 5-HT-positive neurons between *Cdh13* cKO and Ctrls (Ctrl, n=5; *Cdh13* cKO, n=6; P=0.489). Orientation: sagittal. Scale bar 50 µm. Data presented as mean ± s.e.m. *P<0.05. Adapted from Forero et al., 2020.

Once the loss of CDH13 in 5-HT neurons was confirmed in *Cdh13* cKO animals, an initial quantification of the density of 5-HT neurons in the DR at E13.5 was performed. As previously observed in *Cdh13* constitutive knockout mice, our results indicate a significant increase in the cell density of 5-HT-positive neurons in *Cdh13* cKO embryos. While Ctrl animals present an average of $8x10^{-5}$ cells/μm^3 in the DR, *Cdh13* cKO mice have a density of approximately $11x10^{-5}$ cells/μm^3 (*P*=0.0138, Figure 4.2.1-2). No significant difference was found in the DR area between *Cdh13* cKO and Ctrls.

4.2.2. CDH13 deficiency restricted to Pet1-positive neurons increases 5-HT innervation of cortical regions during embryonic stages.

The increase in 5-HT neuron density in the developing DR of *Cdh13* cKO mice led us to investigate the serotonergic innervation of the cortex at E17.5. As it is shown in Figure 4.2.2-1, we measured the area occupied by 5-HT-positive fibers in two regions: the prefrontal cortex (PFC) that will become a relevant cortical region in cognitive functioning, and the somatosensory cortex (SSC) that is shown to be highly affected by 5-HT system alterations during cortical development (Teissier et al., 2017).

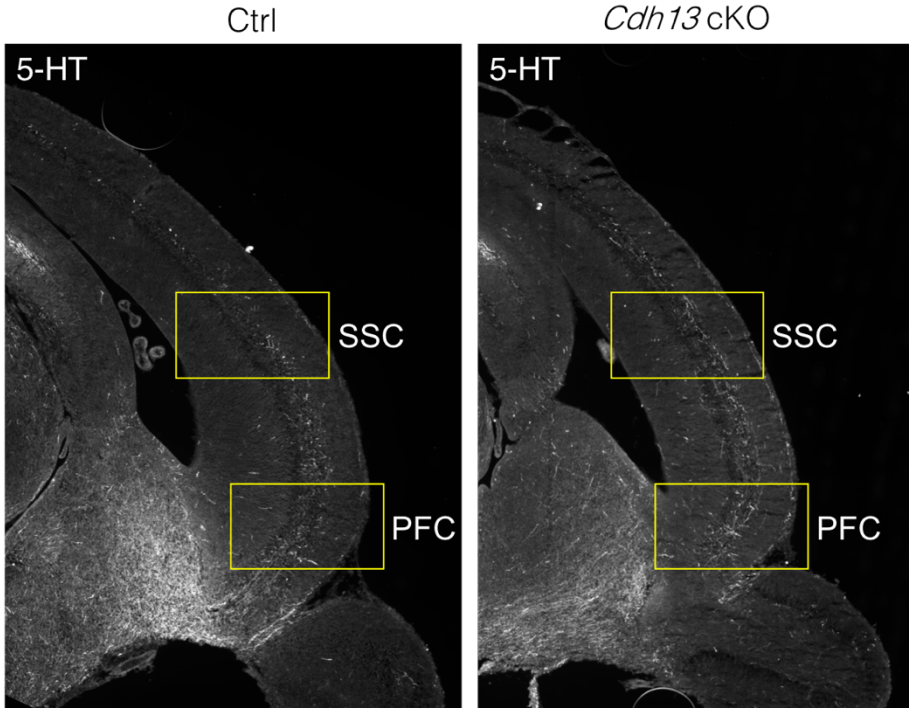

Figure 4.2.2-1. Localization of the prefrontal and somatosensory cortices in the embryonic mouse brain at E17.5. Yellow lines delimit prefrontal cortex (PFC) and somatosensory cortex (SSC). Orientation: sagittal. Scale bar 100 µm. Adapted from Forero et al., 2020.

Our findings show that the absence of CDH13 in 5-HT neurons results in an increase of 5-HT-positive fibers in the developing cortex (Figure 4.2.2-2). In both areas analyzed, the PFC and the SSC, a significant difference between *Cdh13* cKO and Ctrl mice was identified (PFC: *P*=0.0403; SSC: *P*=0.0114; Figure 4.2.2-2).

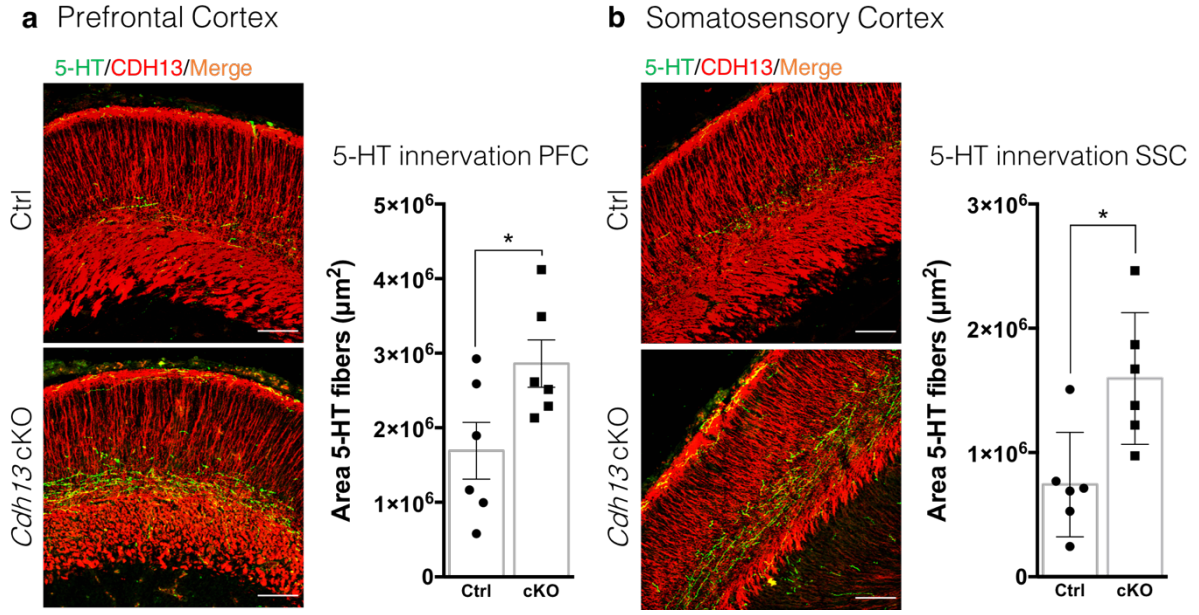

Figure 4.2.2-2. Serotonergic innervation in the prefrontal and somatosensory cortical areas at E17.5. (a) Representative images of CDH13 and 5-HT expression in the PFC. *Cdh13* cKO mice show a significant increase in 5-HT innervation of the PFC compared to Ctrl animals (n=6 per genotype; *P*=0.0403). (b) Representative images of CDH13 and 5-HT expression in the SSC. *Cdh13* cKO mice also show a significant increase in 5-HT innervation of the SSC compared to Ctrl mice (n=6 per genotype; *P*=0.0114). Orientation: sagittal. Scale bar 100 µm. Data presented as mean ± s.e.m. **P*<0.05. Adapted from Forero et al., 2020.

4.2.3. *Cdh13* inactivation in 5-HT neurons differentially alters the number of Tph2-positive neurons in subgroups of the adult dorsal raphe

We next investigated whether the effects on 5-HT neuron density observed in the embryonic DR of *Cdh13* cKO persist into adulthood. Due to the heterogeneity in the identity and projection of the cells constituting the adult DR, a more detailed quantification of Tph2-positive neurons in this region was carried out. We analyzed three subgroups of the DR: the dorsal DR (B7d), the ventral DR (B7v) and the lateral DR (B7l) (Figure 4.2.3-1).

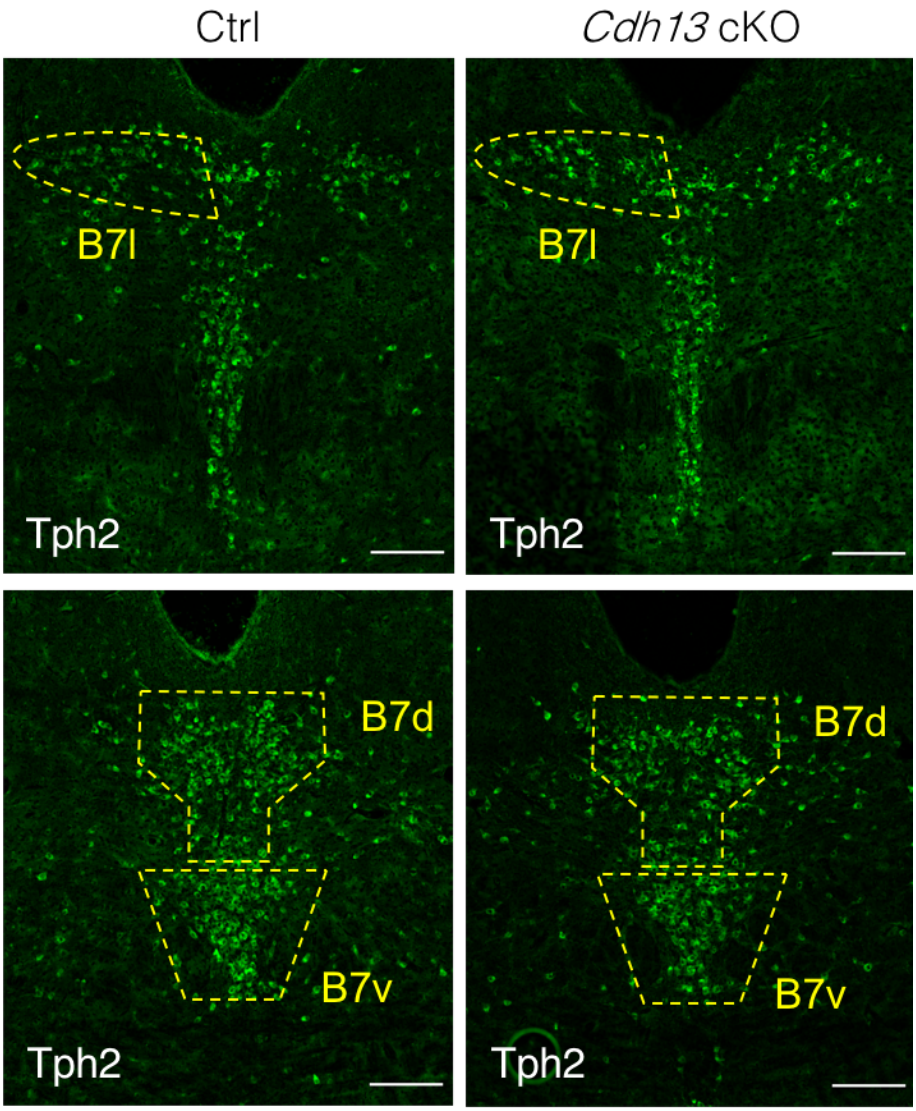

Figure 4.2.3-1. Localization of Tph2-positive neurons in subgroups of the dorsal raphe in adult mice. Yellow lines delimit the lateral (B7l), ventral (B7v) and dorsal (B7d) subgroups of the DR that were evaluated. Orientation: coronal. Scale bar 200 µm. Adapted from Forero et al., 2020.

Our results show that the number of Tph2-positive neurons is differentially altered in these DR subgroups in the absence of CDH13. Specifically, we observed an increase in Tph2-positive neurons in the lateral (P=0.0041) and ventral (P=0.0132) DR regions of *Cdh13* cKO mice compared to Ctrl littermates (Figure 4.2.3-2a, b). However, no difference was detected in the dorsal DR nucleus (Figure 4.2.3-2c).

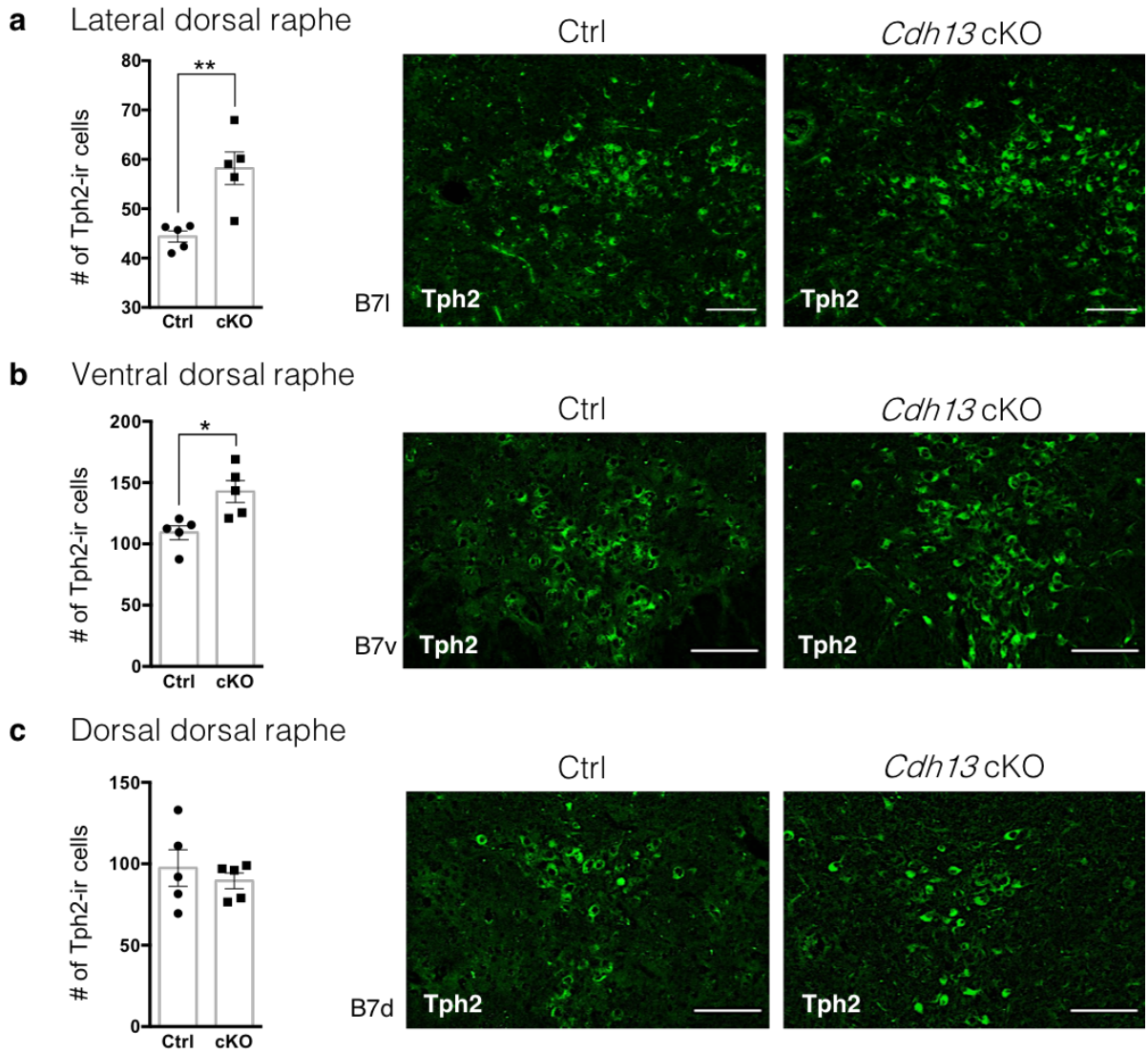

Figure 4.2.3-2. Quantification of Tph2-positive neurons in the lateral (B7l), ventral (B7v) and dorsal (B7d) subgroups of the dorsal raphe in adult mice. (a,b) *Cdh13* cKO mice significantly differ in the Tph2 cell density of B7l (A; n=5 per genotype; P=0.0041) and B7v (B; n=5 per genotype; P=0.0132), showing a higher cell number compared to Ctrl mice. (c) No differences in cell density were observed in the dorsal DR (B7d). Orientation: coronal. Scale bar 100 µm. Data presented as mean ± s.e.m. *P<0.05, **P<0.01. Adapted from Forero et al., 2020.

4.2.4. Altered serotonergic innervation of forebrain regions targeted by the ventral (B7v) subgroup of the dorsal raphe nucleus in conditional *Cdh13* knockouts

Since conditional CDH13 deficiency led to a differential alteration in the cell number of Tph2-positive neurons only in the lateral and ventral DR subgroups, we analyzed the serotonergic innervation of the regions that these cells project to. A robust study using conditional anterograde tracing identified the lateral thalamus, the mammillary bodies, the superior colliculus, and the facial cranial nerve as the main targets of the lateral DR, while the frontal and prefrontal cortex, amygdala, piriform cortex, and olfactory bulb were identified as the targets of the ventral DR (Muzerelle et al., 2016). We decided to analyze 5-Htt fiber density in the lateral

and median thalamus, prefrontal cortex, caudate putamen and amygdala, as these brain regions are known to have a high relevance in the development of psychiatric conditions.

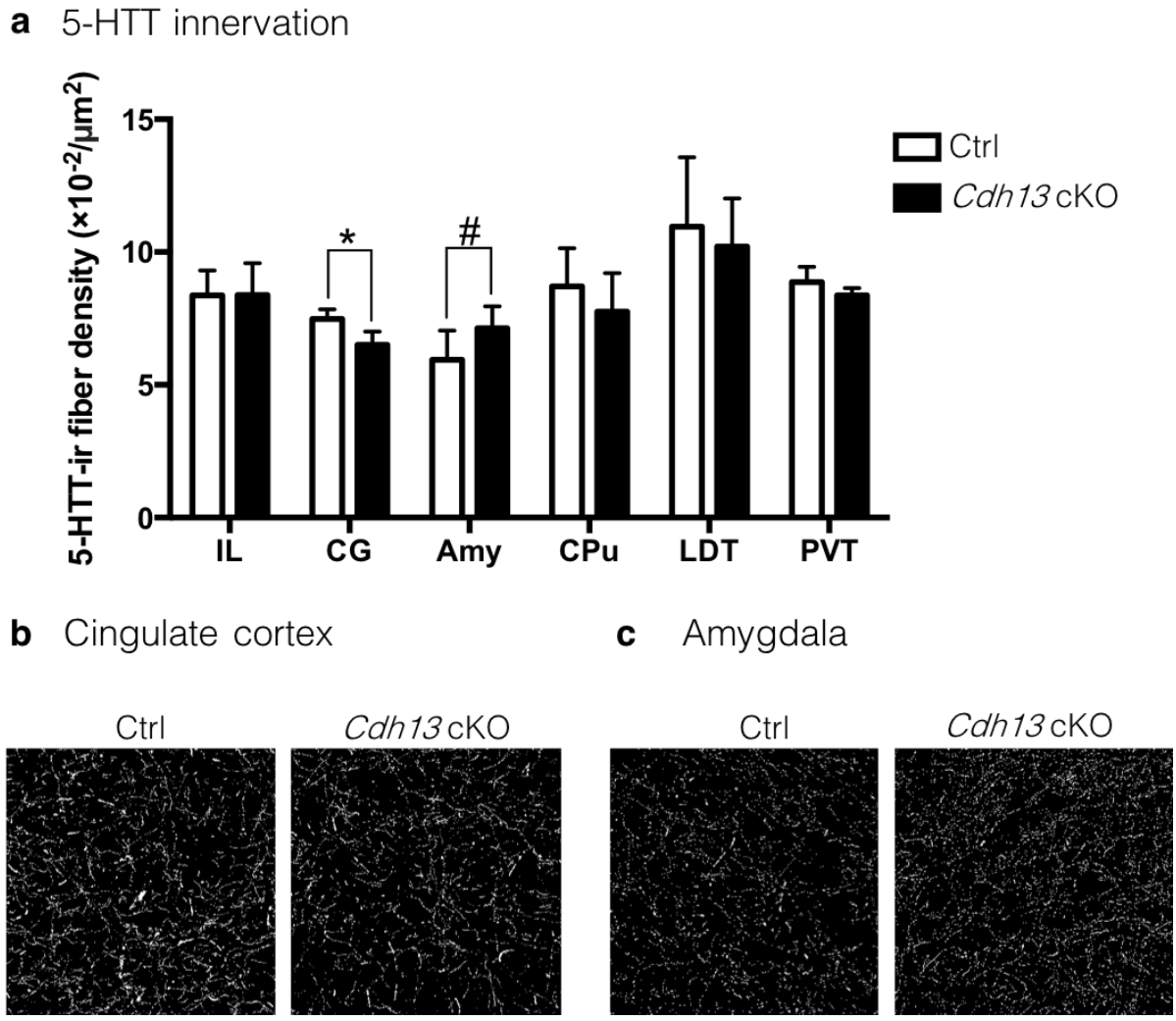

Figure 4.2.4-1. Quantification of 5-Htt innervation in target regions of the dorsal raphe in adult mice. *Cdh13* cKO mice have a significantly decreased 5-Htt- fiber density in the cingulate cortex compared to Ctrl animals (a, b; n=4 per genotype; P=0.0187). Also, a trend toward increased 5-Htt innervation in the amygdala is observed in *Cdh13* cKO mice (a, c; n=6 per genotype; P=0.0598). IL, infralimbic cortex; CG, cingulate cortex; Amy, amygdala; CPu, caudate putamen; LDT, laterodorsal thalamus; PVT, paraventricular thalamus. Data presented as mean ± s.e.m. #P<0.1, *P<0.05. Adapted from Forero et al., 2020.

Our results show a variation in the serotonergic innervation in some of these brain regions in *Cdh13* cKO mice. Specifically, we observed a significantly altered innervation in the cingulate cortex and a trend towards significance in the amygdala; both of which are mainly B7v target regions (Figure 4.2.4-1).

4.2.5. CDH13 deficiency restricted to 5-HT neurons is associated to alterations in learning and impulsivity

Cdh13 cKO mice were subjected to behavioral tests to evaluate the specific effects of 5-HT neuron-specific CDH13 deficiency on anxiety-like behavior, learning and memory, as well as sociability. The analysis revealed no significant genotype effects on anxiety-like behavior, in the elevated plus maze (EPM), the light/dark box (LDB) and the open field (OF) tests (Figure 4.2.5-1).

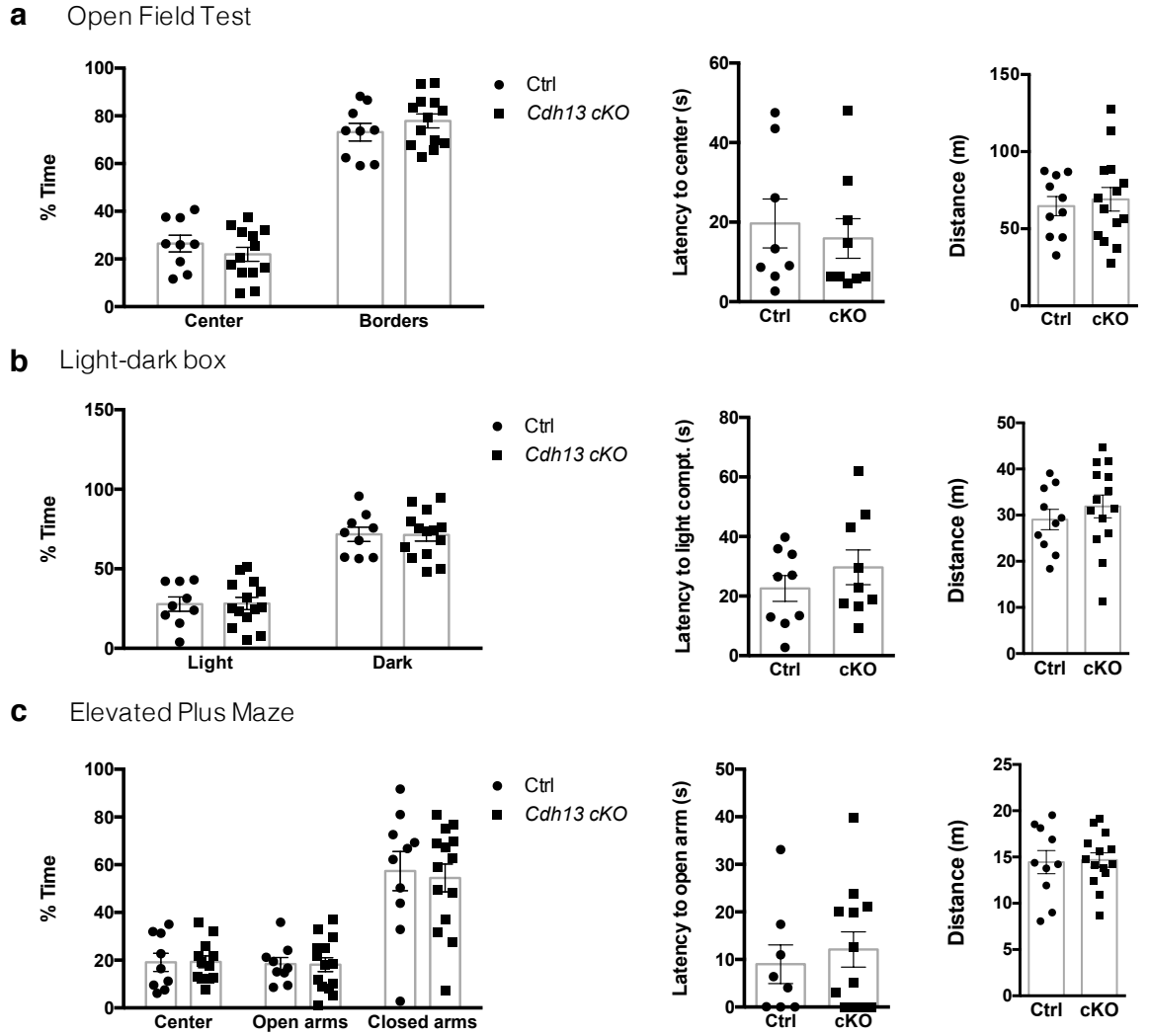

Figure 4.2.5-1. Behavioral assessment of anxiety-like behavior in *Cdh13* conditional knockout mice. No significant differences were observed between *Cdh13* cKO and Ctrl mice in the open field test (a; Ctrl, n=9; *Cdh13* cKO, n=13), light-dark box (b; Ctrl, n=9; *Cdh13* cKO, n=14), and elevated plus maze (c; Ctrl, n=9; *Cdh13* cKO, n=14). Data presented as mean ± s.e.m. Adapted from Forero et al., 2020.

No difference was detected in the time spent in the center versus the borders in the OF (Figure 4.2.5-1a), in the light versus dark compartment in the LDB (Figure 4.2.5-1b), and in the open arms compared to closed arms in the EPM (Figure 4.2.5-1c). Similarly, the total distance travelled and the latencies in all tests conducted did not vary significantly between *Cdh13* cKO and Ctrl mice (Figure 4.2.5-1).

The novel object recognition test was performed as an initial evaluation of recognition memory abilities. However, the ability of the *Cdh13* cKO mice to discriminate between a familiar and a novel object could not be evaluated because the majority of the *Cdh13* cKO animals did not reach the minimum exploration time of 20 s of the familiar object (Figure 4.2.5-2). If this parameter is not met, it is not possible to calculate the discrimination index since it is assumed that the mice did not come in contact with the familiar object enough to later be able to recognize it when presented together with an unfamiliar object.

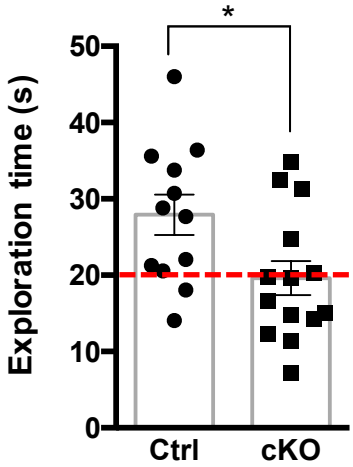

Figure 4.2.5-2. Behavioral assessment of learning and memory through the novel object recognition test. Most of the *Cdh13* cKO mice did not explore the familiar object for a minimum of 20 s (red dotted line) and therefore their recognition memory could not be evaluated (Ctrl, n=12; cKO, n=14; P= 0.024). Data presented as mean ± s.e.m. *P<0.05. Adapted from Forero et al., 2020.

The Barnes Maze (BM) test was used to assess deficits in visuospatial learning and memory. Our results show that all mice were able to learn the location of the escape hole within the allocated given time period. However, a clear delay in the learning process was found in *Cdh13* cKO mice. We observed an increased number of primary errors during the early phases of training and more specifically at the second and fourth days of investigation (Figure 4.2.5-3a; Day 2 P= 0.0066; Day 4 P= 0.0086). A similar effect was observed, in the first trial after a 24 h intermission (Figure 4.2.5-3a; Day 5 P= 0.0297). However, this difference was no longer detectable in the final days of testing, with the *Cdh13* cKO mice committing the same number of errors as Ctrl animals.

Additionally, we observed that *Cdh13* cKO mice showed a significantly shorter latency to start carrying out the task compared to Ctrl animals, both in the initial testing phase as well as in the testing phase after a 24-hour pause (Figure 4.2.5-3b; Pre-pause P= 0.014; Post-pause P= 0.001). As we could not observe a locomotor-initiation phenotype in the open field test, the observed shorter latency in the BM might suggest increased impulsivity or motivation to start exploration.

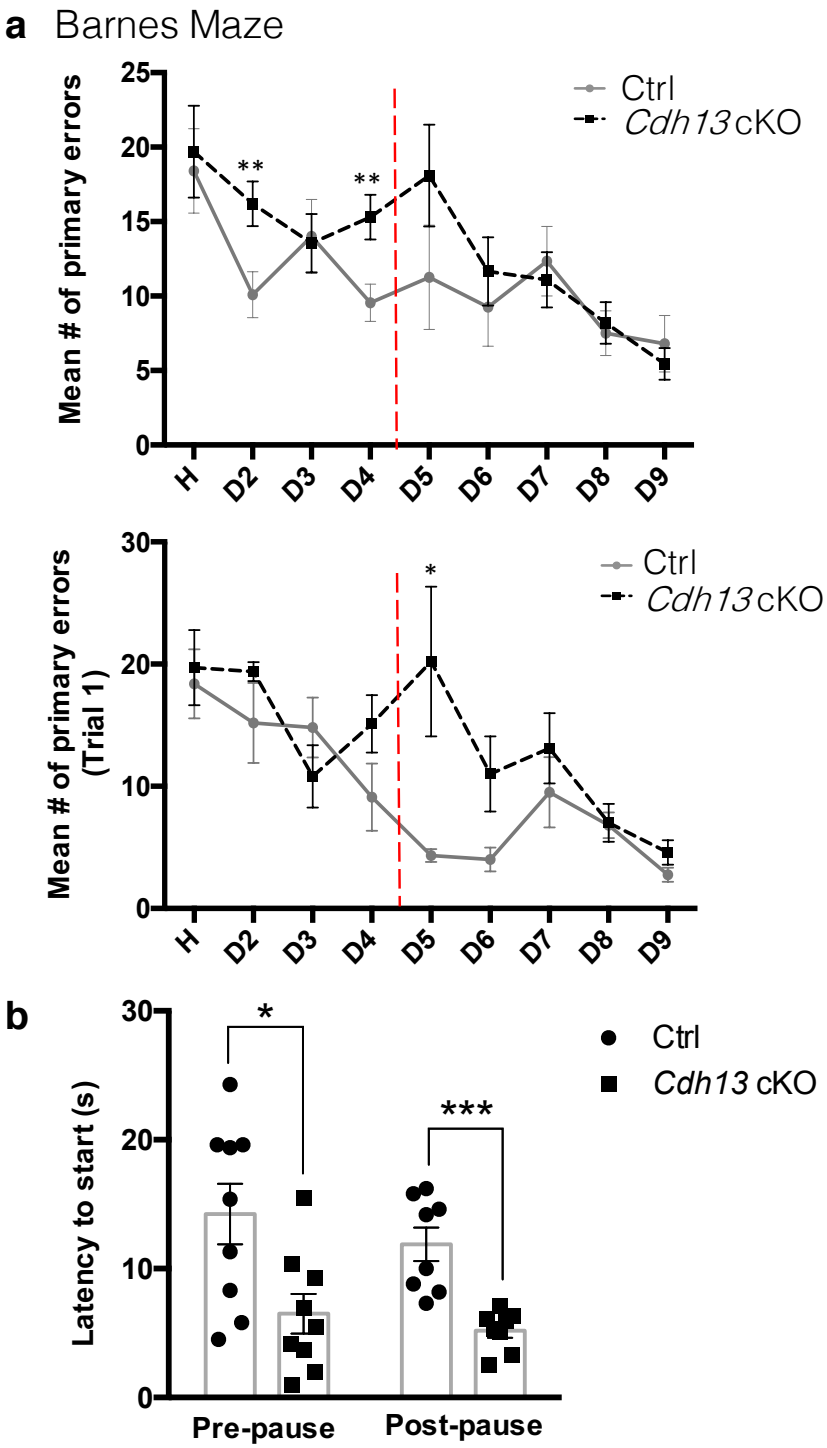

Figure 4.2.5-3. Behavioral assessment of visuospatial learning and memory through the Barnes Maze (BM) test. (a) A significant increase in the number of primary errors committed by *Cdh13* cKO mice compared to Ctrl animals is observed in early stages (n=10 per genotype; D2 P= 0.0066; D4 P= 0.0086), as well as in the first trial after a 24h pause (n=10 per genotype; D5 P= 0.0297; D6 P= 0.0411; 24 h intermission represented by red dotted line). (b) *Cdh13* cKO mice show a significant decrease in the latency to start exploring both in the pre-pause (n=9 per genotype; P= 0.014) and post-pause (n=8 per genotype; P=0.001) phases. Data presented as mean ± s.e.m. *P<0.05, **P<0.01, ***P<0.001. Adapted from Forero et al., 2020.

In order to assess deficits in social interaction and social recognition memory in *Cdh13* cKO mice, we applied a social interaction test, which consists of two consecutive paradigms that evaluate sociability and social novelty preference. During the first trial (sociability; Figure 4.2.5-4a), all mice spent more time interacting with a cage containing a mouse rather than with an empty cage; no genotype differences were detected between *Cdh13* cKO animals and Ctrl littermates. However, a difference in the latency to interact was observed, with *Cdh13* cKO mice being significantly quicker to start exploring the unfamiliar mouse (Figure 4.2.5-4a; P= 0.0085). In addition, a tendency to a reduced latency to explore the empty cage was also observed in *Cdh13* cKO mice (Figure 4.2.5-4a; P= 0.0523). During the second trial performed 30 min later (social novelty preference; Figure 4.2.5-4b), all mice spent longer time with the novel mouse rather than with the familiar mouse, indicating that social recognition memory was intact in the *Cdh13* cKO mice. No genotype difference was observed in the latencies during the social novelty preference task (Figure 4.2.5-4b).

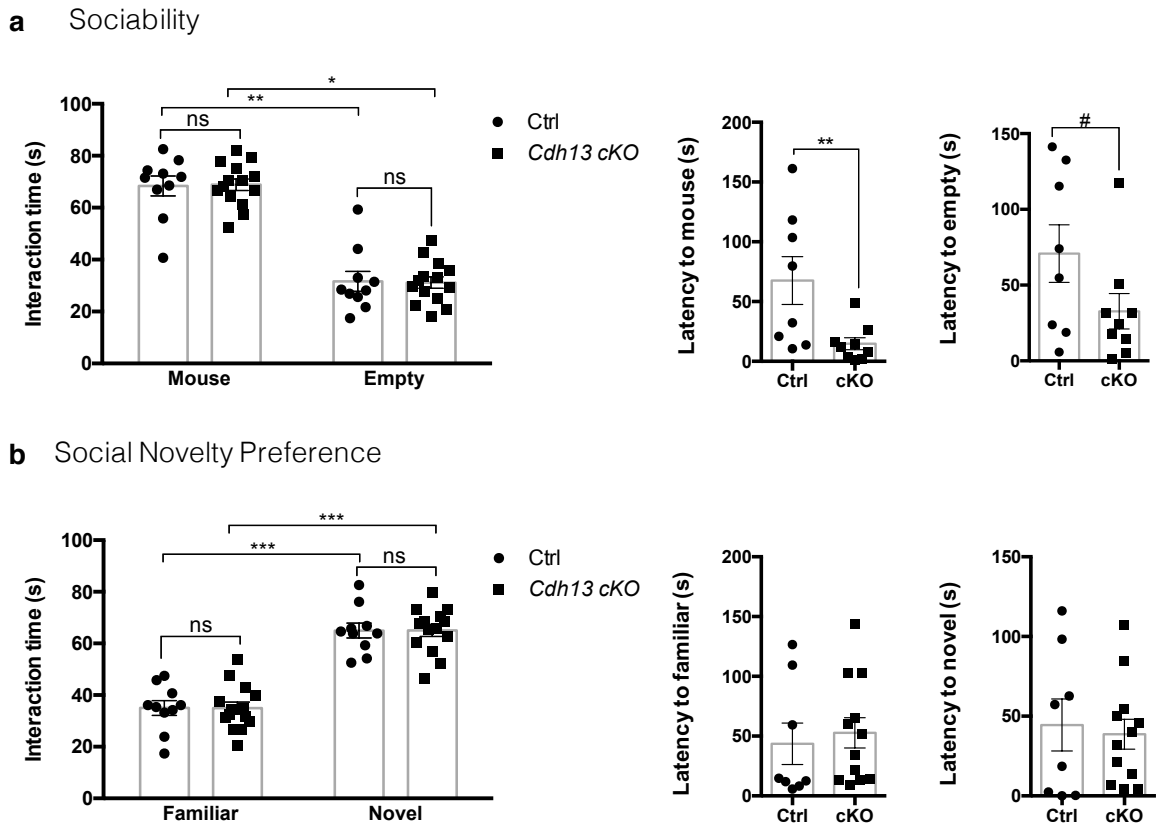

Figure 4.2.5-4. Assessment of social interaction in *Cdh13* conditional knockout mice. (a, b) No genotype difference is observed in sociability and social novelty preference between *Cdh13* cKO and Ctrl mice (Ctrl, n=10; cKO, n=14). However, *Cdh13* cKO do present a significantly reduced latency to interact with the test animal in the sociability test compared to Ctrl animals (Ctrl, n=10; *Cdh13* cKO, n=11; P= 0.0085), as well as, a tendency in the latency to explore the cage presented (Ctrl, n=10; *Cdh13* cKO, n=11; P= 0.0523). Data presented as mean ± s.e.m. #P<0.1, *P<0.05, **P<0.01, ***P<0.00. Adapted from Forero et al., 2020.

4.3. Discussion

The contribution of CDH13 to various neuronal and non-neuronal cellular processes has emphasized its relevance in brain development and function. However, a major remaining challenge is the in-depth study of this protein with relation to the brain serotonin system. The results presented in Project 1 strongly imply the modulation of CDH13 in DR formation and 5-HT innervation in the embryonic and adult murine brain (Forero et al., 2017). However, the impact of constitutive CDH13 deficiency on 5-HT system alterations could not be directly attributed to CDH13 function in 5-HT neurons. The findings we present in this follow-up project allows that by providing evidence that CDH13 deficiency exclusively in 5-HT neurons is sufficient to modify the development of the brain 5-HT system and generate behavioral alterations in mice.

The selective deletion of *Cdh13* increases 5-HT neuron density in the embryonic DR, with persistence into adulthood, and serotonergic hyperinnervation of the developing prefrontal cortex. In the adult brain, CDH13 deficiency exclusively affects the 5-HT neuron density in the lateral (B7l) and ventral (B7v) subgroups of the DR as well as the innervation of the cingulate cortex, a region specifically targeted by the ventral DR subgroup. At the behavioral level, adult *Cdh13* cKO mice display delayed acquisition of several learning tasks and a subtle impulsive-like phenotype, with decreased latency in the sociability paradigm alongside with deficits in visuospatial memory (Forero et al., 2020). No anxiety-related behaviors were observed in *Cdh13* cKO mice. The cellular alterations in the 5-HT network might be responsible for the cognitive deficits and other behavioral features observed in *Cdh13* cKO mice (Forero et al., 2020).

The brain 5-HT system is of considerable relevance to numerous neurodevelopmental and psychiatric conditions, due to its regulatory role in basic cellular processes, such as migration and differentiation of neurons (Gaspar et al., 2003; Lesch & Waider, 2012), but also in the development and plasticity of other transmission systems (Whitaker-Azmitia, 2001). Therefore, the search for modulators of 5-HT neuron development and function is fundamental in neurobiology.

Here, the *Cdh13* conditional knockout mouse serves as a practical tool for a detailed screening of the relationship between CDH13 specifically in the brain 5-HT system. Notably, serotonergic specific *Cdh13* cKO mice display alterations in the 5-HT DR system (i.e. increased 5-HT neuron density), which are similar to those observed in the *Cdh13* constitutive knockout mice. Therefore, we provide evidence that adequate formation of this serotonergic nucleus is directly affected by CDH13 expression, and even though we may hypothesize that other factors are also involved in early prenatal neurodevelopmental processes, the absence of

CDH13 alone from 5-HT expressing neurons is sufficient to lead to morphological and behavioral consequences.

Cdh13 cKO embryos also display serotonergic hyperinnervation in the developing cortex. Cadherins are known to be one of the many molecular cues that provide assistance to establish functional neural circuits through guidance of axons to their specific targets during development (Van Battum, Brignani, & Pasterkamp, 2015). However, only a few members of this superfamily have been implied in 5-HT neuron development in the context of proper target-specific innervation by projecting fibers (Chen et al., 2017; Forero et al., 2017; Hayano et al., 2014; Katori et al., 2009). In this regard, protocadherin-α is strongly expressed in 5-HT neurons and its selective deletion from 5-HT neurons in mice led to abnormal distribution of 5-HT projections in several brain regions (Katori et al., 2009; Katori et al., 2017). Similarly, our results indicate that absence of CDH13 in the 5-HT system enhances the serotonergic innervation in the prefrontal cortex, a brain region that plays a critical role in executive function and decision making, as well as in the somatosensory cortex, a region sensitive to 5-HT system alterations during development (Bennett-Clarke, Leslie, Lane, & Rhoades, 1994; Cases et al., 1996; Miceli et al., 2013). Considering the link between *CDH13* genetic variation and ASD vulnerability, these findings are in agreement with the increase in 5-HTT-immunoreactive axons in the cortex of ASD patients (Azmitia, Singh, & Whitaker-Azmitia, 2011).

The serotonergic hyperinnervation observed in *Cdh13* cKO embryos appears to be accompanied by an increase in 5-HT levels in cortical areas. Coherent with the increased area of 5-Htt-positive fibers in the PFC, HPLC analysis revealed a significant increase of 5-HT levels in the PFC of *Cdh13* cKO embryos at E17.5, when compared to Ctrl littermates (Forero et al., 2020). Notably, hyperserotonemia is one of the most reliable biomarkers in ASD (Ruggeri, Sarkans, Schumann, & Persico, 2014). Although it is not clear which are the consequences that this increased level of serotonin has on ASD pathophysiology, the effects of elevated serotonin levels during early neurodevelopment have been extensively studied using 5-Htt (*Slc6a4*)-deficient mice. The lifelong increase of extracellular 5-HT in cortical regions detected in those mice (Fox et al., 2007; Mathews et al., 2004) leads to an abnormal distribution of GABAergic interneurons in the cerebral cortex (Riccio et al., 2009), which may affect the excitatory-inhibitory balance of brain circuits, one of the underlying mechanisms that have been proposed for several neurodevelopmental disorders (Marin, 2012; Penzes, Buonanno, Passafaro, Sala, & Sweet, 2013; Selten, van Bokhoven, & Nadif Kasri, 2018). Given the existing link between CDH13 deficiency and alterations in the GABAergic system (Paradis et al., 2007; Rivero et al., 2015; Tantra et al., 2018), it would be of utmost relevance to further study the interaction between the serotonergic and GABAergic systems in the *Cdh13* cKO mouse.

Complementary to our investigations of the embryonic brain, we also aimed to clarify how the effects of CDH13 deficiency in 5-HT neurons persisted in the adult brain and ultimately, how behavior was affected. Because the alterations in 5-HT neuron density were only restricted to the lateral and ventral subregions of the adult DR and given the specific properties of each DR serotonin subsystem (Ren et al., 2018) , we subsequently quantified 5-Htt innervation in multiple brain regions that are known to be innervated by these two DR subnuclei (Muzerelle et al., 2016). Contrary to our expectations, we observed that serotonergic innervation was significantly reduced in the cingulate cortex of *Cdh13* cKO mice and unchanged in the infralimbic cortex. Although difficult to explain without any additional data, we speculate that there are compensatory mechanisms in the developing cortex of conditional KO mice that counterbalance the effects produced by CDH13 deficiency and might lead to reduced innervation when adulthood is reached. Serotonergic PFC innervation is shown to be a dynamic process which involves regulatory processes that decrease its density and generate changes in fiber and synapse morphology as age advances (Maddaloni et al., 2017). This same regulation might be involved in the shift that we observe from 5-HT hyperinnervation in late embryonic stages to largely normal innervation in the adult prefrontal cortex and subcortical regions in *Cdh13* cKO mice. In addition, considering the key role of homophilic interactions for cadherin function, the different levels of CDH13 expression throughout the mouse brain (Rivero et al., 2013) might help to understand the variability in the effects induced by CDH13 deficiency in serotonergic fibers.

Correlating with the structural changes in the DR-related serotonergic network, behavioral assessment revealed that the conditional deletion of CDH13 in the 5-HT neurons also had an effect on the acquisition in the Barnes Maze test, a visuo-spatial learning test, and decreased latency in the sociability paradigm. Contrasting this effect, *Cdh13* cKO mice did not differ from controls with respect to locomotor activity or anxiety-like behavior. This finding also agrees with the view of neurodevelopmental disorders as complex conditions where different (genetic and/or environmental) risk factors may mediate specific aspects of the disorder (in this case, cognitive dimensions).

The delayed learning and memory acquisition we observed in *Cdh13* cKO mice is analogous to the moderate learning deficits that are widely reported in ADHD patients (McCann & Roy-Byrne, 2000), and also very similar to the learning deficits we observed in mice (Rivero et al., 2015) and rats (King et al., 2017) with a constitutive inactivation of CDH13. This similarity supports the view that the effect of CDH13 on cognition is largely mediated by its role in serotonergic function, although the (direct or indirect) influence from other systems (e.g. GABAergic) should be considered.

Notably, *Cdh13* cKO mice display a reduced latency in the BM and sociability tests, which may be interpreted as a result of increased impulsivity-like traits or differences in attention to novel stimuli. Testing paradigms have identified the following essential features of increased impulsivity in individuals: (1) shortened response latency to stimulation, (2) difficulty in the ability to inhibit responses and/or (3) increased action (Pattij & Vanderschuren, 2008). With the battery of behavioral tests conducted, we were able to identify two of these features in our mice. Particularly, *Cdh13* cKO mice were significantly faster to respond, therefore exhibiting a shortened response latency in the BM and the sociability test. *Cdh13* cKO also committed a higher number of primary errors in the BM, which could be interpreted as an increase in action.

In addition, an impulsive-like phenotype has recently been identified in *Cdh13* cKO mice in the 5-choice serial-reaction time task (5-CSRTT), a behavioral test used to evaluate visuospatial attentional performance and motor impulsivity (Forero et al., 2020). During the training phase of this test, *Cdh13* cKO mice made more premature responses, an effect that was not detected once the task was acquired, however (Forero et al., 2020). The impulsive-like behaviors we observed may be associated with the altered serotonergic innervation in the cingulate cortex. The integrity and balanced transmission in the anterior cingulate cortex (ACC) are important for inhibitory response control (Hvoslef-Eide et al., 2018), while the extracellular levels of 5-HT in the medial PFC are positively correlated to the premature responses in the 5-CSRTT (Dalley & Roiser, 2012) as well as in the delay discounting task (Winstanley, Theobald, Dalley, Cardinal, & Robbins, 2006). However, further investigation is needed to clarify the existence of a link between the observed impulsive-like phenotype and the detected molecular and cellular changes in the ACC.

In conclusion, we show that inactivation of CDH13 specifically in 5-HT neurons correlates with an increased density of 5-HT neurons in the developing DR and in specific subnuclei of the adult DR, as well as changes in serotonergic innervation of the developing and adult PFC. Notably, conditional CDH13 deficiency is also enough to induce specific cognitive alterations in adult mice that correlate with the specific clinical features observed in neurodevelopmental and psychiatric disorders.

5 | Use of super-resolution microscopy for the visualization of CDH13 in human induced pluripotent stem cells (iPSC)-derived neurons

5.1. Objectives

The possibility of generating human induced pluripotent stem cells (iPSC) and the option to differentiate them into various neuronal cell types has opened a new horizon in understanding the biophysical aspects of neuropsychiatric conditions. For this reason, the adaptation of tools such as super-resolution microscopy for the study of these cells is of great relevance.

In close collaboration with doctoral student C. Jansch (Division of Molecular Psychiatry, Center of Mental Health, University of Würzburg), and Dr. S. Wäldchen (Department of Biotechnology and Biophysics, Biocenter, University of Würzburg), we aimed to establish and optimize two super-resolution microscopy techniques for localization of CDH13 in induced human cells with serotonergic hallmarks: (1) Structured Illumination Microscopy (SIM) and (2) direct Stochastic Optical Reconstruction Microscopy (*d*STORM). The first was used to visualize the expression of CDH13 in TPH2-positive neurons, while the second was used to image synaptic markers Bassoon and Homer also in TPH2-positive neurons (Figure 5.1-1).

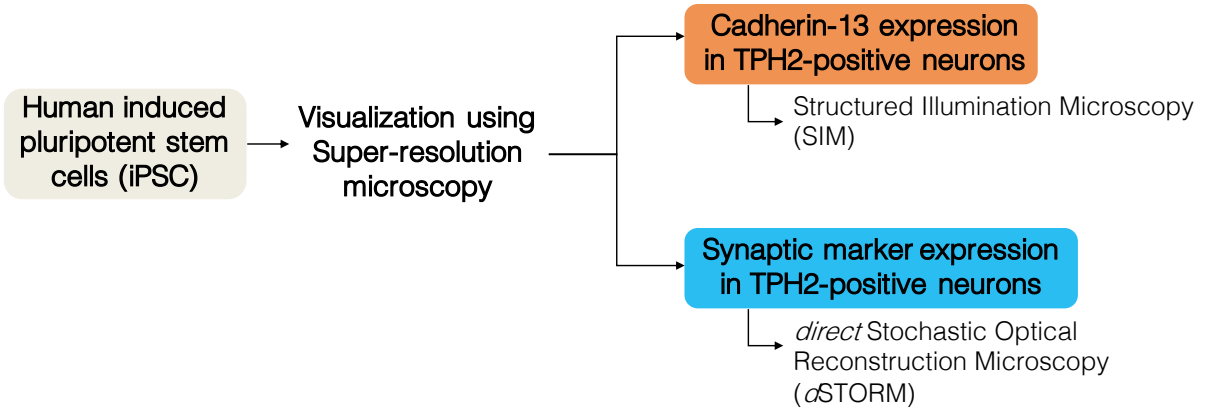

Figure 5.1-1. Outline of principal objectives of Project 3. The project focuses on the optimization of super-resolution microscopy techniques SIM and *d*STORM for the visualization of CDH13 and synaptic markers in TPH2-positive neurons derived from human iPSCs.

5.2. Results

5.2.1. Cadherin-13 expression in TPH2-positive neurons derived from human iPSCs using Structured Illumination Microscopy (SIM)

The recent development of human iPSCs and their neuronal differentiation in direction to 5-HT neurons in our laboratory allowed us to explore the super-resolution localization of CDH13.

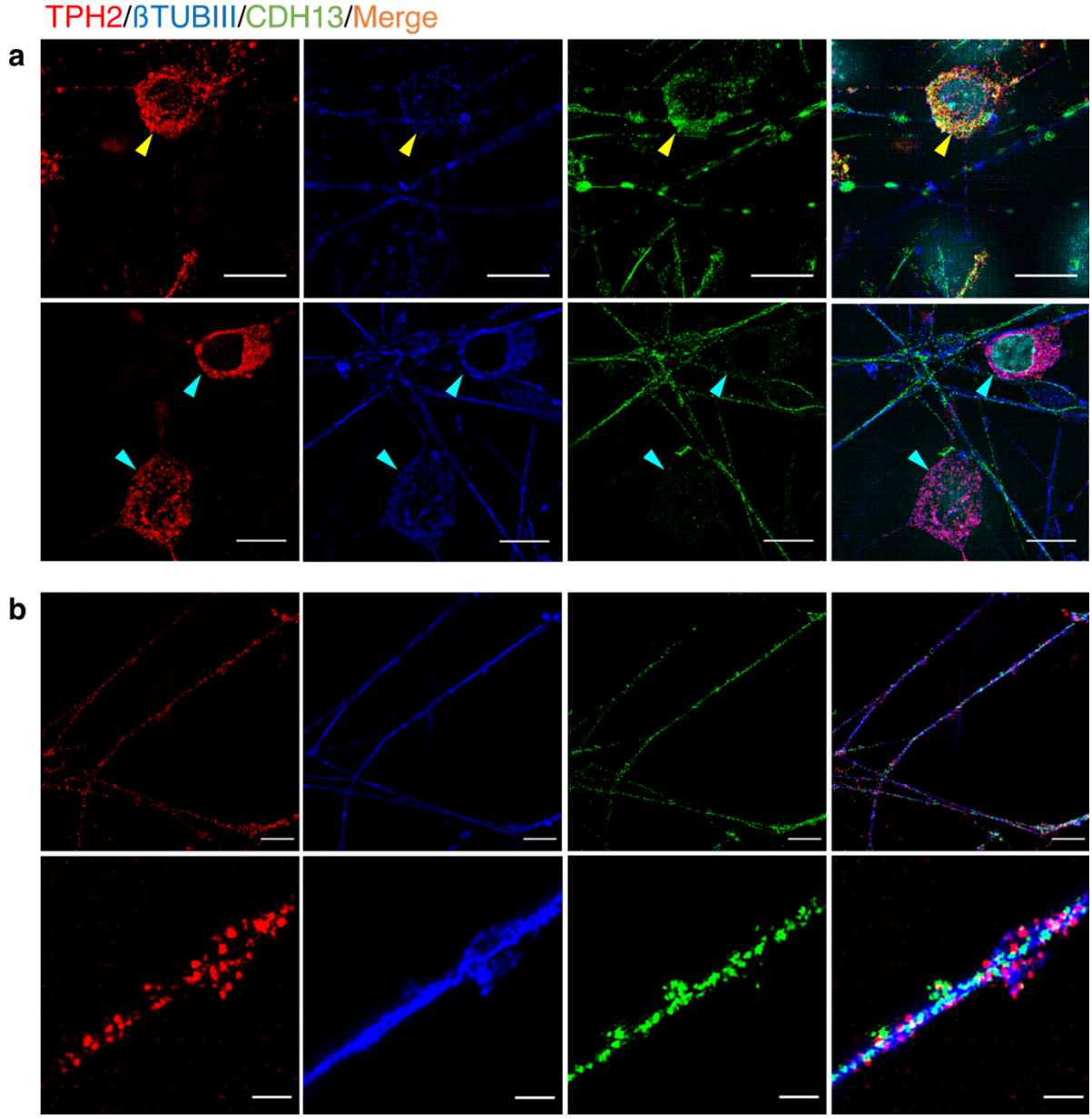

Figure 5.2.1-1. CDH13 expression in TPH2-positive neurons derived from human iPSCs. (a) The cell culture system generated through the differentiation of humans iPSCs contains TPH2-positive neurons that are also positive for CDH13 (yellow arrow). Cyan arrow: single CDH13-negative cells. (b) CDH13 is detected in the soma as well as in the axonal extensions of TPH2-positive neurons. SIM microscopy. Scale bar (a,b): 10 µm.

Our results indicate that CDH13 is highly expressed in a number of TPH2-positive neurons (Figure 5.2.1-1a) but a qualitative observation revealed that it is lacking from the majority of the 5-HT neurons identified in our culture (Figure 5.2.1-1a). In accordance with our findings in murine neurons *in vivo*, CDH13 immunoreactivity outlines both the soma and extending neurites of the corresponding cells (Figure 5.2.1-1a, b).

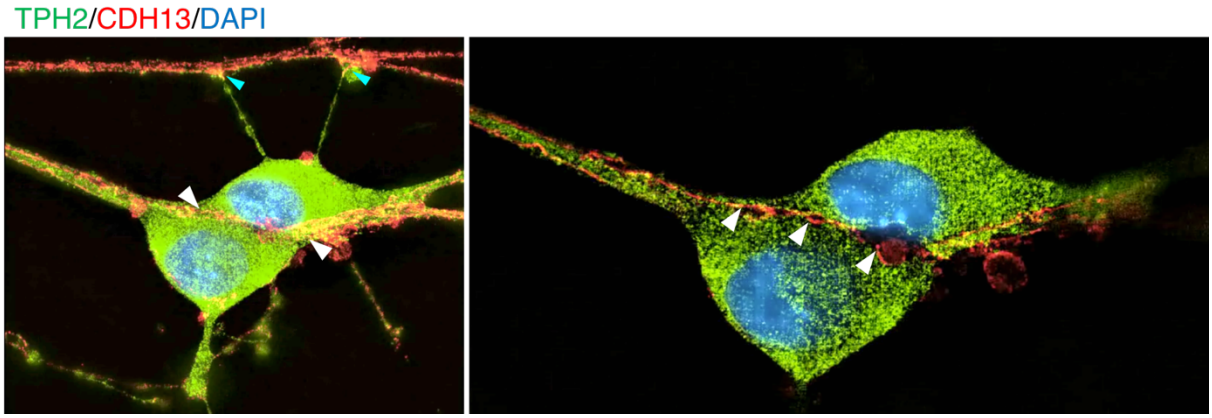

Figure 5.2.1-2. Three-dimensional reconstruction of CDH13 protein distribution in TPH2-positive induced human neurons. Representative images of two TPH2-positive neurons with CDH13 expression (white arrows). Contact between the TPH2-positive neuron and a CDH13-positive fiber are indicated (cyan arrows). Microscopy technique: SIM.

A three-dimensional reconstruction of these CDH13-positive 5-HT neurons suggests a potential role in cell-cell interaction. We observe in our cell culture system TPH2-ir neurons in very close proximity with CDH13 expression at the contact region between them (Figure 5.2.1-2).

5.2.2. Expression of synaptic markers in TPH2-positive neurons using *direct* stochastic optical reconstruction microscopy (*d*STORM)

The expression of the presynaptic marker Bassoon and postsynaptic scaffolding protein Homer was studied in iPSC-derived TPH2-positive neurons using *d*STORM. As it is seen in Figure 5.2.2-1, these neurons appear to have a higher expression of Bassoon compared to Homer. Additionally, we observe a lack of coinciding pre- and post-synaptic bar structures.

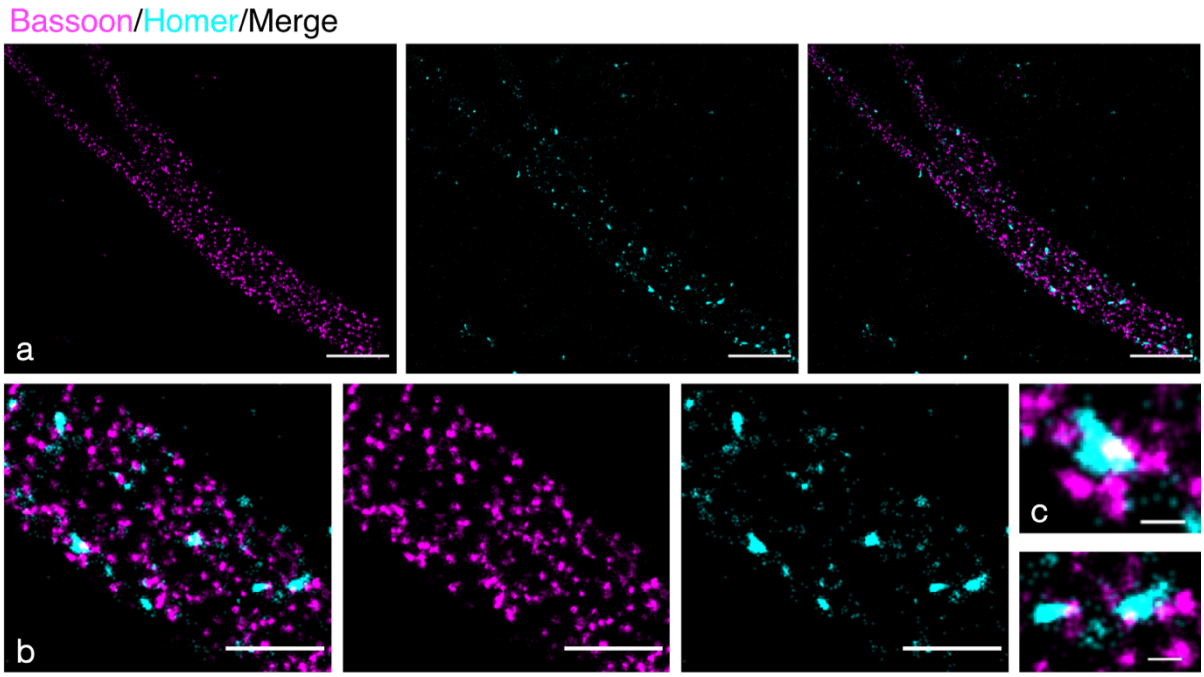

Figure 5.2.2-1. Synaptic markers in TPH2-positive neurons derived from human iPSCs. The presynaptic marker protein Bassoon is visualized with Alexa F647 and postsynaptic scaffolding protein Homer is imaged with Alexa F532. (a) A TPH2-positive fiber is imaged for Bassoon and Homer, close-up images (b) and (c) show the higher expression of Bassoon, and few contact points between the two proteins. Microscopy technique: *d*STORM. Scale bars: (a) 2 µm, (b) 1 µm, (c) 150 nm.

5.3. Discussion

Human iPSCs provide new possibilities in the study of molecules associated with neurodevelopmental and psychiatric disorders. Although the use of animal mouse models is relevant for the systemic understanding of the molecular framework of these disorders, human iPSCs allow patient-derived cellular and organoid models which open new horizons in personalized treatment. The results presented in this project describe a brief characterization of CDH13, a protein extensively studied in mouse models. Through the use of super-resolution microscopy techniques, we provide evidence showing how the expression pattern of CDH13 previously described in mice is similar to that observed in human iPSC-derived neurons. However, it is noteworthy to mention, that the data here presented are purely descriptive and should therefore be replicated in more cell lines and complimented by further analysis with additional markers and the eventual deletion of *CDH13*.

CDH13 is detected in a small subset of the TPH2-positive neurons present in the cell culture. We hypothesize that this could be due to the fact that the differentiation protocol which was followed aims to obtain median raphe 5-HT neurons (Lu et al., 2016). As it is shown in the previous projects presented in this thesis, CDH13 expression is lacking from MR neurons in the mouse brain, and instead concentrates on DR neurons (Forero et al., 2017). Therefore, this protein shows a specificity that could be used as a potential marker for DR cells in human iPSC cell cultures. Various studies have highlighted the difference between these two raphe nuclei in the regions which they innervate and their distinct behavioral functions (Balazsfi et al., 2018; Beliveau et al., 2015; Kusljic, Copolov, & van den Buuse, 2003). However, the generation of both MR and DR Tph2 neurons from iPSCs is also advantageous when creating brain organoids which resemble the human brain.

The qualitative analysis of the synaptic structure of the TPH2-positivie neurons using *d*STORM revealed that they express Bassoon, a presynaptic active zone marker, more extensively than Homer, a post-synaptic density scaffolding protein (Bresler et al., 2004; Dresbach et al., 2006; Tao-Cheng, Thein, Yang, Reese, & Gallant, 2014). 5-HT neurons are more likely to communicate through non-synaptic volume release instead of axonal-dendritic synaptic transmission (Adell, Celada, Abellan, & Artigas, 2002; De-Miguel & Trueta, 2005; Lau, Schneidt, Heimann, Gundelfinger, & Schloss, 2010; Vizi, Kiss, & Lendvai, 2004). This could explain the discrepancy between pre- and post- synaptic structures observed in our *in vitro* 5-HT specific neurons. The contribution of CDH13 to the synapse formation of these cells was not studied in the present project. However, since studies show that CDH13 is required in synapse formation of glutamatergic and GABAergic neurons (Paradis et al., 2007; Rivero et al., 2015), it would be interesting to observe if this is also the case in 5-HT neurons.

In conclusion, iPSC-derived neurons are a relevant mean for the study of human CDH13 and its role in 5-HT system development and function. Our super-resolution images show that CDH13 expression in human 5-HT neurons is similar to that observed in mouse cells and can be used to further investigate its relationship to cellular processes such as axonal outgrowth and migration in a human cellular culture.

6 | Conclusions

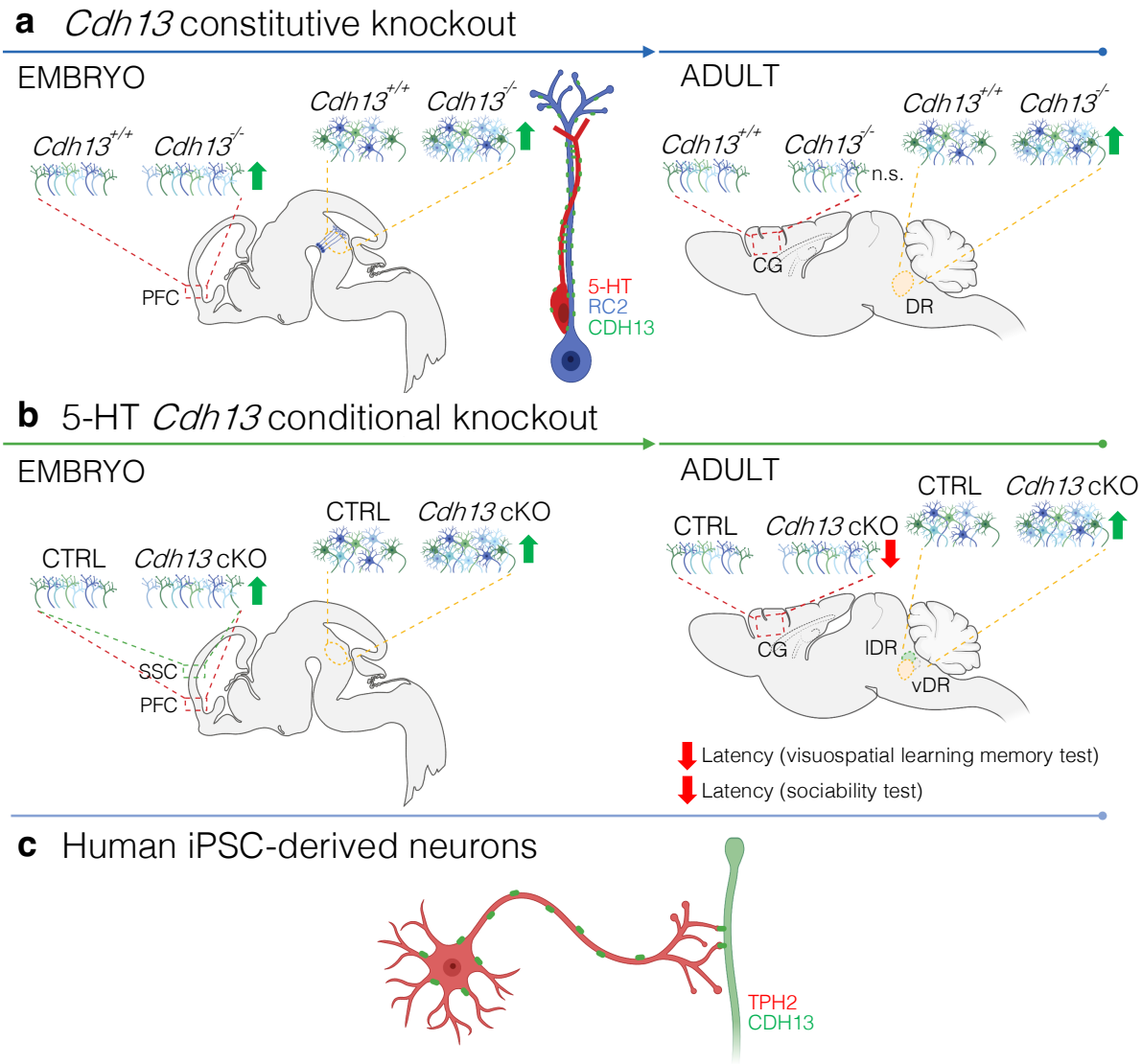

Figure 6.1-1. Summary of the impact of CDH13 deficiency on the brain serotonin system. (a) *Cdh13* constitutive KO mice present a significant increase in 5-HT neuron density in the DR in both the embryonic and adult brain compared to wildtype mice. There is also an increase in 5-HT innervation in the PFC at embryonic stages that is not observed later in the adult. A novel morphology showing 5-HT neurons intertwined with RGCs in the hindbrain region is introduced, with CDH13 present at the intersection points between the two cell types. (b) 5-HT *Cdh13* cKO mice present a significant increase in 5-HT neuron density in the DR in embryonic brain and in the lateral and ventral subgroups of the DR in the adult brain compared to control mice as well as a significant increase in serotonergic innervation of the PFC. A decrease in the latency in both a visuospatial and a sociability paradigm is observed in the *Cdh13* cKO mice. (c) CDH13 expression is confirmed in a number of TPH2-positive neurons derived from human iPSCs. TPH2 neuron extensions are seen attached to CDH13-positive fibers, with CDH13 present at the contact points. Figure created with BioRender.com.

7 | Outlook

The findings presented in this thesis reveal phenotypical alterations in the development of the 5-HT system in the absence of CDH13. We provide evidence that the constitutive and conditional deletion of *Cdh13* generate changes in DR formation and the innervation profile of 5-HT neurons. However, the exact mechanism by which these changes occur remains an open question.

We observe an increase in 5-HT neuron density in both embryonic as well as adult *Cdh13* KO mouse brains. We hypothesize that this alteration is due to a deficit in 5-HT neuron migration since we observe a close interaction with RGCs, a cell type known for aiding in neuronal migration. However, to validate this hypothesis, it is necessary to conduct live-cell imaging of cultured slides from knockout mice and controls to measure migration parameters such as velocity and tortuosity. Albeit a eGFP::Pet1::Cdh13 mouse line was developed for this purpose, but due to limitations in time and equipment it was not possible to conduct the experiment. Besides a migratory deficit, 5-HT neuron density increase in the DR of the embryonic mouse brain might be due to changes in neurogenesis and/or apoptosis. Although a difference in the region occupied by neural progenitor cell (NPC) marker, nestin, was not observed between *Cdh13* KO and wildtype mice, CDH13 is strongly expressed in RGCs, which additionally to having a structural function in migration, have been proven to be NPCs (Noctor, Martinez-Cerdeno, Ivic, & Kriegstein, 2004). Therefore, a further analysis of RGC division and function, as well as the use of markers to measure neurogenesis, such as a BrdU assay, would be worth investigating. Regarding a possible change in apoptosis, *Cdh13* KO mice have an increase in apoptotic cells in the cortex in embryonic stages (Killen et al., 2017), and so this could also hold true in the developing hindbrain. Therefore, it would be worthy to calculate the percentage of apoptotic 5-HT neurons using markers such as CC3.

An important aspect missing from the results presented in this thesis is to confirm the direct correlation between the alterations found. Particularly, our results suggest that the increase in 5-HT cell density might be mediating the increase in 5-HT innervation of prefrontal cortical regions, and ultimately generate the behavioral phenotype observed in the *Cdh13* cKO mice. However, the validation of this model would require the direct manipulation of DR 5-HT neurons as well as rescue experiments through the ectopic re-expression of CDH13 in the KO mouse lines. Since the DR is known to innervate a vast number of cortical and subcortical brain regions, it is necessary to conduct further experiments to decipher its predominant effect on the innervation of the prefrontal cortex.

Finally, the work conducted with Tph2 neurons derived from human iPSCs is only an initial approximation to the study of CDH13 using this human neuronal culture model. As it is evident in the results, major challenges still remain, such as identifying the additional CDH13-positive cells present in the culture system that are interacting with the TPH2-positive neurons. Novel gene editing technique CRISPR-Cas9 could also be applied for the selective deletion of CDH13 and its effect on 5-HT neuron development and function in these patient-derived neurons.

References

Allen Developing Mouse Brain Atlas (2008). Allen Developing Mouse Brain Reference Atlas. Retreived from: https://developingmouse.brain-map.org/

Adams, N. C., Tomoda, T., Cooper, M., Dietz, G., & Hatten, M. E. (2002). Mice that lack astrotactin have slowed neuronal migration. *Development, 129*(4), 965-972. Retrieved from http://www.ncbi.nlm.nih.gov/pubmed/11861479

Adell, A., Celada, P., Abellan, M. T., & Artigas, F. (2002). Origin and functional role of the extracellular serotonin in the midbrain raphe nuclei. *Brain Res Brain Res Rev, 39*(2-3), 154-180. doi:10.1016/s0165-0173(02)00182-0

Alonso, A., Merchan, P., Sandoval, J. E., Sanchez-Arrones, L., Garcia-Cazorla, A., Artuch, R., . . . Puelles, L. (2013). Development of the serotonergic cells in murine raphe nuclei and their relations with rhombomeric domains. *Brain Struct Funct, 218*(5), 1229-1277. doi:10.1007/s00429-012-0456-8

Arias-Vasquez, A., Altink, M. E., Rommelse, N. N., Slaats-Willemse, D. I., Buschgens, C. J., Fliers, E. A., . . . Buitelaar, J. K. (2011). CDH13 is associated with working memory performance in attention deficit/hyperactivity disorder. *Genes Brain Behav, 10*(8), 844-851. doi:10.1111/j.1601-183X.2011.00724.x

Azmitia, E. C., Singh, J. S., & Whitaker-Azmitia, P. M. (2011). Increased serotonin axons (immunoreactive to 5-HT transporter) in postmortem brains from young autism donors. *Neuropharmacology, 60*(7-8), 1347-1354. doi:10.1016/j.neuropharm.2011.02.002

Bai, S., Ghoshal, K., & Jacob, S. T. (2006). Identification of T-cadherin as a novel target of DNA methyltransferase 3B and its role in the suppression of nerve growth factor-mediated neurite outgrowth in PC12 cells. *J Biol Chem, 281*(19), 13604-13611. doi:10.1074/jbc.M513278200

Balazsfi, D., Zelena, D., Demeter, K., Miskolczi, C., Varga, Z. K., Nagyvaradi, A., . . . Haller, J. (2018). Differential Roles of the Two Raphe Nuclei in Amiable Social Behavior and Aggression - An Optogenetic Study. *Front Behav Neurosci, 12*, 163. doi:10.3389/fnbeh.2018.00163

Banasr, M., Hery, M., Printemps, R., & Daszuta, A. (2004). Serotonin-induced increases in adult cell proliferation and neurogenesis are mediated through different and common 5-HT receptor subtypes in the dentate gyrus and the subventricular zone. *Neuropsychopharmacology, 29*(3), 450-460. doi:10.1038/sj.npp.1300320

Banerjee, E., & Nandagopal, K. (2015). Does serotonin deficit mediate susceptibility to ADHD? *Neurochem Int, 82*, 52-68. doi:10.1016/j.neuint.2015.02.001

Beliveau, V., Svarer, C., Frokjaer, V. G., Knudsen, G. M., Greve, D. N., & Fisher, P. M. (2015). Functional connectivity of the dorsal and median raphe nuclei at rest. *Neuroimage, 116*, 187-195. doi:10.1016/j.neuroimage.2015.04.065

Bennett-Clarke, C. A., Leslie, M. J., Lane, R. D., & Rhoades, R. W. (1994). Effect of serotonin depletion on vibrissa-related patterns of thalamic afferents in the rat's somatosensory cortex. *J Neurosci, 14*(12), 7594-7607. Retrieved from https://www.ncbi.nlm.nih.gov/pubmed/7996198

Blakemore, S. J. (2008). The social brain in adolescence. *Nat Rev Neurosci, 9*(4), 267-277. doi:10.1038/nrn2353

Bonnin, A., Goeden, N., Chen, K., Wilson, M. L., King, J., Shih, J. C., . . . Levitt, P. (2011). A transient placental source of serotonin for the fetal forebrain. *Nature, 472*(7343), 347-350. doi:10.1038/nature09972

Borglum, A. D., Demontis, D., Grove, J., Pallesen, J., Hollegaard, M. V., Pedersen, C. B., . . . Mors, O. (2014). Genome-wide study of association and interaction with maternal cytomegalovirus infection suggests new schizophrenia loci. *Mol Psychiatry, 19*(3), 325-333. doi:10.1038/mp.2013.2

Brainstorm, C., Anttila, V., Bulik-Sullivan, B., Finucane, H. K., Walters, R. K., Bras, J., . . . Murray, R. (2018). Analysis of shared heritability in common disorders of the brain. *Science, 360*(6395). doi:10.1126/science.aap8757

Brasch, J., Katsamba, P. S., Harrison, O. J., Ahlsen, G., Troyanovsky, R. B., Indra, I., . . . Shapiro, L. (2018). Homophilic and Heterophilic Interactions of Type II Cadherins Identify Specificity Groups Underlying Cell-Adhesive Behavior. *Cell Rep, 23*(6), 1840-1852. doi:10.1016/j.celrep.2018.04.012

Bresler, T., Shapira, M., Boeckers, T., Dresbach, T., Futter, M., Garner, C. C., . . . Ziv, N. E. (2004). Postsynaptic density assembly is fundamentally different from presynaptic active zone assembly. *J Neurosci, 24*(6), 1507-1520. doi:10.1523/JNEUROSCI.3819-03.2004

Brodski, C., Weisenhorn, D. M., Signore, M., Sillaber, I., Oesterheld, M., Broccoli, V., . . . Wurst, W. (2003). Location and size of dopaminergic and serotonergic cell populations are controlled by the position of the midbrain-hindbrain organizer. *J Neurosci, 23*(10), 4199-4207. Retrieved from http://www.ncbi.nlm.nih.gov/pubmed/12764108

Campbell, K., & Gotz, M. (2002). Radial glia: multi-purpose cells for vertebrate brain development. *Trends Neurosci, 25*(5), 235-238. doi:10.1016/s0166-2236(02)02156-2

Cases, O., Vitalis, T., Seif, I., De Maeyer, E., Sotelo, C., & Gaspar, P. (1996). Lack of barrels in the somatosensory cortex of monoamine oxidase A-deficient mice: role of a serotonin excess during the critical period. *Neuron, 16*(2), 297-307. doi:10.1016/s0896-6273(00)80048-3

Chapman, N. H., Estes, A., Munson, J., Bernier, R., Webb, S. J., Rothstein, J. H., . . . Wijsman, E. M. (2011). Genome-scan for IQ discrepancy in autism: evidence for loci on chromosomes 10 and 16. *Hum Genet, 129*(1), 59-70. doi:10.1007/s00439-010-0899-z

Chen, H., Fan, Y., Zhao, L., Hao, Y., Zhou, X., Guan, Y., & Li, Z. (2017). Successful treatment with risperidone increases 5-HT 3A receptor gene expression in patients with paranoid schizophrenia - data from a prospective study. *Brain Behav, 7*(9), e00798. doi:10.1002/brb3.798

Cho, C. H., Lee, H. J., Woo, H. G., Choi, J. H., Greenwood, T. A., & Kelsoe, J. R. (2015). CDH13 and HCRTR2 May Be Associated with Hypersomnia Symptom of Bipolar Depression: A Genome-Wide Functional Enrichment Pathway Analysis. *Psychiatry Investig, 12*(3), 402-407. doi:10.4306/pi.2015.12.3.402

Ciatto, C., Bahna, F., Zampieri, N., VanSteenhouse, H. C., Katsamba, P. S., Ahlsen, G., . . . Shapiro, L. (2010). T-cadherin structures reveal a novel adhesive binding mechanism. *Nat Struct Mol Biol, 17*(3), 339-347. doi:10.1038/nsmb.1781

Ciranna, L. (2006). Serotonin as a modulator of glutamate- and GABA-mediated neurotransmission: implications in physiological functions and in pathology.

Curr Neuropharmacol, 4(2), 101-114. Retrieved from https://www.ncbi.nlm.nih.gov/pubmed/18615128

Dai, J. X., Han, H. L., Tian, M., Cao, J., Xiu, J. B., Song, N. N., . . . Xu, L. (2008). Enhanced contextual fear memory in central serotonin-deficient mice. *Proc Natl Acad Sci U S A, 105*(33), 11981-11986. doi:10.1073/pnas.0801329105

Dalley, J. W., & Roiser, J. P. (2012). Dopamine, serotonin and impulsivity. *Neuroscience, 215*, 42-58. doi:10.1016/j.neuroscience.2012.03.065

De-Miguel, F. F., & Trueta, C. (2005). Synaptic and extrasynaptic secretion of serotonin. *Cell Mol Neurobiol, 25*(2), 297-312. doi:10.1007/s10571-005-3061-z

Demontis, D., Walters, R. K., Martin, J., Mattheisen, M., Als, T. D., Agerbo, E., . . . Neale, B. M. (2019). Discovery of the first genome-wide significant risk loci for attention deficit/hyperactivity disorder. *Nat Genet, 51*(1), 63-75. doi:10.1038/s41588-018-0269-7

Deneris, E., & Gaspar, P. (2018). Serotonin neuron development: shaping molecular and structural identities. *Wiley Interdiscip Rev Dev Biol, 7*(1). doi:10.1002/wdev.301

Donovan, S. L., Mamounas, L. A., Andrews, A. M., Blue, M. E., & McCasland, J. S. (2002). GAP-43 is critical for normal development of the serotonergic innervation in forebrain. *J Neurosci, 22*(9), 3543-3552. doi:20026295

Dray, A., Davies, J., Oakley, N. R., Tongroach, P., & Vellucci, S. (1978). The dorsal and medial raphe projections to the substantia nigra in the rat: electrophysiological, biochemical and behavioural observations. *Brain Res, 151*(3), 431-442. doi:10.1016/0006-8993(78)91077-6

Dresbach, T., Torres, V., Wittenmayer, N., Altrock, W. D., Zamorano, P., Zuschratter, W., . . . Gundelfinger, E. D. (2006). Assembly of active zone precursor vesicles: obligatory trafficking of presynaptic cytomatrix proteins Bassoon and Piccolo via a trans-Golgi compartment. *J Biol Chem, 281*(9), 6038-6047. doi:10.1074/jbc.M508784200

Drgon, T., Montoya, I., Johnson, C., Liu, Q. R., Walther, D., Hamer, D., & Uhl, G. R. (2009). Genome-wide association for nicotine dependence and smoking cessation success in NIH research volunteers. *Mol Med, 15*(1-2), 21-27. doi:10.2119/molmed.2008.00096

Drgonova, J., Walther, D., Hartstein, G. L., Bukhari, M. O., Baumann, M. H., Katz, J., . . . Uhl, G. R. (2016). Cadherin 13: human cis-regulation and selectively-altered addiction phenotypes and cerebral cortical dopamine in knockout mice. *Mol Med, 22*. doi:10.2119/molmed.2015.00170

Edmondson, J. C., & Hatten, M. E. (1987). Glial-guided granule neuron migration in vitro: a high-resolution time-lapse video microscopic study. *J Neurosci, 7*(6), 1928-1934. Retrieved from http://www.ncbi.nlm.nih.gov/pubmed/3598656

Forero, A., Rivero, O., Waldchen, S., Ku, H. P., Kiser, D. P., Gartner, Y., . . . Lesch, K. P. (2017). Cadherin-13 Deficiency Increases Dorsal Raphe 5-HT Neuron Density and Prefrontal Cortex Innervation in the Mouse Brain. *Front Cell Neurosci, 11*, 307. doi:10.3389/fncel.2017.00307

Forero, A., Ku, H.P., Malpartida, A.B., Wäldchen, S., Alhama-Riba, J., Kulka, C., Aboagye, B., Norton, W., Young, A., Ding, Y.Q., Blum, R., Sauer, M., Rivero, O., Lesch, K.P. (2020). Serotonin (5-HT) neuron-specific inactivation of

Cadherin-13 impacts 5-HT system formation and cognitive function. *Neuropharmacology*. 10.1016/j.neuropharm.2020.108018

Fox, M. A., Andrews, A. M., Wendland, J. R., Lesch, K. P., Holmes, A., & Murphy, D. L. (2007). A pharmacological analysis of mice with a targeted disruption of the serotonin transporter. *Psychopharmacology (Berl), 195*(2), 147-166. doi:10.1007/s00213-007-0910-0

Fredette, B. J., Miller, J., & Ranscht, B. (1996). Inhibition of motor axon growth by T-cadherin substrata. *Development, 122*(10), 3163-3171. Retrieved from http://www.ncbi.nlm.nih.gov/pubmed/8898229

Fredette, B. J., & Ranscht, B. (1994). T-cadherin expression delineates specific regions of the developing motor axon-hindlimb projection pathway. *J Neurosci, 14*(12), 7331-7346. Retrieved from http://www.ncbi.nlm.nih.gov/pubmed/7996179

Frismantiene, A., Dasen, B., Pfaff, D., Erne, P., Resink, T. J., & Philippova, M. (2016). T-cadherin promotes vascular smooth muscle cell dedifferentiation via a GSK3beta-inactivation dependent mechanism. *Cell Signal, 28*(5), 516-530. doi:10.1016/j.cellsig.2016.02.014

Gainetdinov, R. R., Wetsel, W. C., Jones, S. R., Levin, E. D., Jaber, M., & Caron, M. G. (1999). Role of serotonin in the paradoxical calming effect of psychostimulants on hyperactivity. *Science, 283*(5400), 397-401. Retrieved from https://www.ncbi.nlm.nih.gov/pubmed/9888856

Garcia-Gonzalez, D., Khodosevich, K., Watanabe, Y., Rollenhagen, A., Lubke, J. H. R., & Monyer, H. (2017). Serotonergic Projections Govern Postnatal Neuroblast Migration. *Neuron, 94*(3), 534-549 e539. doi:10.1016/j.neuron.2017.04.013

Gaspar, P., Cases, O., & Maroteaux, L. (2003). The developmental role of serotonin: news from mouse molecular genetics. *Nat Rev Neurosci, 4*(12), 1002-1012. doi:10.1038/nrn1256

Gomez, C., Brinon, J. G., Orio, L., Colado, M. I., Lawrence, A. J., Zhou, F. C., . . . Alonso, J. R. (2007). Changes in the serotonergic system in the main olfactory bulb of rats unilaterally deprived from birth to adulthood. *J Neurochem, 100*(4), 924-938. doi:10.1111/j.1471-4159.2006.04229.x

Gupta, A., Tsai, L. H., & Wynshaw-Boris, A. (2002). Life is a journey: a genetic look at neocortical development. *Nat Rev Genet, 3*(5), 342-355. doi:10.1038/nrg799

Gustafsson, M. G. (2000). Surpassing the lateral resolution limit by a factor of two using structured illumination microscopy. *J Microsc, 198*(Pt 2), 82-87. Retrieved from http://www.ncbi.nlm.nih.gov/pubmed/10810003

Harrison, O. J., Bahna, F., Katsamba, P. S., Jin, X., Brasch, J., Vendome, J., . . . Shapiro, L. (2010). Two-step adhesive binding by classical cadherins. *Nat Struct Mol Biol, 17*(3), 348-357. doi:10.1038/nsmb.1784

Hart, A. B., Engelhardt, B. E., Wardle, M. C., Sokoloff, G., Stephens, M., de Wit, H., & Palmer, A. A. (2012). Genome-wide association study of d-amphetamine response in healthy volunteers identifies putative associations, including cadherin 13 (CDH13). *PLoS One, 7*(8), e42646. doi:10.1371/journal.pone.0042646

Haubst, N., Georges-Labouesse, E., De Arcangelis, A., Mayer, U., & Gotz, M. (2006). Basement membrane attachment is dispensable for radial glial cell

fate and for proliferation, but affects positioning of neuronal subtypes. *Development, 133*(16), 3245-3254. doi:10.1242/dev.02486

Hawi, Z., Tong, J., Dark, C., Yates, H., Johnson, B., & Bellgrove, M. A. (2018). The role of cadherin genes in five major psychiatric disorders: A literature update. *Am J Med Genet B Neuropsychiatr Genet, 177*(2), 168-180. doi:10.1002/ajmg.b.32592

Hawthorne, A. L., Wylie, C. J., Landmesser, L. T., Deneris, E. S., & Silver, J. (2010). Serotonergic neurons migrate radially through the neuroepithelium by dynamin-mediated somal translocation. *J Neurosci, 30*(2), 420-430. doi:10.1523/JNEUROSCI.2333-09.2010

Hayano, Y., Zhao, H., Kobayashi, H., Takeuchi, K., Norioka, S., & Yamamoto, N. (2014). The role of T-cadherin in axonal pathway formation in neocortical circuits. *Development, 141*(24), 4784-4793. doi:10.1242/dev.108290

Hendricks, T. J., Fyodorov, D. V., Wegman, L. J., Lelutiu, N. B., Pehek, E. A., Yamamoto, B., . . . Deneris, E. S. (2003). Pet-1 ETS gene plays a critical role in 5-HT neuron development and is required for normal anxiety-like and aggressive behavior. *Neuron, 37*(2), 233-247. doi:10.1016/s0896-6273(02)01167-4

Herve, D., Pickel, V. M., Joh, T. H., & Beaudet, A. (1987). Serotonin axon terminals in the ventral tegmental area of the rat: fine structure and synaptic input to dopaminergic neurons. *Brain Res, 435*(1-2), 71-83. doi:10.1016/0006-8993(87)91588-5

Howard, D. M., Adams, M. J., Clarke, T. K., Hafferty, J. D., Gibson, J., Shirali, M., . . . McIntosh, A. M. (2019). Genome-wide meta-analysis of depression identifies 102 independent variants and highlights the importance of the prefrontal brain regions. *Nat Neurosci, 22*(3), 343-352. doi:10.1038/s41593-018-0326-7

Hvoslef-Eide, M., Nilsson, S. R., Hailwood, J. M., Robbins, T. W., Saksida, L. M., Mar, A. C., & Bussey, T. J. (2018). Effects of anterior cingulate cortex lesions on a continuous performance task for mice. *Brain Neurosci Adv, 2*. doi:10.1177/2398212818772962

Hynes, M., Ye, W., Wang, K., Stone, D., Murone, M., Sauvage, F., & Rosenthal, A. (2000). The seven-transmembrane receptor smoothened cell-autonomously induces multiple ventral cell types. *Nat Neurosci, 3*(1), 41-46. doi:10.1038/71114

Jansch, C., Gunther, K., Waider, J., Ziegler, G. C., Forero, A., Kollert, S., . . . Lesch, K. P. (2018). Generation of a human induced pluripotent stem cell (iPSC) line from a 51-year-old female with attention-deficit/hyperactivity disorder (ADHD) carrying a duplication of SLC2A3. *Stem Cell Res, 28*, 136-140. doi:10.1016/j.scr.2018.02.005

Johnson, C., Drgon, T., Walther, D., & Uhl, G. R. (2011). Genomic regions identified by overlapping clusters of nominally-positive SNPs from genome-wide studies of alcohol and illegal substance dependence. *PLoS One, 6*(7), e19210. doi:10.1371/journal.pone.0019210

Joshi, M. B., Ivanov, D., Philippova, M., Erne, P., & Resink, T. J. (2007). Integrin-linked kinase is an essential mediator for T-cadherin-dependent signaling via Akt and GSK3beta in endothelial cells. *FASEB J, 21*(12), 3083-3095. doi:10.1096/fj.06-7723com

Joshi, M. B., Philippova, M., Ivanov, D., Allenspach, R., Erne, P., & Resink, T. J. (2005). T-cadherin protects endothelial cells from oxidative stress-induced apoptosis. *FASEB J, 19*(12), 1737-1739. doi:10.1096/fj.05-3834fje

Katori, S., Hamada, S., Noguchi, Y., Fukuda, E., Yamamoto, T., Yamamoto, H., . . . Yagi, T. (2009). Protocadherin-alpha family is required for serotonergic projections to appropriately innervate target brain areas. *J Neurosci, 29*(29), 9137-9147. doi:10.1523/JNEUROSCI.5478-08.2009

Katori, S., Noguchi-Katori, Y., Okayama, A., Kawamura, Y., Luo, W., Sakimura, K., . . . Yagi, T. (2017). Protocadherin-alphaC2 is required for diffuse projections of serotonergic axons. *Sci Rep, 7*(1), 15908. doi:10.1038/s41598-017-16120-y

Killen, A. C., Barber, M., Paulin, J. J. W., Ranscht, B., Parnavelas, J. G., & Andrews, W. D. (2017). Protective role of Cadherin 13 in interneuron development. *Brain Struct Funct, 222*(8), 3567-3585. doi:10.1007/s00429-017-1418-y

King, C. P., Militello, L., Hart, A., St Pierre, C. L., Leung, E., Versaggi, C. L., . . . Meyer, P. J. (2017). Cdh13 and AdipoQ gene knockout alter instrumental and Pavlovian drug conditioning. *Genes Brain Behav, 16*(7), 686-698. doi:10.1111/gbb.12382

Kiser, D. P., Popp, S., Schmitt-Bohrer, A. G., Strekalova, T., van den Hove, D. L., Lesch, K. P., & Rivero, O. (2019). Early-life stress impairs developmental programming in Cadherin 13 (CDH13)-deficient mice. *Prog Neuropsychopharmacol Biol Psychiatry, 89*, 158-168. doi:10.1016/j.pnpbp.2018.08.010

Kiser, D. P., Rivero, O., & Lesch, K. P. (2015). Annual research review: The (epi)genetics of neurodevelopmental disorders in the era of whole-genome sequencing--unveiling the dark matter. *J Child Psychol Psychiatry, 56*(3), 278-295. doi:10.1111/jcpp.12392

Kiyasova, V., Fernandez, S. P., Laine, J., Stankovski, L., Muzerelle, A., Doly, S., & Gaspar, P. (2011). A genetically defined morphologically and functionally unique subset of 5-HT neurons in the mouse raphe nuclei. *J Neurosci, 31*(8), 2756-2768. doi:10.1523/JNEUROSCI.4080-10.2011

Kiyasova, V., & Gaspar, P. (2011). Development of raphe serotonin neurons from specification to guidance. *Eur J Neurosci, 34*(10), 1553-1562. doi:10.1111/j.1460-9568.2011.07910.x

Ku, H.P. (2017). Effects of Cadherin 13 Deficiency in the Development of the Serotonergic System with Emphasis on Prefrontal Cortex Innervation. University of Würzburg, Würzburg, Germany.

Kusljic, S., Copolov, D. L., & van den Buuse, M. (2003). Differential role of serotonergic projections arising from the dorsal and median raphe nuclei in locomotor hyperactivity and prepulse inhibition. *Neuropsychopharmacology, 28*(12), 2138-2147. doi:10.1038/sj.npp.1300277

Kyriakakis, E., Frismantiene, A., Dasen, B., Pfaff, D., Rivero, O., Lesch, K. P., . . . Philippova, M. (2017). T-cadherin promotes autophagy and survival in vascular smooth muscle cells through MEK1/2/Erk1/2 axis activation. *Cell Signal, 35*, 163-175. doi:10.1016/j.cellsig.2017.04.004

Lasky-Su, J., Neale, B. M., Franke, B., Anney, R. J., Zhou, K., Maller, J. B., . . . Faraone, S. V. (2008). Genome-wide association scan of quantitative traits for attention deficit hyperactivity disorder identifies novel associations and

confirms candidate gene associations. *Am J Med Genet B Neuropsychiatr Genet, 147B*(8), 1345-1354. doi:10.1002/ajmg.b.30867

Lau, T., Schneidt, T., Heimann, F., Gundelfinger, E. D., & Schloss, P. (2010). Somatodendritic serotonin release and re-uptake in mouse embryonic stem cell-derived serotonergic neurons. *Neurochem Int, 57*(8), 969-978. doi:10.1016/j.neuint.2010.10.003

Lendahl, U., Zimmerman, L. B., & McKay, R. D. (1990). CNS stem cells express a new class of intermediate filament protein. *Cell, 60*(4), 585-595. Retrieved from http://www.ncbi.nlm.nih.gov/pubmed/1689217

Lesch, K. P. (2016). Maturing insights into the genetic architecture of neurodevelopmental disorders - from common and rare variant interplay to precision psychiatry. *J Child Psychol Psychiatry, 57*(6), 659-661. doi:10.1111/jcpp.12574

Lesch, K. P., Timmesfeld, N., Renner, T. J., Halperin, R., Roser, C., Nguyen, T. T., . . . Jacob, C. (2008). Molecular genetics of adult ADHD: converging evidence from genome-wide association and extended pedigree linkage studies. *J Neural Transm (Vienna), 115*(11), 1573-1585. doi:10.1007/s00702-008-0119-3

Lesch, K. P., & Waider, J. (2012). Serotonin in the modulation of neural plasticity and networks: implications for neurodevelopmental disorders. *Neuron, 76*(1), 175-191. doi:10.1016/j.neuron.2012.09.013

Leventhal, A. M., Kirkpatrick, M. G., Pester, M. S., McGeary, J. E., Swift, R. M., Sussman, S., & Kahler, C. W. (2017). Pharmacogenetics of stimulant abuse liability: association of CDH13 variant with amphetamine response in a racially-heterogeneous sample of healthy young adults. *Psychopharmacology (Berl), 234*(2), 307-315. doi:10.1007/s00213-016-4462-z

Li, J. Y., & Joyner, A. L. (2001). Otx2 and Gbx2 are required for refinement and not induction of mid-hindbrain gene expression. *Development, 128*(24), 4979-4991. Retrieved from http://www.ncbi.nlm.nih.gov/pubmed/11748135

Lidov, H. G., & Molliver, M. E. (1982). An immunohistochemical study of serotonin neuron development in the rat: ascending pathways and terminal fields. *Brain Res Bull, 8*(4), 389-430. Retrieved from https://www.ncbi.nlm.nih.gov/pubmed/6178481

Lionel, A. C., Crosbie, J., Barbosa, N., Goodale, T., Thiruvahindrapuram, B., Rickaby, J., . . . Scherer, S. W. (2011). Rare copy number variation discovery and cross-disorder comparisons identify risk genes for ADHD. *Sci Transl Med, 3*(95), 95ra75. doi:10.1126/scitranslmed.3002464

Liu, Q. R., Drgon, T., Johnson, C., Walther, D., Hess, J., & Uhl, G. R. (2006). Addiction molecular genetics: 639,401 SNP whole genome association identifies many "cell adhesion" genes. *Am J Med Genet B Neuropsychiatr Genet, 141B*(8), 918-925. doi:10.1002/ajmg.b.30436

Lu, J., Zhong, X., Liu, H., Hao, L., Huang, C. T., Sherafat, M. A., . . . Zhang, S. C. (2016). Generation of serotonin neurons from human pluripotent stem cells. *Nat Biotechnol, 34*(1), 89-94. doi:10.1038/nbt.3435

Maddaloni, G., Bertero, A., Pratelli, M., Barsotti, N., Boonstra, A., Giorgi, A., . . . Pasqualetti, M. (2017). Development of Serotonergic Fibers in the Post-Natal Mouse Brain. *Front Cell Neurosci, 11*, 202. doi:10.3389/fncel.2017.00202

Maitre, J. L., & Heisenberg, C. P. (2013). Three functions of cadherins in cell adhesion. *Curr Biol, 23*(14), R626-633. doi:10.1016/j.cub.2013.06.019

Marin, O. (2012). Interneuron dysfunction in psychiatric disorders. *Nat Rev Neurosci, 13*(2), 107-120. doi:10.1038/nrn3155

Mathews, T. A., Fedele, D. E., Coppelli, F. M., Avila, A. M., Murphy, D. L., & Andrews, A. M. (2004). Gene dose-dependent alterations in extraneuronal serotonin but not dopamine in mice with reduced serotonin transporter expression. *J Neurosci Methods, 140*(1-2), 169-181. doi:10.1016/j.jneumeth.2004.05.017

McCann, B. S., & Roy-Byrne, P. (2000). Attention-deficit/hyperactivity disorder and learning disabilities in adults. *Semin Clin Neuropsychiatry, 5*(3), 191-197. Retrieved from https://www.ncbi.nlm.nih.gov/pubmed/11291014

Miceli, S., Negwer, M., van Eijs, F., Kalkhoven, C., van Lierop, I., Homberg, J., & Schubert, D. (2013). High serotonin levels during brain development alter the structural input-output connectivity of neural networks in the rat somatosensory layer IV. *Front Cell Neurosci, 7*, 88. doi:10.3389/fncel.2013.00088

Miller, E. K., & Cohen, J. D. (2001). An integrative theory of prefrontal cortex function. *Annu Rev Neurosci, 24*, 167-202. doi:10.1146/annurev.neuro.24.1.167

Muzerelle, A., Scotto-Lomassese, S., Bernard, J. F., Soiza-Reilly, M., & Gaspar, P. (2016). Conditional anterograde tracing reveals distinct targeting of individual serotonin cell groups (B5-B9) to the forebrain and brainstem. *Brain Struct Funct, 221*(1), 535-561. doi:10.1007/s00429-014-0924-4

Nadarajah, B., & Parnavelas, J. G. (2002). Modes of neuronal migration in the developing cerebral cortex. *Nat Rev Neurosci, 3*(6), 423-432. doi:10.1038/nrn845

Neale, B. M., Lasky-Su, J., Anney, R., Franke, B., Zhou, K., Maller, J. B., . . . Faraone, S. V. (2008). Genome-wide association scan of attention deficit hyperactivity disorder. *Am J Med Genet B Neuropsychiatr Genet, 147B*(8), 1337-1344. doi:10.1002/ajmg.b.30866

Neale, B. M., Medland, S., Ripke, S., Anney, R. J., Asherson, P., Buitelaar, J., . . . Group, I. I. C. (2010). Case-control genome-wide association study of attention-deficit/hyperactivity disorder. *J Am Acad Child Adolesc Psychiatry, 49*(9), 906-920. doi:10.1016/j.jaac.2010.06.007

Neale, B. M., Medland, S. E., Ripke, S., Asherson, P., Franke, B., Lesch, K. P., . . . Psychiatric, G. C. A. S. (2010). Meta-analysis of genome-wide association studies of attention-deficit/hyperactivity disorder. *J Am Acad Child Adolesc Psychiatry, 49*(9), 884-897. doi:10.1016/j.jaac.2010.06.008

Noctor, S. C., Martinez-Cerdeno, V., Ivic, L., & Kriegstein, A. R. (2004). Cortical neurons arise in symmetric and asymmetric division zones and migrate through specific phases. *Nat Neurosci, 7*(2), 136-144. doi:10.1038/nn1172

Okaty, B. W., Freret, M. E., Rood, B. D., Brust, R. D., Hennessy, M. L., deBairos, D., . . . Dymecki, S. M. (2015). Multi-Scale Molecular Deconstruction of the Serotonin Neuron System. *Neuron, 88*(4), 774-791. doi:10.1016/j.neuron.2015.10.007

Otsuka, I., Watanabe, Y., Hishimoto, A., Boku, S., Mouri, K., Shiroiwa, K., . . . Sora, I. (2015). Association analysis of the Cadherin13 gene with

schizophrenia in the Japanese population. *Neuropsychiatr Dis Treat, 11*, 1381-1393. doi:10.2147/NDT.S84736

Paradis, S., Harrar, D. B., Lin, Y., Koon, A. C., Hauser, J. L., Griffith, E. C., . . . Greenberg, M. E. (2007). An RNAi-based approach identifies molecules required for glutamatergic and GABAergic synapse development. *Neuron, 53*(2), 217-232. doi:10.1016/j.neuron.2006.12.012

Park, D., Xiang, A. P., Zhang, L., Mao, F. F., Walton, N. M., Choi, S. S., & Lahn, B. T. (2009). The radial glia antibody RC2 recognizes a protein encoded by Nestin. *Biochem Biophys Res Commun, 382*(3), 588-592. doi:10.1016/j.bbrc.2009.03.074

Patel, S. D., Ciatto, C., Chen, C. P., Bahna, F., Rajebhosale, M., Arkus, N., . . . Shapiro, L. (2006). Type II cadherin ectodomain structures: implications for classical cadherin specificity. *Cell, 124*(6), 1255-1268. doi:10.1016/j.cell.2005.12.046

Pattij, T., & Vanderschuren, L. J. (2008). The neuropharmacology of impulsive behaviour. *Trends Pharmacol Sci, 29*(4), 192-199. doi:10.1016/j.tips.2008.01.002

Pellow, S., Chopin, P., File, S. E., & Briley, M. (1985). Validation of open:closed arm entries in an elevated plus-maze as a measure of anxiety in the rat. *J Neurosci Methods, 14*(3), 149-167. Retrieved from https://www.ncbi.nlm.nih.gov/pubmed/2864480

Penzes, P., Buonanno, A., Passafaro, M., Sala, C., & Sweet, R. A. (2013). Developmental vulnerability of synapses and circuits associated with neuropsychiatric disorders. *J Neurochem, 126*(2), 165-182. doi:10.1111/jnc.12261

Philippova, M., Ivanov, D., Allenspach, R., Takuwa, Y., Erne, P., & Resink, T. (2005). RhoA and Rac mediate endothelial cell polarization and detachment induced by T-cadherin. *FASEB J, 19*(6), 588-590. doi:10.1096/fj.04-2430fje

Philippova, M., Ivanov, D., Joshi, M. B., Kyriakakis, E., Rupp, K., Afonyushkin, T., . . . Resink, T. J. (2008). Identification of proteins associating with glycosylphosphatidylinositol- anchored T-cadherin on the surface of vascular endothelial cells: role for Grp78/BiP in T-cadherin-dependent cell survival. *Mol Cell Biol, 28*(12), 4004-4017. doi:10.1128/MCB.00157-08

Philippova, M., Joshi, M. B., Kyriakakis, E., Pfaff, D., Erne, P., & Resink, T. J. (2009). A guide and guard: the many faces of T-cadherin. *Cell Signal, 21*(7), 1035-1044. Retrieved from http://www.ncbi.nlm.nih.gov/pubmed/19399994

Pinto, D., Delaby, E., Merico, D., Barbosa, M., Merikangas, A., Klei, L., . . . Scherer, S. W. (2014). Convergence of genes and cellular pathways dysregulated in autism spectrum disorders. *Am J Hum Genet, 94*(5), 677-694. doi:10.1016/j.ajhg.2014.03.018

Prakasam, A. K., Maruthamuthu, V., & Leckband, D. E. (2006). Similarities between heterophilic and homophilic cadherin adhesion. *Proc Natl Acad Sci U S A, 103*(42), 15434-15439. doi:10.1073/pnas.0606701103

Prata, D. P., Costa-Neves, B., Cosme, G., & Vassos, E. (2019). Unravelling the genetic basis of schizophrenia and bipolar disorder with GWAS: A systematic review. *J Psychiatr Res, 114*, 178-207. doi:10.1016/j.jpsychires.2019.04.007

Rakic, P. (1978). Neuronal migration and contact guidance in the primate telencephalon. *Postgrad Med J, 54 Suppl 1*, 25-40. Retrieved from https://www.ncbi.nlm.nih.gov/pubmed/364453

Rakic, P. (2003). Elusive radial glial cells: historical and evolutionary perspective. *Glia, 43*(1), 19-32. doi:10.1002/glia.10244

Ranscht, B., & Bronner-Fraser, M. (1991). T-cadherin expression alternates with migrating neural crest cells in the trunk of the avian embryo. *Development, 111*(1), 15-22. Retrieved from http://www.ncbi.nlm.nih.gov/pubmed/1707785

Ranscht, B., & Dours-Zimmermann, M. T. (1991). T-cadherin, a novel cadherin cell adhesion molecule in the nervous system lacks the conserved cytoplasmic region. *Neuron, 7*(3), 391-402. Retrieved from http://www.ncbi.nlm.nih.gov/pubmed/1654948

Read, D. E., & Gorman, A. M. (2009). Involvement of Akt in neurite outgrowth. *Cell Mol Life Sci, 66*(18), 2975-2984. doi:10.1007/s00018-009-0057-8

Ren, J., Friedmann, D., Xiong, J., Liu, C. D., Ferguson, B. R., Weerakkody, T., . . . Luo, L. (2018). Anatomically Defined and Functionally Distinct Dorsal Raphe Serotonin Sub-systems. *Cell, 175*(2), 472-487 e420. doi:10.1016/j.cell.2018.07.043

Riccio, O., Potter, G., Walzer, C., Vallet, P., Szabo, G., Vutskits, L., . . . Dayer, A. G. (2009). Excess of serotonin affects embryonic interneuron migration through activation of the serotonin receptor 6. *Mol Psychiatry, 14*(3), 280-290. doi:10.1038/mp.2008.89

Rivero, O., Selten, M. M., Sich, S., Popp, S., Bacmeister, L., Amendola, E., . . . Lesch, K. P. (2015). Cadherin-13, a risk gene for ADHD and comorbid disorders, impacts GABAergic function in hippocampus and cognition. *Transl Psychiatry, 5*, e655. doi:10.1038/tp.2015.152

Rivero, O., Sich, S., Popp, S., Schmitt, A., Franke, B., & Lesch, K. P. (2013). Impact of the ADHD-susceptibility gene CDH13 on development and function of brain networks. *Eur Neuropsychopharmacol, 23*(6), 492-507. doi:10.1016/j.euroneuro.2012.06.009

Ruggeri, B., Sarkans, U., Schumann, G., & Persico, A. M. (2014). Biomarkers in autism spectrum disorder: the old and the new. *Psychopharmacology (Berl), 231*(6), 1201-1216. doi:10.1007/s00213-013-3290-7

Sacristan, M. P., Vestal, D. J., Dours-Zimmermann, M. T., & Ranscht, B. (1993). T-cadherin 2: molecular characterization, function in cell adhesion, and coexpression with T-cadherin and N-cadherin. *J Neurosci Res, 34*(6), 664-680. doi:10.1002/jnr.490340610

Saito, M., Tucker, D. K., Kohlhorst, D., Niessen, C. M., & Kowalczyk, A. P. (2012). Classical and desmosomal cadherins at a glance. *J Cell Sci, 125*(Pt 11), 2547-2552. doi:10.1242/jcs.066654

Salatino-Oliveira, A., Genro, J. P., Polanczyk, G., Zeni, C., Schmitz, M., Kieling, C., . . . Hutz, M. H. (2015). Cadherin-13 gene is associated with hyperactive/impulsive symptoms in attention/deficit hyperactivity disorder. *Am J Med Genet B Neuropsychiatr Genet, 168B*(3), 162-169. doi:10.1002/ajmg.b.32293

Sanders, S. J., Ercan-Sencicek, A. G., Hus, V., Luo, R., Murtha, M. T., Moreno-De-Luca, D., . . . State, M. W. (2011). Multiple recurrent de novo CNVs, including duplications of the 7q11.23 Williams syndrome region, are

strongly associated with autism. *Neuron, 70*(5), 863-885. doi:10.1016/j.neuron.2011.05.002

Sanders, S. J., He, X., Willsey, A. J., Ercan-Sencicek, A. G., Samocha, K. E., Cicek, A. E., . . . State, M. W. (2015). Insights into Autism Spectrum Disorder Genomic Architecture and Biology from 71 Risk Loci. *Neuron, 87*(6), 1215-1233. doi:10.1016/j.neuron.2015.09.016

Sargin, D., Jeoung, H. S., Goodfellow, N. M., & Lambe, E. K. (2019). Serotonin Regulation of the Prefrontal Cortex: Cognitive Relevance and the Impact of Developmental Perturbation. *ACS Chem Neurosci, 10*(7), 3078-3093. doi:10.1021/acschemneuro.9b00073

Schatz, D. B., & Rostain, A. L. (2006). ADHD with comorbid anxiety: a review of the current literature. *J Atten Disord, 10*(2), 141-149. doi:10.1177/1087054706286698

Schneider, C. A., Rasband, W. S., & Eliceiri, K. W. (2012). NIH Image to ImageJ: 25 years of image analysis. *Nat Methods, 9*(7), 671-675. Retrieved from http://www.ncbi.nlm.nih.gov/pubmed/22930834

Selten, M., van Bokhoven, H., & Nadif Kasri, N. (2018). Inhibitory control of the excitatory/inhibitory balance in psychiatric disorders. *F1000Res, 7*, 23. doi:10.12688/f1000research.12155.1

Seong, E., Yuan, L., & Arikkath, J. (2015). Cadherins and catenins in dendrite and synapse morphogenesis. *Cell Adh Migr, 9*(3), 202-213. doi:10.4161/19336918.2014.994919

Shikanai, M., Nakajima, K., & Kawauchi, T. (2011). N-cadherin regulates radial glial fiber-dependent migration of cortical locomoting neurons. *Commun Integr Biol, 4*(3), 326-330. doi:10.4161/cib.4.3.14886

Song, N. N., Xiu, J. B., Huang, Y., Chen, J. Y., Zhang, L., Gutknecht, L., . . . Ding, Y. Q. (2011). Adult raphe-specific deletion of Lmx1b leads to central serotonin deficiency. *PLoS One, 6*(1), e15998. doi:10.1371/journal.pone.0015998

Takeichi, M. (1988). The cadherins: cell-cell adhesion molecules controlling animal morphogenesis. *Development, 102*(4), 639-655. Retrieved from https://www.ncbi.nlm.nih.gov/pubmed/3048970

Tantra, M., Guo, L., Kim, J., Zainolabidin, N., Eulenburg, V., Augustine, G. J., & Chen, A. I. (2018). Conditional deletion of Cadherin 13 perturbs Golgi cells and disrupts social and cognitive behaviors. *Genes Brain Behav, 17*(6), e12466. doi:10.1111/gbb.12466

Tao-Cheng, J. H., Thein, S., Yang, Y., Reese, T. S., & Gallant, P. E. (2014). Homer is concentrated at the postsynaptic density and does not redistribute after acute synaptic stimulation. *Neuroscience, 266*, 80-90. doi:10.1016/j.neuroscience.2014.01.066

Teissier, A., Soiza-Reilly, M., & Gaspar, P. (2017). Refining the Role of 5-HT in Postnatal Development of Brain Circuits. *Front Cell Neurosci, 11*, 139. doi:10.3389/fncel.2017.00139

Teraoka, H., Russell, C., Regan, J., Chandrasekhar, A., Concha, M. L., Yokoyama, R., . . . Wilson, S. W. (2004). Hedgehog and Fgf signaling pathways regulate the development of tphR-expressing serotonergic raphe neurons in zebrafish embryos. *J Neurobiol, 60*(3), 275-288. doi:10.1002/neu.20023

Tiihonen, J., Rautiainen, M. R., Ollila, H. M., Repo-Tiihonen, E., Virkkunen, M., Palotie, A., . . . Paunio, T. (2015). Genetic background of extreme violent behavior. *Mol Psychiatry, 20*(6), 786-792. doi:10.1038/mp.2014.130

Treutlein, J., Cichon, S., Ridinger, M., Wodarz, N., Soyka, M., Zill, P., . . . Rietschel, M. (2009). Genome-wide association study of alcohol dependence. *Arch Gen Psychiatry, 66*(7), 773-784. doi:10.1001/archgenpsychiatry.2009.83

Uhl, G. R., Drgon, T., Liu, Q. R., Johnson, C., Walther, D., Komiyama, T., . . . Lin, S. K. (2008). Genome-wide association for methamphetamine dependence: convergent results from 2 samples. *Arch Gen Psychiatry, 65*(3), 345-355. doi:10.1001/archpsyc.65.3.345

Uhl, G. R., Liu, Q. R., Drgon, T., Johnson, C., Walther, D., Rose, J. E., . . . Lerman, C. (2008). Molecular genetics of successful smoking cessation: convergent genome-wide association study results. *Arch Gen Psychiatry, 65*(6), 683-693. doi:10.1001/archpsyc.65.6.683

Van Battum, E. Y., Brignani, S., & Pasterkamp, R. J. (2015). Axon guidance proteins in neurological disorders. *Lancet Neurol, 14*(5), 532-546. doi:10.1016/S1474-4422(14)70257-1

van de Linde, S., Loschberger, A., Klein, T., Heidbreder, M., Wolter, S., Heilemann, M., & Sauer, M. (2011). Direct stochastic optical reconstruction microscopy with standard fluorescent probes. *Nat Protoc, 6*(7), 991-1009. doi:10.1038/nprot.2011.336

Vestal, D. J., & Ranscht, B. (1992). Glycosyl phosphatidylinositol--anchored T-cadherin mediates calcium-dependent, homophilic cell adhesion. *J Cell Biol, 119*(2), 451-461. doi:10.1083/jcb.119.2.451

Vitalis, T., Ansorge, M. S., & Dayer, A. G. (2013). Serotonin homeostasis and serotonin receptors as actors of cortical construction: special attention to the 5-HT3A and 5-HT6 receptor subtypes. *Front Cell Neurosci, 7*, 93. doi:10.3389/fncel.2013.00093

Vitalis, T., Cases, O., Passemard, S., Callebert, J., & Parnavelas, J. G. (2007). Embryonic depletion of serotonin affects cortical development. *Eur J Neurosci, 26*(2), 331-344. doi:10.1111/j.1460-9568.2007.05661.x

Vizi, E. S., Kiss, J. P., & Lendvai, B. (2004). Nonsynaptic communication in the central nervous system. *Neurochem Int, 45*(4), 443-451. doi:10.1016/j.neuint.2003.11.016

Walf, A. A., & Frye, C. A. (2007). The use of the elevated plus maze as an assay of anxiety-related behavior in rodents. *Nat Protoc, 2*(2), 322-328. doi:10.1038/nprot.2007.44

Wallace, J. A., & Lauder, J. M. (1983). Development of the serotonergic system in the rat embryo: an immunocytochemical study. *Brain Res Bull, 10*(4), 459-479. Retrieved from http://www.ncbi.nlm.nih.gov/pubmed/6344960

Wallman, M. J., Gagnon, D., & Parent, M. (2011). Serotonin innervation of human basal ganglia. *Eur J Neurosci, 33*(8), 1519-1532. doi:10.1111/j.1460-9568.2011.07621.x

Waselus, M., Valentino, R. J., & Van Bockstaele, E. J. (2011). Collateralized dorsal raphe nucleus projections: a mechanism for the integration of diverse functions during stress. *J Chem Neuroanat, 41*(4), 266-280. doi:10.1016/j.jchemneu.2011.05.011

Wegel, E., Gohler, A., Lagerholm, B. C., Wainman, A., Uphoff, S., Kaufmann, R., & Dobbie, I. M. (2016). Imaging cellular structures in super-resolution with

SIM, STED and Localisation Microscopy: A practical comparison. *Sci Rep, 6*, 27290. doi:10.1038/srep27290

Whitaker-Azmitia, P. M. (2001). Serotonin and brain development: role in human developmental diseases. *Brain Res Bull, 56*(5), 479-485. doi:10.1016/s0361-9230(01)00615-3

Winstanley, C. A., Theobald, D. E., Dalley, J. W., Cardinal, R. N., & Robbins, T. W. (2006). Double dissociation between serotonergic and dopaminergic modulation of medial prefrontal and orbitofrontal cortex during a test of impulsive choice. *Cereb Cortex, 16*(1), 106-114. doi:10.1093/cercor/bhi088

Wurst, W., & Bally-Cuif, L. (2001). Neural plate patterning: upstream and downstream of the isthmic organizer. *Nat Rev Neurosci, 2*(2), 99-108. doi:10.1038/35053516

Wyler, S. C., Donovan, L. J., Yeager, M., & Deneris, E. (2015). Pet-1 Controls Tetrahydrobiopterin Pathway and Slc22a3 Transporter Genes in Serotonin Neurons. *ACS Chem Neurosci, 6*(7), 1198-1205. doi:10.1021/cn500331z

Wyler, S. C., Spencer, W. C., Green, N. H., Rood, B. D., Crawford, L., Craige, C., . . . Deneris, E. (2016). Pet-1 Switches Transcriptional Targets Postnatally to Regulate Maturation of Serotonin Neuron Excitability. *J Neurosci, 36*(5), 1758-1774. doi:10.1523/JNEUROSCI.3798-15.2016

Wylie, C. J., Hendricks, T. J., Zhang, B., Wang, L., Lu, P., Leahy, P., . . . Deneris, E. S. (2010). Distinct transcriptomes define rostral and caudal serotonin neurons. *J Neurosci, 30*(2), 670-684. doi:10.1523/JNEUROSCI.4656-09.2010

Xu, C., Funahashi, Y., Watanabe, T., Takano, T., Nakamuta, S., Namba, T., & Kaibuchi, K. (2015). Radial Glial Cell-Neuron Interaction Directs Axon Formation at the Opposite Side of the Neuron from the Contact Site. *J Neurosci, 35*(43), 14517-14532. doi:10.1523/JNEUROSCI.1266-15.2015

Xu, W., Cohen-Woods, S., Chen, Q., Noor, A., Knight, J., Hosang, G., . . . Vincent, J. B. (2014). Genome-wide association study of bipolar disorder in Canadian and UK populations corroborates disease loci including SYNE1 and CSMD1. *BMC Med Genet, 15*, 2. doi:10.1186/1471-2350-15-2

Ye, W., Shimamura, K., Rubenstein, J. L., Hynes, M. A., & Rosenthal, A. (1998). FGF and Shh signals control dopaminergic and serotonergic cell fate in the anterior neural plate. *Cell, 93*(5), 755-766. Retrieved from http://www.ncbi.nlm.nih.gov/pubmed/9630220

Yokota, Y., Eom, T. Y., Stanco, A., Kim, W. Y., Rao, S., Snider, W. D., & Anton, E. S. (2010). Cdc42 and Gsk3 modulate the dynamics of radial glial growth, inter-radial glial interactions and polarity in the developing cerebral cortex. *Development, 137*(23), 4101-4110. doi:10.1242/dev.048637

Zhang, Z. W. (2003). Serotonin induces tonic firing in layer V pyramidal neurons of rat prefrontal cortex during postnatal development. *J Neurosci, 23*(8), 3373-3384. Retrieved from https://www.ncbi.nlm.nih.gov/pubmed/12716945

Zhou, K., Dempfle, A., Arcos-Burgos, M., Bakker, S. C., Banaschewski, T., Biederman, J., . . . Asherson, P. (2008). Meta-analysis of genome-wide linkage scans of attention deficit hyperactivity disorder. *Am J Med Genet B Neuropsychiatr Genet, 147B*(8), 1392-1398. doi:10.1002/ajmg.b.30878

Affidavit

I hereby confirm that my thesis entitled "Impact of Cadherin-13 deficiency on the brain serotonin system using mouse models and human iPSC-derived neurons" is the result of my own work. I did not receive any help or support from commercial consultants. All sources and / or materials applied are listed and specified in the thesis.
Furthermore, I confirm that this thesis has not yet been submitted as part of another examination process neither in identical nor in similar form.

_____ _____

Place, Date Signature

Eidesstattliche Erklärung

Hiermit erkläre ich an Eides statt, die Dissertation mit dem Titel " Einfluss einer Cadherin-13 Defizienz auf das Serotonin- System des Gehirns unter Verwendung von Mausmodellen und humanen iPSC-abgeleiteten Neuronen" eigenständig, d.h. insbesondere selbständig und ohne Hilfe eines kommerziellen Promotionsberaters, angefertigt und keine anderen als die von mir angegebenen Quellen und Hilfsmittel verwendet zu haben.
Ich erkläre außerdem, dass die Dissertation weder in gleicher noch in ähnlicher Form bereits in einem anderen Prüfungsverfahren vorgelegen hat.

_____ _____

Ort, Datum Unterschrift

List of publications

Forero, A., Rivero, O., Waldchen, S., Ku, H. P., Kiser, D. P., Gartner, Y., . . . Lesch, K. P. (2017). Cadherin-13 Deficiency Increases Dorsal Raphe 5-HT Neuron Density and Prefrontal Cortex Innervation in the Mouse Brain. *Front Cell Neurosci, 11*, 307. doi:10.3389/fncel.2017.00307

Forero, A., Ku, H.P., Malpartida, A.B., Wäldchen, S., Alhama-Riba, J., Kulka, C., Aboagye, B., Norton, W., Young, A., Ding, Y.Q., Blum, R., Sauer, M., Rivero, O., Lesch, K.P. (2020) Serotonin (5-HT) neuron-specific inactivation of Cadherin-13 impacts 5-HT system formation and cognitive function. *Neuropharmacology*. 10.1016/j.neuropharm.2020.108018

Jansch, C., K. Günther, J. Waider, G. C. Ziegler, **A. Forero**, S. Kollert, E. Svirin, D. Pühringer, C. K. Kwok, R. Ullmann, A. Maierhofer, J. Flunkert, T. Haaf, F. Edenhofer and K.-P. Lesch (2018). Generation of a human induced pluripotent stem cell (iPSC) line from a 51-year-old female with attention-deficit/hyperactivity disorder (ADHD) carrying a duplication of SLC2A3. *Stem Cell Research* 28: 136-140.

Jansch, C., **A. Forero**, S. Kollert, S. Wäldchen, E. Svirin, J. Waider, G. C. Ziegler, F. Edenhofer, M. Sauer, E. Wischmeyer and K.-P. Lesch (submitted). Serotonin-specific neurons differentiated from human iPSCs form distinct subtypes with synaptic protein assembly.

Acknowledgements

This five-year journey has been so much more than getting a degree. I've stumbled, fallen, and gotten back up, and in doing so I was lucky to have wonderful people around me to offer support in every step of the way. I would like to acknowledge the German Excellence Initiative to the Graduate School of Life Sciences and the Colombian Department of Science, Technology and Innovation (Colciencias) for the financial support provided for this project. Following, I would like to express my gratitude for my thesis supervisors. I thank Prof. Dr. Klaus-Peter Lesch for allowing me to be part of his wonderful team, thank you for encouraging critical thinking and collaborative work. I greatly appreciate your guidance and support over these past years. I would like to thank Prof. Dr. Markus Sauer for accepting to be my thesis supervisor and for all his constructive criticism on this project. I also would like to recognize Dr. Robert Blum, thank you for your mentoring, for always being available to discuss ideas and plans, for your motivating words and always honest opinion, I will remember this kindly in my future endeavors. Next, I would like to acknowledge the wonderful people that I worked with, many of which more than colleagues, I now consider friends. Gracias a Olga, amiga me ha encantando trabajar contigo estos años, has sido un gran apoyo para mi, tanto en mi vida profesional como personal. Thank you to Dr. Jonas Waider and Dr. Angelika Schmitt for your scientific support. A special thanks goes out to Sina, Charline and Hsing-Ping for making even the most difficult work enjoyable, and to Johanna, Maria, Leonie, Jann, Christoph, Ben and Dominik for all the nice conversations, it was great having you as colleagues. I also appreciate the excellent assistance from Judith, Gaby, Marion, Eva, Nicole and Julia in my project, and also thank everyone else in the lab who contributed in any way.

I would also like to gratefully recognize the GSLS team, Dr. Gabriele Blum-Oehler, Katrin, Jenny and Sebastian, for all their dedication to help and ease the way for us doctoral students. Thank you for supporting us as we pursue our goals. I would also like to give a special thanks to Dr. Stephan Schöder-Köhne, my first contact in Germany, for the constant support and feedback during every step of my education in Würzburg.

Finally, I would like to thank my family and friends. Diego, gracias por todo, por acompañarme y apoyarme en todas mis decisiones, tu y Oliver han sido el regalo más bello que me ha dado la vida. Gracias a mis padres, por su apoyo incondicional; a mi padre por despertar en mi una curiosidad casi insaciable por la vida, y a mi madre por ser mi mejor amiga. Gracias también a mis hermanos, a mis tías, primas y amigas que con mensajes o llamadas hicieron que la distancia no se sintiera tan grande. I would like to thank my FOKUS family, thank you for all the moments shared, you've made Germany feel like home.